

**Aus der Medizinischen Klinik und Poliklinik IV
der Ludwig-Maximilians-Universität München
Direktor: Prof. Dr. med. Martin Reincke**

Chemokines and Cysteine Proteases in Diabetic Kidney Disease

Dissertation

**zum Erwerb des Doktorgrades der Humanbiologie
an der Medizinischen Fakultät der
Ludwig-Maximilians-Universität zu München**

Vorgelegt von

Venkata Surya Narayana Murthy Darisipudi

Aus

Annavaram, India

2013

**Mit Genehmigung der Medizinischen Fakultät
der Universität München**

Berichterstatter : Prof. Dr. Hans-Joachim Anders

**Mitberichterstatter : Priv. Doz. Dr. Andreas Helck
Prof. Dr. Jochen Seißler
Priv. Doz. Dr. Peter Fraun Bergei**

Dekan : Herr Prof. Dr. med. Dr.h.c. Maximilian Reiser, FACR, FRCR

Tag der mündlichen Prüfung: 19.12.2013

Dedicated to
My Mother

Venkata Surya Narayana Murthy Darisipudi M.Sc.,
Medizinische Klinik und Poliklinik IV,
Klinikum der Universität Muenchen,
Nephrologisches Zentrum,
Arbeitsgruppe Prof. Hans Joachim Anders,
Schillerstraße-42,
80336 Munich, Germany
Tel. +49 89 218075856

DECLARATION

I hereby declare that the present work embodied in this thesis was carried out by me under the supervision of Prof. Hans Joachim Anders, Medizinische Klinik und Poliklinik IV, Klinikum der Universität München. This work has not been submitted in part or full to any other university or institute for any degree or diploma.

Publications

Darisipudi MN, Kulkarni OP, Sayyed SG, Ryu M, Migliorini A, Sagrinati C, Parente E, Vater A, Eulberg D, Klussmann S, Romagnani P, Anders HJ. Dual blockade of the homeostatic chemokine CXCL12 and the proinflammatory chemokine CCL2 has additive protective effects on diabetic kidney disease. *Am J Pathol.* 2011 Jul; 179(1):116-24

Darisipudi MN, Ryu M, Hägele H, Kulkarni OP, Mulay SR, Jana D, Uhl B, Reichel Ch, Krombach F, Moll S, Schott B, Gruner S, Haap W, Hartmann G, Anders HJ. Cathepsin S promotes endothelial dysfunction and its therapeutic inhibition protects from proteinuria, podocyte loss, and glomerulosclerosis in type 2 diabetes. (Submitted)

Part of the work was done by collaborators, as mentioned below:

1. Prof. Paola Romagnani, University of Florence, Italy.
She has performed the *in vitro* studies on human kidney renal progenitor cells to find out the effect of CXCL12 blockade on podocyte regeneration. These data are presented in the results-part I (figure 21) of this thesis.

2. Dr. Guido Hartmann, Dr. Brigitte Schott, Sabine Gruner, Wolfgang Haap, Roche Pharmaceuticals, Basel, Switzerland. They have provided the *in-situ* hybridization images, splenocyte p10 accumulation and enzymatic assay data. These data are presented in the results-part II (figure 24B and 26B, table 8) of this thesis.

3. Dr. Chistoph Reichel, Fritz Krombach and Bernd Uhl, Walther-Straub-Institut for Pharmakologie und Toxikologie, University of Munich, Munich, Germany. They have performed the *in vivo* experiments with mouse cremaster muscles to see the effect of R05461111 on vascular damage. These data are presented in the results-part II (figure 31A-B) of this thesis.

Venkata Surya Narayana Murthy Darisipudi
Date:

ACKNOWLEDGEMENTS

As my doctoral journey is reaching its end, I wish to take this opportunity to express my sincere gratitude to all around me who have helped in numerous ways to be able to accomplish my research goals.

At this point, I feel greatly indebted to Prof. Hans Joachim Anders who presented me with a wonderful opportunity to realize my research objectives under his esteemed supervision. His incredible foresight, deeper insights and keen interest in my ideas and opinions have always been a source of guidance and motivation at each and every step of my doctoral journey. Apart from refining my research and scientific thinking skills; this experience has brought along numerous learning opportunities where the prized wisdom, constant encouragement and endless support of my supervisor inspired me to cultivate personal qualities like dedication towards work, conviction in my own ideas as well as developing amicable and constructive relationships with people around me.

I would like to acknowledge Prof. S. Klussmann (Noxxon Pharma, Berlin) and Dr. Guido Hartmann (Roche, Switzerland) for providing me the experimental drug molecules for the research work. I specially thank Dr. Guido Hartmann for his constant support, discussions and cooperation to complete the thesis. I thank Prof. Paola Romagnani, University of Florence, for her support and kind collaboration.

My sincere thanks go to Dr. Peter Nelson, Dr. Bruno Luckow and Dr. Volker Vielhauer for their constant encouragement and constructive suggestions throughout my stay at Klinische Biochemie.

I am very grateful to all my colleagues of the institute for the cooperative spirit, the warm and friendly working atmosphere and sharing scientific discussion. Many thanks to Adrinana, Dana, Khader, Kirstin, Maciej, Santosh, Simone, Shrikant, and Onkar and all other medical students who are too many to enumerate but are still deeply in my heart. My special thanks to Henny, Dan, Jana, Nuru and Ewa for their skillful technical assistance to carry out the research work successfully.

My special thanks to Anji for his great help professionally and personally.

I would like take this opportunity to thank my friends Kushekar, Sai Prasad and Prathyush for their support in providing scientific papers to write my thesis.

I am always indebted to my dear friends, Naresh, Sudhakar and Praneeth who always cared for me and helped me when I was in need. You are always close to my heart. To the amazing friends who have spent this period of my life with me who made who made my stay in Munich enjoyable and unforgettable. Thanks to Harish, Khader, Santhosh, Ramakrishna, Sukumar, Narotham and Jigna. I would also like to thank my ever dearest friends, Preethi, Rambabu and Amrutha for their love and warm encouragement. I expand my sincere thanks to all my seniors, Pavan, Vikas, Sumit, Neeraj, Pranav and Jaya prakash who helped me in all aspects during my stay in delhi. I feel highly indebted to Satish for his extended brotherly love towards me.

My heartfelt thanks to Prof. D. N. Rao, All India Institute of Medical Sciences, New Delhi, for his support and encouragement.

It is my duty to express my tearful acknowledgement to the animals, which have been sacrificed for the betterment of human being.

TABLE OF CONTENTS

1. Introduction	1
1.1 Chronic kidney disease	1
1.2 Diabetic nephropathy	3
1.2.1 Pathophysiology	6
1.2.2 The role of inflammation	8
1.3 Chemokines and chemokine receptors	9
1.3.1 Chemokines	9
1.3.2 Chemokine receptors	10
1.3.3 Role of chemokines and chemokine receptors	14
1.3.4 CCL2/ MCP-1.....	14
1.3.5 CXCL12/ SDF-1.....	16
1.4 Cathepsins	18
1.4.1 Cysteine cathepsins	19
1.4.2 Pathophysiological role of cysteine cathepsins	20
1.4.3 Role of cysteine cathepsins in proteinuric kidney diseases	21
1.4.4 Cathepsin S	21
1.5 Animal models of diabetic nephropathy	23
1.6 Spiegelmers-next generation Aptamers	25
2. Research hypothesis	28
3. Material and methods	29
3.1 Materials	31
3.2 Methods part I	34
3.3 Methods part II	45
4. Results	54
4.1 Part I	54
4.1.1 Plasma CCL2 and CXCL12 levels	54
4.1.2 Body weight and blood glucose	55
4.1.3 Glomerulosclerosis	56
4.1.4 Renal functional parameters in db/db mice	58
4.1.5 Ki-67+ proliferating glomerular cells	59
4.1.6 Leukocyte numbers in glomeruli	60
4.1.7 Renal mRNA expression of proinflammatory and podocyte parameters in db/db mice	62
4.1.8 Podocyte numbers in db/db mice	63

4.1.9 CXCL12 suppresses nephrin <i>de novo</i> expression of podocyte progenitors	65
4.2 Part II	67
4.2.1 Cathepsin S expression in murine and human type 2 diabetic kidney disease	67
4.2.2 RO5461111 inhibits cathepsin S activity	71
4.2.3 RO5461111 reduces glomerulosclerosis	73
4.2.4 RO5461111 treatment reduces podocyte loss	73
4.2.5 RO5461111 treatment reduces albuminuria	75
4.2.6 Cathepsin S directly injures glomerular endothelial cells	76
4.2.7 RO5461111 reduces oxidative stress-induced vascular permeability <i>in vivo</i>	78
4.2.8 RO5461111 reduces glomerular leukocyte recruitment and inflammation	80
5. Discussion	83
5.1 Part I- Chemokine blockade in diabetic nephropathy	83
5.2 Part II- Cathepsin S inhibition in diabetic nephropathy	86
6. Summary and conclusion	91
7. Zusammenfassung und Fazit	93
8. References	95
9. Abbreviations	104
10. Appendix	106
11. Curriculum vitae	108

1. Introduction

1.1 Chronic Kidney Disease

Chronic Kidney Disease (CKD) is a gradual and progressive loss of kidney function that often leads to End Stage Renal Disease (ESRD). The loss of renal function usually takes many years to occur and there may be no symptoms at early stages of the disease¹. In fact, progression may be so gradual that symptoms do not occur until kidney function is less than one-tenth of normal. ESRD is the most advanced form of CKD which requires kidney replacement to ensure survival².

The development and progression to CKD involves many complications and consequences that finally lead to ESRD. Kidney Disease Improving Global Outcomes (KDIGO) conceptual model describes the various stages, risk factors and complications associated with the progression of CKD to kidney failure and death¹ (Figure 1). KDIGO defined CKD as abnormalities of kidney structure or function present for 3 months or longer. The CKD is classified into different stages based on the decline in the glomerular filtration rate (GFR) and the severity of albuminuria³ (Table 1).

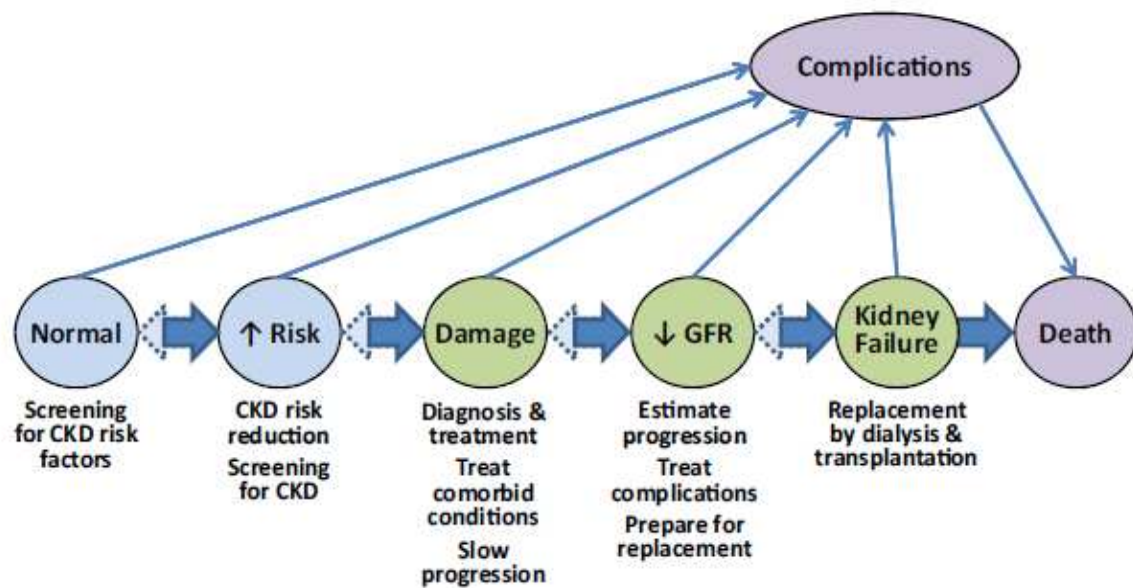


Figure 1: Conceptual model of chronic kidney disease. This diagram presents the continuum of development, progression, and complications of chronic kidney disease. Green circles represent stages of chronic kidney disease, aqua circles represent potential antecedents, lavender circles represent consequences, and thick arrows between ellipses represent risk factors associated with the development, progression, and remission of chronic kidney disease. ‘Complications’ refers to all complications of chronic kidney disease and interventions for its treatment and prevention, including complications of decreased glomerular filtration rate and cardiovascular disease. Adapted from A.S.Levey *et. al.*³

Table 1: Prognosis of chronic kidney disease: The revised classification of Chronic Kidney Disease by KDIGO. Adapted from KDIGO, *Kidney International*, 2013

Prognosis of CKD by GFR and Albuminuria Categories: KDIGO 2012				Persistent albuminuria categories Description and range		
				A1	A2	A3
				Normal to mildly increased	Moderately increased	Severely increased
				<30 mg/g <3 mg/mmol	30-300 mg/g 3-30 mg/mmol	>300 mg/g >30 mg/mmol
GFR categories (ml/min/ 1.73 m ²) Description and range	G1	Normal or high	≥90			
	G2	Mildly decreased	60-89			
	G3a	Mildly to moderately decreased	45-59			
	G3b	Moderately to severely decreased	30-44			
	G4	Severely decreased	15-29			
	G5	Kidney failure	<15			

The colours represent the intensities of risk. Green: low risk (if no other markers of kidney disease, no CKD); Yellow: moderately increased risk; Orange: high risk; Red: very high risk
Abbreviations: GFR, glomerular filtration rate

Though the abnormalities of kidney damage generally ascertained from albuminuria, other objective measures (urine sediment, pathology or imaging studies, acid-base and electrolyte disorders due to tubular disorders, or history of kidney transplantation) also help in assessing the disease (KDIGO Kidney International 2013).

The prevalence of CKD continues to increase worldwide and approximately 600 million people are affected worldwide. For example, CKD affects about 14 to 15% of the adult US population and is projected to increase by 50% in the next 20 years⁴. Diabetes, obesity and hypertension are the most common causes that account for approximately two thirds of the cases of chronic renal failure and ESRD³. Other diseases and conditions such as autoimmune and hereditary disorders^{5,6}, infections^{7,8} (HBV, HCV and HIV) and diabetic nephropathy (DN)^{9,10} have shown to be associated with the development and progression of CKD. Among these, DN is one of the major causes of CKD⁹.

1.2 Diabetic Nephropathy

Diabetes Mellitus

Diabetes Mellitus (DM) is characterized by hyperglycaemia with disturbances in carbohydrate, protein and fat metabolism caused by complete or relative insufficiency of insulin secretion and/or insulin action¹¹.

There are mainly two forms of diabetes mellitus, insulin-dependent diabetes mellitus (IDDM) and non-insulin dependent diabetes mellitus (NIDDM). IDDM or type 1 diabetes (T1D) is characterized by a progressive destruction of the insulin-producing β -cells in the pancreas, usually due to auto-immune response, which leads to insulin deficiency. In addition to that, various genetic and environmental factors, for example, exposure to viruses also contribute to T1D which accounts for about 10-15% of all people with DM¹².

Non-insulin-dependent or adult-onset diabetes mellitus or type 2 diabetes (T2D) is characterized by insulin resistance or relative insulin deficiency. This is the most common form of diabetes and accounts for almost 90-95% of all cases of diabetes in adults worldwide. The incidence of T2D is mainly due to lifestyle changes, such as high-fat diet and physical inactivity and yet, several genetic epidemiological studies demonstrate that both obesity and T2D are highly inherited traits¹³. There are other forms of DM namely, maturity onset diabetes of the young (MODY) and gestational diabetes (GD) occurring with relatively low prevalence.

Prevalence of Diabetes

The worldwide prevalence of diabetes for all age groups is estimated to be 2.8%; of which 8.3% are reported to be adults between 20-79 age in year 2011¹⁴. According to International Diabetes Federation (IDF), the total number of people living with diabetes across the world is around 366 million and expected to hit 552 million by the year 2030 and it is equal to 3 new cases every 10 second or 10 million per year. In general, on an average, nearly 8% of adults living in highly developed countries have diabetes¹⁴. According to 'London School of Economics (LSE) diabetes report' 2012, diabetes prevalence in European population has been increasing over the past two decades and it has estimated that among all European countries, Germany has the highest diabetes prevalence rate of 8.9% and approximately 6 people per every hour die from diabetes and complications associated with it¹⁵. Today, it is estimated that one in

every 13 persons in Germany has diabetes. The IDF estimates that by 2030 the number of people with diabetes will increase to 8 million, which corresponds to 13.5% of total diabetic population (www.dzd-ev.de).

Diabetes and its complications

Uncontrolled and prolonged hyperglycaemia in diabetic patients often leads to several macro and micro vascular complications. Major microvascular complications include retinal abnormalities (diabetic retinopathy), autonomic, sensory, and motor neuropathies (diabetic neuropathy) and renal impairment (DN).

Diabetic nephropathy

DN is the leading cause of CKD in the Western world, and is one of the most significant long-term complications leading to increased morbidity and mortality in patients with T2D¹⁶. Approximately 25-30% of patients with T1D or T2D will develop overt DN, where half of all patients will require hemodialysis treatment¹⁷. DN is characterized by hypertension, progressive albuminuria, glomerulosclerosis, and decline in GFR, leading to ESRD. Based on the decline in the GFR and albuminuria, DN is classified into 5 stages¹⁸ (Table 2).

In DN, the glomerular tuft undergoes a slow but progressive structural remodelling characterized by glomerular hypertrophy, accumulation of extracellular mesangial matrix, and podocyte damage¹⁹ (Figure 2). The latter have been shown to account for the progression of micro-albuminuria from early stages to overt proteinuria. These changes eventually lead to glomerular sclerosis at late stage DN which progressively destroys the renal function and finally leads to kidney failure. The development and progression of DN to ESRD involves multiple pathomechanisms (Figure 3) that finally contribute to the scarring of glomerulus, known as glomerulosclerosis which is manifested by either nodular or diffuse lesions (www.emedline.com).

Table 2: KDOQI classification of different stages associated with various stages of DN.

Stage	Description	Characteristic features	GFR*	Prevalence %
1	Kidney damage with normal or slight increase in GFR	Glomerular hyperfiltration	>90	3.3
2	Kidney damage with mildly reduced GFR	Thickened GBM, expanded mesangium	60-90	3
3	Moderately impaired GFR	Microalbuminuria	30-59	4.3
4	Severe impaired GFR	Macroalbuminuria	15-29	0.2
5	Kidney failure	ESRD	<15 or dialysis	0.2

Adapted and modified from Levey *et. al*¹⁸.

*mL/min/1.73 m²

Abbreviations: GFR, glomerular filtration rate;
 GBM, glomerular basement membrane;
 ESRD, end stage renal disease;
 KDOQI, Kidney Disease Outcomes Quality Initiative

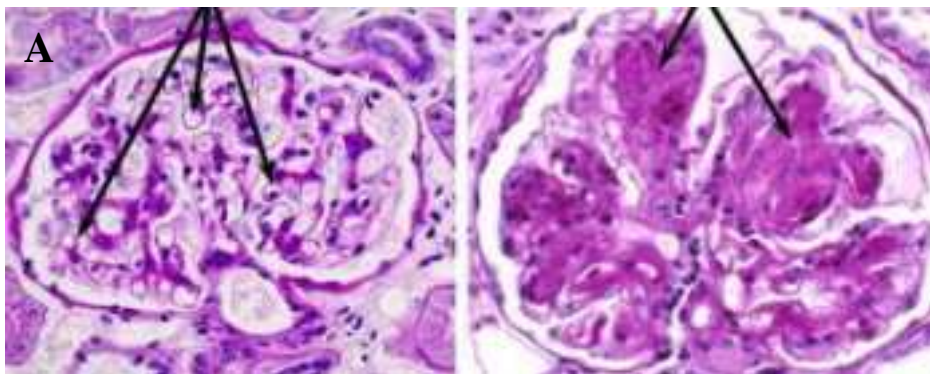


Figure 2: Periodic acid–Schiff stain of glomeruli. (A) Normal glomerular with wide open capillaries and normal vasculature. (B) Mesangial matrix accumulation, thickened GBM and collapsed capillaries (Obtained from <http://drugline.org>).

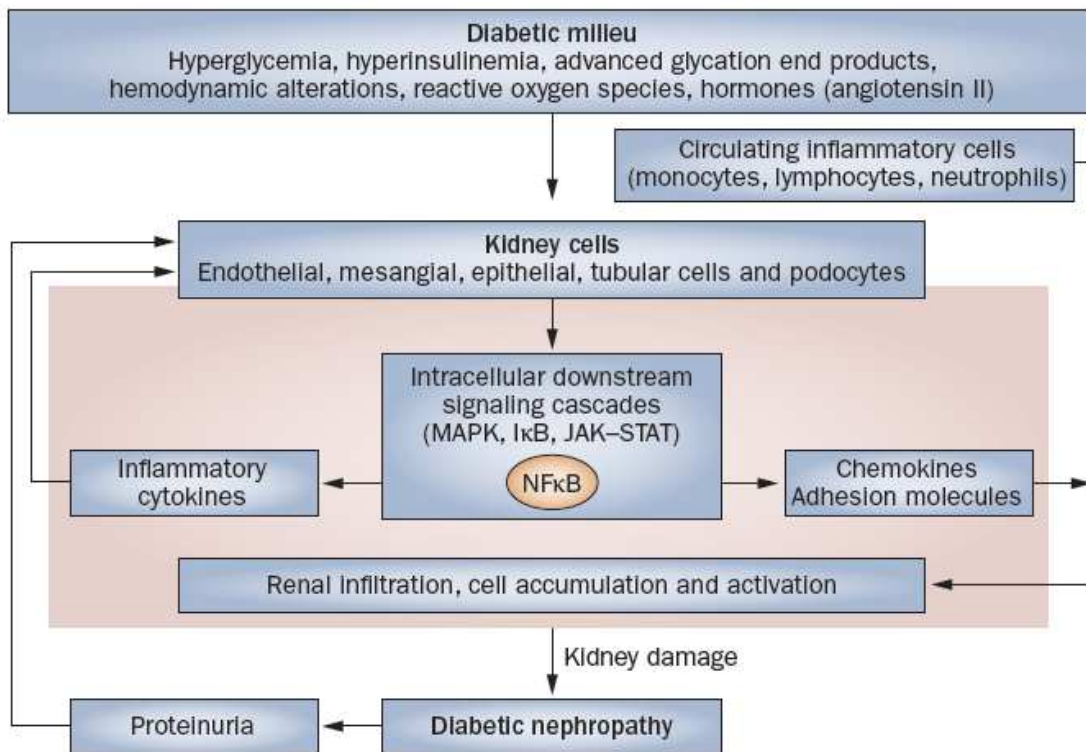


Figure 3: Overview of multiple pathomechanisms involved in the progression of DN. Adapted from J.F Navarro *et al.*²⁰

1.2.1 Pathophysiology of diabetic nephropathy

Glomerulosclerosis

Glomerulosclerosis is a major cause of DN. The development and progression of DN to glomerulosclerosis involves all cell types (mesangial cells, endothelial cells and podocytes) in the glomerular tuft. Recent studies report that both the glomerulus and the tubulointerstitium are involved in the pathophysiologic changes contributing to progression of the disease¹⁹. Though mesangial cells are in front in the development and progression of the disease, the cross talk between all cell types plays an important role in the evolution of diabetic glomerulosclerosis. However, the loss of podocytes, the glomerular epithelial cell that represents the main constituent of the glomerular filtration barrier (GFB), is the crucial driver of progression towards glomerulosclerosis^{21,22}. A number of factors, including genetic, mechanical, and immunological stresses, as well as toxins, can cause podocyte injury²³⁻²⁶.

Podocytes loss

The GFB is a highly specialized blood filtration unit consisting of three major components: the fenestrated endothelial cell, the glomerular basement membrane (GBM), and the visceral epithelial cells, called podocytes. Podocytes are highly specialized epithelial cells of mesenchymal origin located on the urinary aspect of the GFB^{27,28}. Growing evidences suggest that loss of podocytes plays a key role in the progression towards glomerulosclerosis. For example, reduction in the number of podocytes is proportional to the extent of albuminuria in many diseases including DN²⁹⁻³¹, focal segmental glomerulosclerosis (FSGS) and IgA nephropathy^{29,32}. Various insults, including genetic, mechanical, and immunological stress, as well as toxins, alter the structural and functional cytoskeleton of the podocytes and its slit diaphragm³³⁻³⁵. Since these podocytes are terminally differentiated and cannot undergo cell division, any repair/proliferative response of surviving podocytes often lead to podocyte detachment from the GBM either as a consequence of sublethal injury or from apoptotic or necrotic death^{36,37}, now referred to as “mitotic catastrophe”^{38,39}. Mitotic catastrophe is defined as “cell death during mitosis” by an incomplete assembly of the chromosomes and the mitotic spindle in the pro-metaphase which then leads to aberrant chromosome segregation⁴⁰. Such cells die either immediately within mitosis or shortly after via apoptosis or necrosis. Morphologic features of mitotic catastrophe include multiple nuclei, micronuclei or irregularly shaped nuclei^{36,41,42}. *In vitro* studies suggest that cultured podocytes lack the ability to reproduce the *in vivo* podocyte cytoskeletal phenotype⁴³. In addition, several experimental models have addressed that either podocyte depletion or podocyte injury is sufficient to induce glomerulosclerosis and the degree of podocyte depletion positively correlates with the severity of the glomerulosclerosis^{44,45}. Furthermore, it has been show that replacement of podocytes (either recovery or repair) contributes to the regression of glomerulosclerosis^{44,46-48}. However, a large body of evidence over the past decade suggest the involvement of many inflammatory pathways that finally leads to podocyte loss and glomerulosclerosis in DN²⁰.

1.2.2 The role of inflammation in the pathophysiology of diabetic nephropathy

As depicted in figure 3, all components of diabetic milieu (high glucose, hemodynamic changes, metabolic abnormalities, advanced glycation end products (AGEs), and oxidative stress act on all types of kidney cells (endothelial, mesangial, epithelial, tubular cells, and podocytes) and activate diverse molecular signal cascades. Activation of these signalling pathways result in infiltration of circulating inflammatory cells, which amplifies and perpetuates the inflammatory process in the kidney to produce various cytokine and chemokines, finally resulting in development and progression of DN. Many studies have shown that chronic inflammation is associated with the progression of kidney disease in T2D, implying the role of inflammatory processes in the disease progression⁴⁹.

Recruitment of inflammatory cells

There are increasing evidences suggesting the involvement of immune cells in the DN^{50,51}. The chemokines produced by elements of diabetic milieu direct the migration of leukocytes into kidney and promote further inflammation^{52,53}. The steps involved in the recruitment of leukocytes into kidney are discussed in detail in “chemokines and chemotaxis” section.

Macrophages

Macrophages are one of the central mediators of renal vascular inflammation in diabetes mellitus, and promote DN⁵⁴. It has been shown in renal biopsies of human DN, macrophages accumulate in the glomeruli and interstitium even in the early stages of the disease. Recent studies also demonstrate that macrophage-derived products can induce further inflammation in the diabetic kidney. After infiltration into tissues, these macrophages produce various cytokines, reactive oxygen species (ROS), profibrotic and anti-angiogenic factors which are crucial mediators of renal damage. In different experimental models of DN, renal macrophage accumulation correlates with increased chemokine production, glomerular and tubule-interstitial injury, and progressive fibrosis. Adoptive transfer studies in a mouse model of experimental glomerulonephritis showed that macrophages can induce proteinuria and mesangial proliferation⁵⁵. Together, macrophages and their products exacerbate inflammation in the kidneys of patients with DM implicating their pathological role in DN.

Macrophages recruitment

Research during the past decade demonstrated that diabetic patients with nephropathy have elevated plasma levels of ICAM-1 (intercellular adhesion molecule-1)⁵⁶. ICAM-1 on vascular endothelium actively controls the homing of macrophages into the kidney. ICAM-1 serves as a ligand for LFA-1 on monocytes, facilitating leukocyte adhesion and transmigration. It has been demonstrated that various factors such as hyperglycemia⁵⁷, AGEs⁵⁸, oxidative stress⁵⁹, and hyper-insulinemia can induce ICAM-1 expression in kidneys of both type 1 and type 2 diabetic mice. ICAM-1 deficient db/db mice showed significant reduction in albuminuria, glomerular and tubulointerstitial injury and associated with reduction in the number of glomerular and interstitial macrophages⁶⁰. In addition, in experimental DN, blockade of c-fms, the receptor for colony stimulating factor-1, and the major cytokine known to promote local macrophage proliferation, prevented the progression and development of the disease^{61,62}.

1.3 Chemokines and chemokine receptors

1.3.1 Chemokines

Chemokines constitute a large family of small, secreted and structurally related proteins that are mainly involved in leukocyte attraction⁶³. Like cytokines, chemokines have other activities, including regulation of angiogenesis, fibrosis, proliferation, and apoptosis⁶⁴⁻⁶⁶. Almost all cell types have the ability to produce these proteins whose molecular weight is in the range between 8 and 10 kDa. To date, approximately 50 chemokines have been discovered⁶⁶ (Table 3).

Chemokines are classified on the basis of number and position of the first two conserved N-terminal cysteine residues, CXC and CC, depending on whether they have an intervening amino acid (X) between them (CXC) or are adjacent (CC)^{67,68}. In addition, two other classes of chemokines have been described: lymphotactin (C or *SCYc*) and fractalkine (CX3C or *SCYd*). The former one lacks an N-terminal cysteine, while the latter exhibit three amino acids between the first two cysteines and is also the only membrane-bound chemokine attached via a mucin like stalk⁶⁹. In 2000, a nomenclature system was introduced to describe the chemokines based on the ligand (L), their receptors (R) and subgroups they belong to^{68,70,71}. Some CXC chemokines are further classified by the presence of three amino acid motif 'E-L-R' (glutamic acid-

leucine-arginine) at N-terminal of the first conserved cysteine residue. These E-L-R-CXC chemokines are the potential neutrophil chemo attractants. In contrast, the CXC chemokines that lack the E-L-R motif bind different CXC receptors on lymphocytes and inhibit angiogenesis^{64,72}.

In addition, chemokines are further divided according to their function, homeostatic and inflammatory chemokines (Table 3). Inflammatory chemokines or inducible cytokines are produced in response to acute and chronic inflammatory processes, while homeostatic chemokines are produced constitutively and usually control the homeostatic trafficking of leukocytes under steady state conditions and have so-called "housekeeping" functions, like homing and migration, haematopoiesis, immune surveillance, and adaptive immune responses^{67,70,73}. For example, consistent expression of CCL17/TARC and CCL19/MIP-3 β at high levels in thymus and lymph nodes are responsible for physiological migration of T and B lymphocytes into the lymphoid organs^{74,75}. However, some chemokines fall into both categories depending on the biological context or pathological state, called "dual function chemokines"⁷⁶. These chemokines are involved in adaptive immunity, T- lymphopoiesis, trafficking of T and B cell in small intestine, dendritic cell development, and homing to particular anatomic compartments^{77,78}.

1.3.2 Chemokine receptors

Interaction with specific receptors is a crucial determinant of the chemokines spectrum. Chemokine receptors belong to the G-protein-coupled receptor (GPCR) serpentine super family and contain extra, intra and cytoplasmic domains^{79,80}. As with any G-protein-mediated activation cascade, the external interface contributes to the specificity of ligand recognition, which triggers the exchange of GDP for GTP on the α -Subunit of the G-protein. This G-protein, then dissociates from the receptor and binds to the effector molecules which then activate the signaling cascade in the cytoplasmic loop of the effector cell. This process ultimately leads to cell mobilization and activation^{80,81}. In addition, chemokine receptors with structural features that are inconsistent with a signalling function have also been described. These receptors are called "silent or non-signalling receptors" which do not signal via the typical G-protein-mediated pathways, but regulate inflammatory and immune reactions in several ways, including by acting as decoy receptors and scavenger receptors^{66,82,83}. To date, more than 20 chemokine receptors have been molecularly defined (Table 3).

Table 3: List of chemokines and chemokine receptors

Nomenclature	Old name	Receptor
<u>Proinflammatory chemokines</u>		
<u>CC family</u>		
CCL1	I-309	CCR8
CCL2	CCL2	CCR2
CCL3	MIP1 α S	CCR1, CCR4
CCL3L1	MIP1 α P	CCR1, CCR5
CCL4	MIP1 β	CCR5
CCL5	RANTES	CCR1, CCR3, CCR5
CCL7	MCP3	CCR1, CCR2, CCR3
CCL8	MCP2	CCR2, CCR5
CCL11	Eotaxin	CCR3
CCL13	MCP4	CCR1, CCR2
CCL23	MPIF-1	CCR1
CCL24	Eotaxin-2	CCR3
CCL26	Eotaxin-3	CCR3
CCL28	MEC	CCR10
<u>CXC family</u>		
CXCL1	GRO- α	CXCR2
CXCL2	GRO- β	CXCR2
CXCL3	GRO- γ	CXCR2
CXCL5	ENA-78	CXCR2
CXCL6	GCP-2	CXCR1, CXCR2
CXCL7	NAP-2	CXCR1, CXCR2
CXCL8	IL-8	CXCR1, CXCR2
CXCL9	MIG	CXCR3A, CXCR3B
CXCL10	IP-10	CXCR3A, CXCR3B
CXCL11	ITAC	CXCR3A, CXCR3B, CXCR7
CXCL14	BRAK, BMAC, MIP-2 γ	Unknown
CXCL16		CXCR6
CX ₃ CL1	Fractalkine	CX ₃ CR1
<u>Mixed function chemokine and receptors</u>		
<u>CC family</u>		
CCL17	TARC	CCR4
CCL20	MIP3 α	CCR6
CCL21	SLC	CCR7
CCL22	MDC	CCR4
<u>X-C family</u>		
XCL1	Lymphotactin	XCR1
XCL2	SCM1 β	XCR1

Nomenclature	Old name	Receptor
<u>Homeostatic chemokine and receptors</u>		
<u>CC family</u>		
CCL14	HCC-1	CCR1
CCL15	HCC-2	CCR1, CCR3
CCL16	HCC-4	CCR1, CCR3
CCL18	PARC	PITPNM3
(Jingqi Chen <i>et. al.</i> 2011)		
CCL19	ELC	CCR7
CCL25	TECK	CCR9
CCL27	CTACK	CCR10
<u>CXC family</u>		
CXCL4	PF4	CXCR3B
CXCL12	CXCL12 α/β	CXCR4, CXCR7
CXCL13	BCA-1	CXCR5
<u>Silent chemokine receptors</u>		
Receptor	Ligand	
CCX CKR	CCL19, 21, 25	
DARC	CCL1, 2, 5, 7, 8, 11, 13, 14, 16, 17, 18 CXCL1, 35, 6, 8	
D6	CCL2, 3, 4, 5, 7, 8, 11, 12, 13, 14, 17, 22, 23, 24	
CCRL2	CCL19	

Chemokines and chemotaxis

The immune system has adapted to respond to any foreign antigen and/or tissue damage, and other physiological insults⁸⁴. This ability is greatly depending on chemokine networks to recruit specific leukocytes to the right place by process called, chemotaxis, which involves three steps: rolling, adhesion and transmigration^{85,86} (Figure 4).

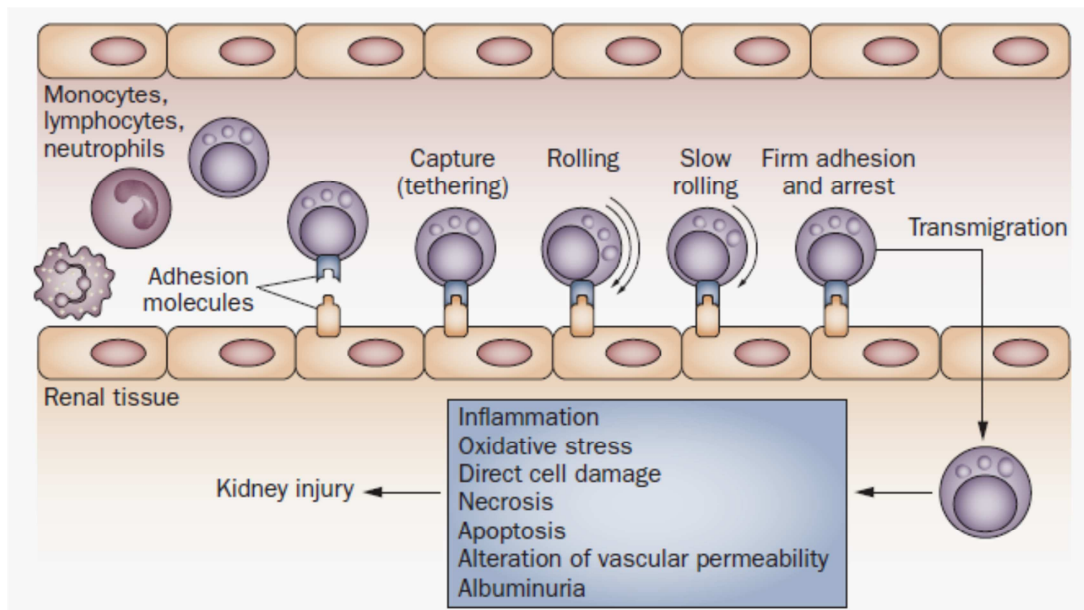


Figure 4: The mechanism of chemotaxis. Adapted from J.F. Navarro *et. al.* 2011²⁰

E-selectin, ICAM-1 and vascular cell adhesion molecule-1 (VCAM-1) are cell adhesion molecules that actively control the transmigration of leukocytes into renal tissue via the adhesion cascade⁸⁷. First step is "rolling" of leukocytes through the capillary endothelium. This transient process involves the selectins on the endothelium which interact with mucin receptors on the leukocytes via labile interactions causing a rolling behaviour of the leukocyte along the cell surface and this allows the firm adhesion of leukocytes to the endothelium^{86,88}. Chemokines secreted in response to pro-inflammatory signals, are thought to bind GAGs on endothelial cell surface as a mechanism for retention at the inflammatory site⁸⁹. This adhesion is an irreversible process required for the subsequent trans-endothelial extravagation of the cells from the blood into tissue along chemokine gradients^{90,91}. This process is called "haptotaxis"⁹². Once the activated leukocyte reaches the site of tissue damage, it produces more effective chemokines and cytokines locally and thus exacerbates tissue damage⁷⁶.

Function of chemokines

In addition to chemotaxis, chemokines have other effects including, changes in cell shape, extension of lamellipodia through cytoskeletal restructuring, release of oxygen radicals, and cytotoxic proteins from neutrophils, basophils, and eosinophils. Besides these pro-inflammatory effects, chemokines have also attributed to other

growth promoting functions. For example, the CXC family chemokines are identified as growth factors^{93,94}. The chemokine growth-related oncogene- α (GRO- α) was originally identified as an autocrine growth factor for melanoma cells⁹⁵. IL-8 and epithelial cell-derived neutrophil attractant-78 (ENA-78) have shown to be angiogenic^{96,97}, while platelet factor-4 (PF-4), interferon (IFN)-inducible protein (IP-10), monokine induced by interferon- γ (MIG), stromal cell-derived factor-1 (SDF-1), and IFN-inducible T-cell alpha chemoattractant (I-TAC)/CXCL11 act as angiostatic factors⁹⁸⁻¹⁰¹. Chemokine RANTES (regulated upon activation, normal T cell expressed and secreted) can induce eosinophil and basophil degranulation¹⁰². To summarize, the expression of chemokines helps in determining the micro-vascularization within the tissue during embryogenesis, wound healing, tumor growth and chronic inflammation.

1.3.3 Role of chemokines and chemokine receptors in chronic kidney disease

Chemo-attraction is an essential component of the host defence mechanism to attract leukocytes to sites of inflammation and infection¹⁰³. Chemokines and chemokine receptors are an integral part of this process and have been implicated in the pathophysiology of many infectious and inflammatory diseases¹⁰⁴. Since inflammation is often a double-edged sword, this robust protective response can sometimes be deleterious in many inflammatory diseases characterized by recruitment of inflammatory cells into tissues including DN, resulting in organ dysfunction^{20,62}. Since MCP-1 (monocyte chemo-attractant protein-1) or CCL2 and CXCL12 are amongst the chemokines of interest, I would like to elaborately discuss these molecules and their role in DN.

1.3.4 CCL2/MCP-1

CCL2 is the first discovered and most extensively studied chemokine¹⁰⁵. It belongs to CC-class chemokine family that exhibits its most potent chemo-tactic activity towards monocytes-macrophage (M/M \emptyset) lineage and promotes their transmigration into various tissues¹⁰⁶. It is expressed by various cells in the kidney, including M/M \emptyset , mesangial cells, podocytes, and tubular cells¹⁰⁷⁻¹¹¹. Recent studies in experimental glomerulonephritis model have demonstrated that CCL2/CCR2 system plays an important role in the pathogenesis of crescent formation and progressive tubulo-interstitial lesions via M/M \emptyset recruitment¹¹². There are numerous evidences

suggesting the role of this chemokine in kidney diseases of various etiologies. For example, unilateral ureteral obstruction in rats increased the urinary CCL2 levels which are correlated with the degree of obstruction¹¹³. The presence of collagen types III and IV deposits in mesangial region and interstitial infiltration of M/MØ in experimental obstructive uropathy model indicate the role of CCL2 in the pathophysiology of kidney diseases¹¹⁴. It is also postulated that the degree of albuminuria is proportional to the active tubular chemokine expression in the proximal tubules¹¹⁵.

Role of CCL2/MCP-1 in diabetic nephropathy

Almost all components of the diabetic milieu induce the over expression of CCL2 in renal cells. Previous studies have demonstrated the role of CCL2 and its receptor CCR2 in the pathogenesis of DN. In patients with T2 DN, increased urinary excretion of CCL2 was correlated with CD68- positive infiltrated macrophages in the interstitium⁶⁰. In addition, increased urinary CCL2 excretion was positively correlated with N-acetyl- β -D-glucosaminidase (NAG) excretion, a marker of tubular injury, implicating the role of CCL2 in tubulointerstitial damage¹¹⁶. This was evident by immuno-histochemical analysis and *in situ* hybridization, where a strong up regulation of CCL2 expression was found in tubular cells. It has also been shown that type 1 diabetics with micro-albuminuria have increased plasma levels of CCL2¹¹⁷. Targeted deletion or inhibition of CCL2 in T1 or T2 diabetic mice prevented the glomerulosclerosis by blocking macrophage recruitment to the glomeruli^{118,119}. In another study, administration of anti-CCL2 antibodies protected the kidney from glomerular sclerosis and interstitial fibrosis¹²⁰. Hemodynamic factors and renin angiotensin system (RAS) are also shown to induce CCL2 in the kidney^{121,122}. Inhibition of angiotensin converting enzyme (ACE) or the mineralo-corticoid receptor also suppressed renal CCL2 production and improved the renal function in patients with T1D and T2D¹²³⁻¹²⁵.

Numerous *in vitro* studies also revealed the role of CCL2 in diabetic kidney disease. High glucose treatment on endothelial cells isolated from diabetic subjects resulted in an increase of CCL2 release¹²⁶. Several recent studies have also demonstrated that the cultured podocytes express CCR2 and thus, with exogenous CCL2 treatment, they reorganize their actin cytoskeleton and show increased motility, suggesting the direct effects of CCL2 on the glomerular cells¹²⁷. *In vivo*, these signalling

changes translate into foot process effacement and podocytopenia^{20,128}. In addition, CCL2 targets the slit diaphragm and induces the down regulation of nephrin via Rho-kinase-dependent mechanisms¹²⁹.

Furthermore, studies have convincingly demonstrated the role of CCL2 in the development of DN. For example, in *Lepr*^{db/db} mice and in streptozotocin (STZ) induced DN, CCL2 deficiency reduced renal monocyte and/or macrophage accumulation and abrogated the progression of diabetic renal injury^{118,119}. Previous studies from our lab have documented that, in uninephrectomized db/db mice with T2D, blockade of CCL2 with mNOX-E36 spiegelmer prevented the diabetic glomerulosclerosis and restored the GFR by inhibiting glomerular macrophage recruitment in late-stage of DN¹³⁰. This study represents the CCL2 as promising therapeutic target in DN.

Collectively, the pro-inflammatory chemokine, CCL2 promotes tissue inflammation and remodelling by recruiting and activating immune cells in DN.

1.3.5 CXCL12/SDF-1

The first identified lymphocyte homing chemokine, CXCL12, chemokine (C-X-C motif) ligand 12, also known as stromal cell-derived factor-1 alpha (CXCL12 α), is a unique homeostatic chemokine that signals through CXCR4 and CXCR7 (also known as RDC-1), but, with greater affinity to CXCR7^{131,132}. CXCL12 was originally isolated as a pre-B-cell growth-stimulating factor¹³³ and subsequently shown to regulate trans-endothelial migration, proliferation and differentiation of hematopoietic cells¹³⁴. Moreover, it is important for the regulation of homeostatic trafficking and distribution of cells in the different compartments and sub-compartments of the immune system¹³⁵⁻¹³⁷.

CXCL12 exhibits pro-inflammatory activities by recruiting immune cells to inflamed tissues in autoimmune diseases such as rheumatoid arthritis (RA), nephritis, or murine lupus erythematosus¹³⁸⁻¹⁴⁰. On the other hand, CXCL12 also exhibits anti-inflammatory activities by augmenting antigen-specific T cell response^{141,142}; suggesting that CXCL12 acts as a double edged sword in mediating the inflammation.

Furthermore, studies have shown that CXCL12/CXCR4 axis plays a key role in tissue repair and regeneration in a number of disease models like pancreatic beta cell loss in T1D¹⁴³, endovascular injury¹⁴⁴, and ischemic acute renal failure¹⁴⁵. For example, CXCL12 plays a protective role in renal pathogenesis by mediating tubular

epithelial cells (TECs) protection (by preventing TECs apoptosis) against ischemia-reperfusion injury¹⁴⁶, suggesting its role in tissue repair. In ischemic myocardium, CXCL12 executes a tissue protective and tissue regenerative function by decreasing the apoptosis and up-regulation of vascular endothelial growth factor (VEGF). The study by Yoshitsugu *et.al.* reported the key role of CXCL12/CXCR4 axis in the development of renal vasculature during embryogenesis, where CXCL12-secreting stromal cells surround CXCR4-positive epithelial components of early nephrons and blood vessels in the embryonic kidney¹⁴⁷. In glomeruli, the CXCL12-secreting podocytes were found in close proximity to CXCR4 positive endothelial cells, demonstrating the role of CXCL12 in kidney development^{147,148}. In addition, CXCL12 or CXCR4 KO embryos display defects in vascularization of the gastrointestinal tract, demonstrating the organ-specific essential functions of CXCL12/CXCR4 in blood vessel formation^{149,150}.

The role of CXCL12 is not restricted to tissue repair and regeneration. Various studies demonstrate that the CXCL12 plays a key role in auto-immune diseases¹⁵¹. In lupus-like immune complex glomerulonephritis in NZB/NZW mice, CXCL12 blockade prevented the glomerulonephritis which was attributed to less autoantibody production and T cell recruitment to glomeruli, indicating its potential in ameliorating lupus nephritis¹⁴⁰.

In addition, CXCL12 promotes tumor metastasis in various organs expressing increased CXCL12 levels, including lymph nodes, lung, liver, and bone marrow; and also in lower expressing organs including small intestine, kidney, skin, brain, and skeletal muscle¹⁵². CXCL12 signaling also supports tumor growth either by promoting cancer cell survival or by promoting angiogenesis¹⁵³. Recent studies have shown that inhibition of CXCL12 and CXCR4 decreased endothelial activation and organ injury and improved animal survival in shiga toxin induced renal injury where CXCR7/CXCR4/CXCL12 pathway plays a key role in the pathogenesis of uremic syndrome in human and mice¹⁵⁴. It has been shown that, transgenic mice over expressing CXCR4 selectively in podocytes, caused proteinuria and glomerular crescent formation¹⁴⁸. It is also evidenced by Balabanian *et.al.* that, glomerulonephritis was prevented by blocking CXCL12, and this activity was attributed to less podocyte proliferation and T-cell recruitment¹⁴⁰. These studies suggest that CXCL12 creates a microenvironment for the homing of other cells including progenitor cells during repair and hence contributes to tissue regeneration.

Role of CXCL12 in diabetic nephropathy

So far little is known about the role of CXCL12 in DN. By its name, “homeostatic” chemokines, CXCL12 display functions that are independent of tissue inflammation. Homeostatic chemokines are rather constitutively expressed, as they contribute to the physiological homing and migration of immune cells in bone marrow or lymphoid organs. For example, recent work from our laboratory has shown that, CXCL12 is constitutively expressed by podocytes and CXCL12 blockade with NOX-A12 spiegelmer prevented diabetic glomerulosclerosis in a way that was independent of glomerular macrophage recruitment. CXCL12 blockade was shown to have a profound effect on podocyte count and proteinuria¹⁵⁵. However, the mechanism underlying the protective effect of CXCL12 blockade on DN remained unclear. In addition, there was no increase in bone marrow-derived progenitor cells in kidneys of treated db/db mice observed. Thus, this enhancer effect on the capacity of intra-glomerular progenitors to restore podocytes in DN is suspected and hence should be studied further.

1.4 Cathepsins

The lysosomal/endosomal compartments are rich in proteases involved in degradation of proteins. The human genome encodes more than 600 proteases which are involved in various physiological functions including complement activation, signal transduction, intracellular house keeping and degradation of intra and extra cellular matrix proteins¹⁵⁶. Cathepsins (Cats) are a class of globular proteases which are predominantly distributed in the lysosomal compartments involved in protein turnover¹⁵⁷. The term “Cathepsin (Cat)” was derived from the Greek word, *kata-* “down” and *hepsein* “boil”, meaning “digest”. Normally Cats are located in lysosomes of the cells, but also reside in other compartments, such as phagosomes, and endosomes and they can be secreted in certain pathological conditions. Studies revealed that secreted forms of Cats are critical for degradation of the extracellular matrix during inflammatory or adaptive response¹⁵⁶. Based on the mechanism of catalysis and structure, Cats are classified into three groups: cysteine, serine and aspartic Cats (Table 4).

Table 4: Classification of cathepsins and their tissue distribution

Family	Group	Organs showing the most expression
<u>Cysteine cathepsins</u>		
CCs expressed ubiquitously	Cathepsin B	Liver, thyroid gland, kidney, spleen
	Cathepsin F	Heart, skeletal muscle, brain, testis, ovary, macrophages
	Cathepsin H	Liver, kidney, spleen
	Cathepsin L	Liver, thyroid gland, kidney
	Cathepsin O	Liver, kidney, placenta, ovary
	Cathepsin X	Liver, lung, kidney, placenta
	Cathepsin C	Kidney, placenta, lung, spleen, cytotoxic T lymphocytes
CCs expressed in limited tissues	Cathepsin S	Spleen, lymph nodes, antigen presenting cells, heart, cornea, testis, thymus
	Cathepsin K	Osteoclasts, macrophages, epithelial cells of gastrointestinal, respiratory and urinary tract of human embryo and fetus, adult human lung
	Cathepsin V	Cornea, testis, thymus
	Cathepsin W	Spleen, lymph nodes
<u>Serine cathepsins</u>	Cathepsin A	Testis, epididymis
	Cathepsin G	Human cerebral cortex, intervertebral discs
<u>Aspartic cathepsins</u>	Cathepsin E	Surface of epithelial mucus-producing cells of the stomach
	Cathepsin D	Retina, human epithelial breast cancer cells

Adapted and modified from Ki Young Choi, et.al 2012 and Berdowska, 2004^{158,159}

1.4.1 Cysteine cathepsins

The cysteine cathepsins (CCs) are predominantly endopeptidases, and are located intracellularly in endolysosomal vesicles. The majority of Cats fall into this category which consists of 11 Cats in humans and 10 of their counterparts in mice. In addition, eight additional Cats have been identified which are expressed only in the placenta of mice¹⁶⁰ (Table 4). Cats activity is regulated intracellularly by stefins (stefin A and B) and extracellularly by cystatins (cystatin C) and kininogens¹⁶¹. CCs represent the major types of proteases abundantly found in mammals as well as in microorganisms (bacteria and virus)¹⁶². They are expressed throughout different types

of tissues and cells. Cats B, C, F, H, L, O, and Z are expressed constitutively and are thought to have housekeeping functions¹⁵⁷, whereas, the expression of some CCs is regulated and is noticeably high in specific cell types. For example, Cat K is mainly found in osteoclasts¹⁶³, Cat W is expressed only in cytotoxic cells, in particular NK cells^{164,165}, while Cat V is expressed only in humans and absent in mice¹⁶⁶. Moreover, Cat S is selectively expressed in antigen presenting cells such as B-cells, macrophages and dendritic cells. However, it has been shown that the expression levels of Cats may alter in many patho-physiological conditions. It is well documented that CCs are over expressed in many cancers, cardiovascular and auto-immune diseases^{167,168}.

1.4.2 Pathophysiological role of cysteine cathepsins

CCs participate in various physiological systems and are upregulated in many inflammatory disorders. Due to their increased expression and activity, CCs serve as candidate disease markers in many diseases including rheumatoid arthritis, multiple sclerosis, atherosclerosis and various cancers. It has been shown that Cats D, F, L, S and V are important participants in antigen processing and presentation, while Cats K, L and S play a key role in the development of atherosclerosis^{167,169,170}. Moreover, the novel insights into CCs function in many human diseases have been gained by the generation of knockout and transgenic mice. Studies in mice deficient for Cat K or Cat S have confirmed a role of Cat K in bone remodelling and Cat S in MHC II presentation respectively¹⁷¹. In addition, Cat L-deficiency has been shown to cause development of myocardial fibrosis and phenotypes in skin, while Cat B-deficient mice exhibit reduced TNF-induced apoptosis of hepatocytes¹⁷⁰. On the other hand, Cat S and B have been shown to be involved in the clearance of immune complexes and thereby protect the mice from neuronal death. Mice deficient in both Cat S and B exhibited reduced degradation of immune complexes and thereby inducing apoptosis of cerebral neurons, resulting in death¹⁷². In addition, these two Cats are also shown to be involved in tumour angiogenesis¹⁶⁷. It is well documented that Cat B is involved in regulation of innate immunity via activation of inflammasomes¹⁷³. Moreover, Cats B, H, K, L, and S are involved in other inflammatory conditions such as silicosis and sarcoidosis characterized by ECM degradation, suggesting the role of Cats in disease pathogenesis¹⁷⁰. More recent studies have demonstrated that CCs play an important role in the development of renal diseases¹⁷⁴.

1.4.3 Role of cysteine cathepsins in proteinuric kidney diseases

In 1994, Shechter *et.al.* published that, in STZ induced rats, the development of diabetic renal hypertrophy with increased renal protein content was correlated with decreased activity of Cats B and L in kidneys¹⁷⁵. In another study, the altered expression of Cats B, L and H in tubules of rats with polycystic kidney disease has also been demonstrated¹⁷⁶. These two studies described that, the expression pattern of Cats varies at different stages of the disease for different Cats. But, until recently, the exact role of Cats in the kidney has not been well studied. In 2004, Reiser *et.al.* demonstrated that, Cat L is involved in the pathogenesis of podocyte foot process effacement (migration and detachment from GBM) which leads to proteinuria¹⁷⁷. Later in 2007, Sanja *et.al.* demonstrated the direct role of Cat L in the development of proteinuric kidney diseases¹⁷⁴. The authors demonstrated that dynamin is normally required to maintain the ultra-filtration barrier in kidneys, possibly via regulation of the actin cytoskeleton in podocytes. In LPS or puromycin amino nucleoside induced nephropathy, the induction of Cat L expression in podocytes cleaves the dynamin at an evolutionary conserved site, resulting in reorganization of the podocyte actin cytoskeleton, leading to podocytes loss and proteinuria¹⁷⁴. In addition, various cytokines induce the up regulation of CCs *in vitro* and *in vivo*. It has been noticed that cytokines IL-4 and IL-13 induce the up-regulation of Cat L in glomerular epithelial cells¹⁷⁸.

Recent studies revealed that Cat L serves as a potential and sensitive biomarker to assess the degree of kidney injury (gender specific) and management of chronic kidney disease¹⁷⁹. On the other hand, immunostaining on bovine kidneys revealed that Cat S is localized in proximal tubules¹⁸⁰. Further, studies in mice and humans have confirmed that, elevated levels of Cats S, L and B in plasma are associated with worsening of diabetes¹⁸¹.

1.4.4 Cathepsin S

Cat S, a major catalytic papain cysteine protease which is predominately present in the spleen, lymph nodes, and all antigen presenting cells, such as monocytes, macrophages, B cells and dendritic cells where it plays a pivotal role in antigen presentation¹⁷⁰. Unlike other proteases, Cat S shows its proteolytic activity both at neutral and slightly basic pH and can function both inside and outside the lysosomes¹⁸². Its activity is tightly regulated by its endogenous inhibitor cystatin C¹⁸³. Cat S activity is

reported to be involved in the pathophysiology of many inflammatory and auto immune diseases, including rheumatoid arthritis, osteoporosis, atherosclerosis and cancers. Indeed, recent studies indicate that increased serum levels of Cat S are associated with increased mortality risk in patients with cardiovascular and renal disease, cancer, obesity and diabetes¹⁸⁴⁻¹⁸⁶. In addition, Cat S inhibition in various inflammatory mouse models showed promising protective effects suggesting that, Cat S can be a potent therapeutic target for autoimmune and inflammatory disorders^{187,188}.

It was shown that macrophages express high levels of active Cat S, which contribute to extensive ECM remodelling. For example, Cat S deficiency or small molecule inhibitors reduced the atherosclerotic plaques by reducing the macrophage infiltration and accumulation, suggesting that Cat S plays an important role in leukocyte migration^{169,189}. Recent studies have demonstrated that angiotensin II was found to stimulate the mRNA expression of Cat S in smooth muscle cells and modulated the inflammation and apoptosis in atherosclerosis¹⁹⁰. Various factors and cytokines are known to induce Cat S in many other cell types including adipocytes, endothelial cells and smooth muscle cells. For example, various proinflammatory cytokines including TNF- α and IFN- γ are potent inducers of Cat S in endothelial cells and play a role in the degradation of extracellular elements such as laminin and collagens^{186,189}.

Apart from its potent proteolytic activity and mediating the inflammation, recent studies have shown that Cat S is differentially expressed during kidney and fetal lung development¹⁹¹. In contrast, Cat S activity has also been proposed to play a part in the development of cancer by tumor angiogenesis¹⁹². DNA microarray analysis revealed that in Ochatoxin A (OTA) nephropathy, proximal tubule cells (PTC) expressed high levels of Cat S, indicating the role of Cat S in the development of kidney diseases¹⁹³.

1.5 Animal models of diabetic nephropathy

Ideal animal models which provide an experimental system of unparalleled flexibility are very essential for studying any mammalian diseases. The advantage of using mouse model attributes to their fully studied genome, the lower maintenance, cost effectiveness, and short reproductive cycles. The use of experimental models of DN has provided valuable information regarding many aspects of DN, including pathophysiology, progression, and new therapeutic strategies¹⁹⁴.

According to “The Animal Models of Diabetic Complications Consortium” (AMDCC), any mouse models used to study human diabetes and diabetic complications should meet the minimum criteria and exhibit >50% decline in GFR over the lifetime of the animal, >10-fold increase in albuminuria compared with controls for that strain at the same age and gender, and pathology of kidneys (advanced mesangial matrix expansion, \pm nodular sclerosis mesangiolysis, any degree of arteriolar hyalinosis, glomerular basement membrane thickening by >50% over baseline and tubulointerstitial fibrosis)¹⁹⁵.

In recent years, there were several genetic mouse models of diabetes (Table 5) established and the best characterized model is *LepR*^{db/db} type 2 diabetic mice. The db/db mouse is the most widely used mouse model of T2D. First described in 1966 in Jackson laboratories, the *db* gene encodes a G-to-T point mutation of the leptin receptor, which is transmitted in an autosomal recessive fashion. This leptin receptor mutation (*LepR*^{db/db}) results in abnormal splicing and a defective receptor for the adipocyte-derived hormone leptin which is altered in the hypothalamus. Due to this fact, these mice do not feel a sense of satiety due to hyperphagia and develop obesity with high leptin levels and hyper-insulinemia. Kidney function in these mice on the C57BL/KS background has been intensively investigated and exhibits some features similar to early human DN, class I to III. DN in the C57BL/KsJ (db/db) mouse is initially expressed as increased urinary albumin excretion at the age of 8 weeks without evidence of glomerular lesions by light microscopy. After 16 week of age, there is a very consistent three fold increase in mesangial matrix expansion and at about 6 month of life, signs of diabetic kidney damage are visible. The animals show an increasing necrosis and tubular dilatation, tubular atrophy, interstitial fibrosis and leukocyte infiltrates.

Table 5: List of mouse models studied for diabetic nephropathy

Animal model	Strains reported	Diabetic type
Streptozotocin	C57BL/6J, C57BLKS, Balb/c, ICR, DBA2, ROP	Type I
Encephalomyocarditis- -virus D variant	DBA, Balb/c	Type I
Ins2 Akita	C57BL/6, C3H	Type I
NOD	Inbred line derived from ICR (out bred line)	Type I
db/db	C57BL/6, C57BLKS, DBA, FVB, CBA	Type II
ob/ob	C57BL/6, DBA2, FVB/N	Type II
Agouti (Ay)	KK, C57BL/6 C3H, FVB	Type II
High-fat diet	C57BL/6 is a main -susceptible strain	Type II
db/db eNOS -/-	BKS	Type II
NONcNZO10/LtJ	NON/LtJ+NZO/HILt	Type II
BTBR ^{ob/ob}	BTBR	Type II
GIPR ^{dn} transgenic	CD1	Type II
GLUT1 transgenic	C57BL/6J	Non-diabetic -transgenic mice
podIR -/- (podocin or - nephrin promoter) FVB)	Mixed genetic background- (C57BL/6, 129/SV and FVB)	

1.6 Spiegelmers-next generation Aptamers

To achieve CCL2 and CXCL12 antagonism, we used RNA-aptamers (Spiegelmer), a patented technology of NOXXON Pharma (Berlin). RNA-aptamer binds to the active site of target chemokines and makes them biologically non-functional.

An aptamer is a nucleic acid structure that can bind to a target molecule conceptually similar to an antibody that recognizes an antigen. Aptamers have binding characteristics similar to peptides or antibodies, with affinities in the low nanomolar to the picomolar range. However, there are several drawbacks to aptamers as useful therapeutic products. As relatively small molecules, aptamers demonstrate circulating half-lives *in vivo* in the order of minutes. This situation can be addressed by attaching large inert molecules to aptamers (e.g. polyethylene glycol) to reduce their elimination via the kidney and hence increase their presence in the circulation. Nevertheless, aptamers, as natural nucleic acid polymers, are prone to rapid degradation by nucleases that are present in all tissues in the body.

Spiegelmers are bio-stable aptamers, have all the diverse characteristics of aptamers but possess a structure that prevents enzymatic degradation. While aptamers are created from the natural D-nucleotides, which are recognized by the nucleic acid degrading enzymes, Spiegelmers are synthesized as the mirror image L-oligonucleotide and are not degraded by any nucleases since there are no such enzymes in the body capable of interacting with these unnatural molecules¹⁹⁶. Spiegelmer technology is based on the simple concept that if an aptamer binds its natural target, the mirror image of the aptamer will identically bind the mirror image of the natural target (Figure 5). The process of aptamer selection is carried out against the mirror image target protein; an aptamer against this unnatural mirror image is obtained. More important, this Spiegelmer is now resistant to nuclease degradation. Spiegelmers should not be confused with antisense RNAs as in that, they do not directly interfere with transcription or translation of their target molecules¹⁹⁶. They are designed to bind specifically to extracellular proteins, either a receptor or its ligand, similar to the behaviour of a monoclonal antibody, aptamer or peptide. Spiegelmers appear to be non-immunogenic, even under the most inductive conditions for antibody formation in rabbits. These molecules are termed “Spiegelmer” from the German word “Spiegel” meaning “mirror”.

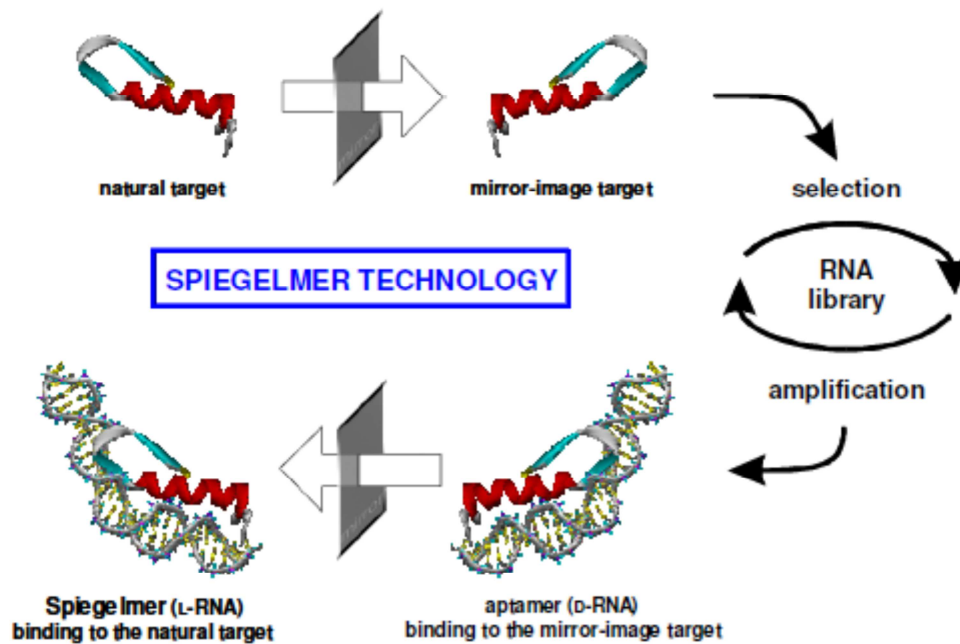


Figure 5: Representation of Spiegelmer generation. L-enantiomer of the target is processed to get the selective binding D-aptamer. Highly selective D-aptamer for mirror image (L-target) is then amplified and then mirrored to get L-aptamer which has the selective binding property for natural D-target. (Taken from www.noxxon.net)

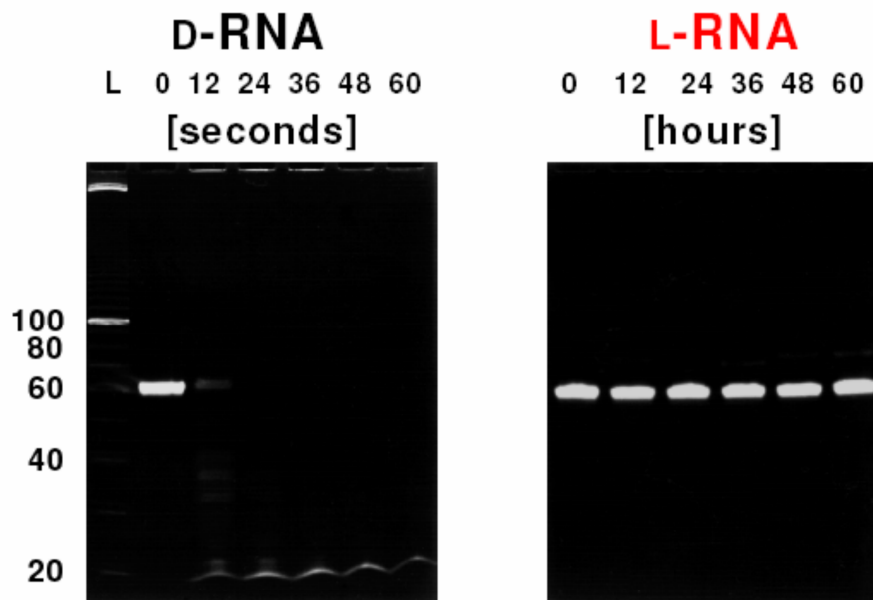


Figure 6: Representation of Spiegelmer stability. Left panel with D-enantiomeric RNA which degrades in seconds when incubated in human plasma at 37°C., while L-enantiomeric RNA is stable even at 60 h of incubation in human plasma (right panel) (Taken from www.noxxon.net)

Summary of Spiegelmer properties

- High binding specificity to their target
- Comparable binding affinity as antibodies (low nanomolar-picomolar)
- Stable in human plasma and after injection into animals
- Non-immunogenic
- Low toxicity (target-based)
- Synthesized using standard chemistry (scalable)
- No biological contaminants
- Easy to formulate (polar) with excellent solubility

2. Research hypothesis

Targeting chemokines

Previous work from our laboratory has shown that CCL2/MCP-1 and CXCL12/SDF-1 both contribute to glomerulosclerosis in mice with T2DM through different mechanisms. CCL2 mediates macrophage-related inflammation, whereas CXCL12 contributes to podocyte loss. Inhibition of CCL2 by mNOX-E36 showed the protection from diabetic glomerulosclerosis and restored the GFR by preventing glomerular macrophage recruitment. Thus, CCL2 blockade prevents the progression of DN by interfering with macrophage-driven glomerular inflammation. Inhibition of CXCL12 by NOX-A12 significantly reduced the degree of glomerulosclerosis, increased the number of podocytes, prevented the onset of albuminuria and maintained the peritubular vasculature without affecting glomerular macrophage infiltration. Nevertheless, the mechanism underlying the protective effect of CXCL12 blockade on DN remains unclear. Therefore, the aim of the study was to evaluate the effect of dual blockade of both chemokines on the progression of DN. We hypothesized that dual blockade of both chemokines; compared to monotherapies of either CCL2 or CXCL12 antagonists, might have beneficial effects in an accelerated mouse model of DN.

Targeting cathepsins

Cat S is a member of cysteine protease family involved in pathogenesis of various inflammatory and auto-immune diseases. Various pro-inflammatory cytokines upregulate the Cat S expression in various cells, especially in macrophages and promote their infiltration to the inflamed tissue. In addition, Cat S is also known to degrade the extracellular matrix in various compartments and promote vascular remodelling. Previous studies with inhibitors for Cats other than Cat S confirmed their role in the progression of kidney diseases, but, so far, the role of Cat S in DN has not been explored. Cat S inhibition was immunosuppressive in several models of autoimmune diseases, implicating its use as a potential target to treat autoimmune and inflammatory diseases. Since inflammation and vascular damage are the major mediators in the progression and development of DN, we hypothesized that Cat S inhibition might be protective in progressive DN.

3. Material and methods

3.1 Materials

Instruments and chemicals

Instruments

Anaesthesia

Isoflurane anaesthesia chamber Harvard Anaesthesia system, UK.

Balances

Analytic balance, BP110S Sartorius, Göttingen, Germany
Mettler PJ 3000 Mettler-Toledo, Greifensee, Switzerland

Cell culture incubators

Type B5060 EC-CO₂ Heraeus Sepatech, München, Germany

Centrifuges

Heraeus, Minifuge T VWR International, Darmstadt, Germany
Heraeus, Biofuge primo Kendro Laboratory Products GmbH, Hanau, Germany
Heraeus, Sepatech Biofuge A Heraeus Sepatech, München, Germany

ELISA reader

Tecan, GENios Plus Tecan, Crailsheim, Germany

Fluorescence microscopes

Leica DC 300F Leica Microsystems, Cambridge, UK
Olympus BX50 Olympus Microscopy, Hamburg, Germany

TaqMan sequence detection system

ABI prism™ 7700 sequence detector PE Biosystems, Weiterstadt, Germany
RT-PCR Light cycler 480, Roche, Germany

Other equipment

Cryostat RM2155	Leica Microsystems, Bensheim, Germany
Cryostat CM 3000	Leica Microsystems, Bensheim, Germany
Glucometer accu check sensor	Roche, Mannheim, Germany
Homogenizer ULTRA-TURRAX T25	IKA GmbH, Staufen, Germany
Microtome HM 340E	Microm, Heidelberg, Germany
Nanodrop	PEQLAB Biotechnology GmbH, Erlangen, Germany
pH meter WTW	WTW GmbH, Weilheim, Germany
Thermomixer 5436	Eppendorf, Hamburg, Germany
Vortex Genie 2™	Bender&Hobein AG, Zurich, Switzerland
Water bath HI 1210	Leica Microsystems, Bensheim, Germany

Chemicals and reagents

RNeasy mini kit	Qiagen GmbH, Hilden, Germany
RT-PCR primers	Metabion, Martinsreid, Germany

Cell culture

DMEM-medium	Biochom KG, Berlin, Germany
Dulbecco's PBS (1X)	PAA Laboratories GmbH, Cölbe, Germany
FSC	Biochom KG, Berlin, Germany
Penicillin/streptomycin (100X)	PAA Laboratories GmbH, Cölbe, Germany
RPMI-1640 medium	GIBCO/Invitrogen, Paisley, Scotland, UK
Trypsin/EDTA (1X)	PAA Laboratories GmbH, Cölbe, Germany

Antibodies

7/4	AbD Serotec, Düsseldorf, Germany
β-Actin	Cell signalling, Danvers, MA
Cat S	R&D Systems, Minneapolis, MN, USA
CD3	BD Pharmingen, Hamburg, Germany
CD11b	BD Pharmingen, Hamburg, Germany
CD45	BD Biosciences, Mannheim, Germany
F4/80 FITC	Caltag Laboratories, Bulingame, CA, USA

Goat anti-rat HP	Dianova, Hamburg, Germany
HP linked anti-Rabbit secondary Ab	Cell signalling, Danvers, MA
Ki-67	Dako Deutschland GmbH, Hamburg, Germany
Ly6C+	BD Pharmingen, Hamburg, Germany
Ly6G	BD Pharmingen, Hamburg, Germany
Mac2	Cederlane, Ontario, Canada
Rat anti-mouse neutrophils	AbD Serotec, Düsseldorf, Germany
Rat anti-mouse CD74	BD Biosciences
WT-1	Santa Cruz Biotechnology, CA, USA

ELISA kits

Albumin	Bethyl Laboratories, TX, USA
MCP-1/CCL2	R &D Systems, Minneapolis, MN, USA
Creatinine FS	DiaSys Diagnostic System, GmbH, Holzheim, Germany
CXCL12	R &D Systems, Wiesbaden, Germany

Chemicals

Acetone	Merck, Darmstadt, Germany
Acrylamide 30%	Carl Roth GmbH, Karlsruhe, Germany
AEC substrate packing	Biogenex, San Ramon, USA
Beta-mercapto ethanol	Roth, Karlsruhe, Germany
Bovine Serum Albumin	Roche Diagnostics, Mannheim, Germany
Calcium chloride	Merck, Darmstadt, Germany
Calcium dihydrogen phosphate	Merck, Darmstadt, Germany
Calcium hydroxide	Merck, Darmstadt, Germany
DAPI	Sigma-Aldrich, Steinheim, Germany
DEPC	Fluka, Buchs, Switzerland
Diluent C for PKH26 dye	Sigma-Aldrich Chemicals, Germany
DMSO	Merck, Darmstadt, Germany
EDTA	Calbiochem, SanDiego, USA
Eosin	Sigma, Deisenhofen, Germany
Ethanol	Merck, Darmstadt, Germany

Formalin	Merck, Darmstadt, Germany
Hydroxyethyl cellulose	Sigma-Aldrich, Steinheim, Germany
HCl (5N)	Merck, Darmstadt, Germany
Inulin-FITC	Sigma-Aldrich, Steinheim, Germany
Isopropanol	Merck, Darmstadt, Germany
MACS-Buffer	Miltenyi Biotec, Bergisch Gladbach, Germany
Oxygenated water	DAKO, Hamburg, Germany
Penicillin	Sigma, Deisenhofen, Germany
Phosphate Buffer Saline (DPBS)	PAN Biotech GmbH, Germany
Roti-Aqua-Phenol	Carl Roth GmbH, Karlsruhe, Germany
Skim milk powder	Merck, Darmstadt, Germany
Sodium acetate	Merck, Darmstadt, Germany
Sodium chloride	Merck, Darmstadt, Germany
Sodium citrate	Merck, Darmstadt, Germany
Sodium dihydrogenphosphate	Merck, Darmstadt, Germany
Streptomycin	Sigma, Deisenhofen, Germany
TEMED	Santa Cruz Biotechnology, Santa Cruz, CA
Tissue freezing medium	Leica, Nussloch, Germany
Trypan Blue	Sigma, Deisenhofen, Germany
Xylol	Merck, Darmstadt, Germany
<u>Miscellaneous</u>	
Anti-FITC micro beads	Miltenyi Biotec, Germany
Cat S activity assay kit	BioVision, Inc., Milpitas, CA, USA
Cell death detection (TUNEL) kit	Roche Diagnostics, Mannheim, Germany
CellTiter 96 proliferation assay	Promega, Mannheim, Germany
Needles	BD Drogheda, Ireland
Pipette's tip 1-1000 μ L	Eppendorf, Hamburg, Germany
Plastic histo-cassettes	NeoLab, Heidelberg, Germany
Pre-separation filters	Miltenyi Biotec, Bergisch Gladbach, Germany
SuperFrost® Plus microscope slides	Menzel-Gläser, Braunschweig, Germany
Syringes	Becton Dickinson GmbH, Heidelberg, Germany

Tissue culture dishes 100x20 mm	TPP, Trasadingen, Switzerland
Tissue culture dishes 150x20 mm	TPP, Trasadingen, Switzerland
Tissue culture dishes 35x10 mm	Becton Dickinson, Franklin Lakes, NJ, USA
Tissue culture flasks 150 cm ²	TPP, Trasadingen, Switzerland
Tubes 15 and 50 mL	TPP, Trasadingen, Switzerland
Tubes 1.5 and 2 mL	TPP, Trasadingen, Switzerland

- All other reagents were of analytical grade and are commercially available from Invitrogen, SIGMA or ROTH.

3.2 Methods

3.2.1 Part I

3.2.1 Animal studies

Male diabetic C57BLKS db/db mice or non-diabetic C57BL/6 mice 5-6 week old were obtained from Taconic (Ry, Denmark) and housed in filter top cages with a 12 hrs dark/light cycle. All animals had unlimited access to food and water throughout the study duration. At the age of 6 weeks uninephrectomy (1K mice) or sham surgery (2K mice) was performed as described below. All animal experiments were approved by the local government authorities.

Animal model-Uninephrectomized db/db mice

Surgical procedure of Uninephrectomy

Uninephrectomy (1K mice) or sham surgery (2K mice) was performed under general anaesthesia using isoflurane. Anesthetized mice were positioned laterally on the operation bed. Under deep anaesthesia a flank incision of about 1-1.5 cm was made on the dorsolateral side just below the thoracic cage so as to reach kidney easily. A silk suture (2-0) was passed around the right kidney and after tying off all blood vessels and ureter the kidney was rapidly excised out using a curved scissors. In sham operated group of mice, the kidney was left *in situ*. Skin incision was closed with silk suture and wound clamps (Figure 7). All mice received analgesic (1 drop of Novaminsulfon, Ratiopharm GmbH, Germany, 1:200, orally administered) before and after surgery.

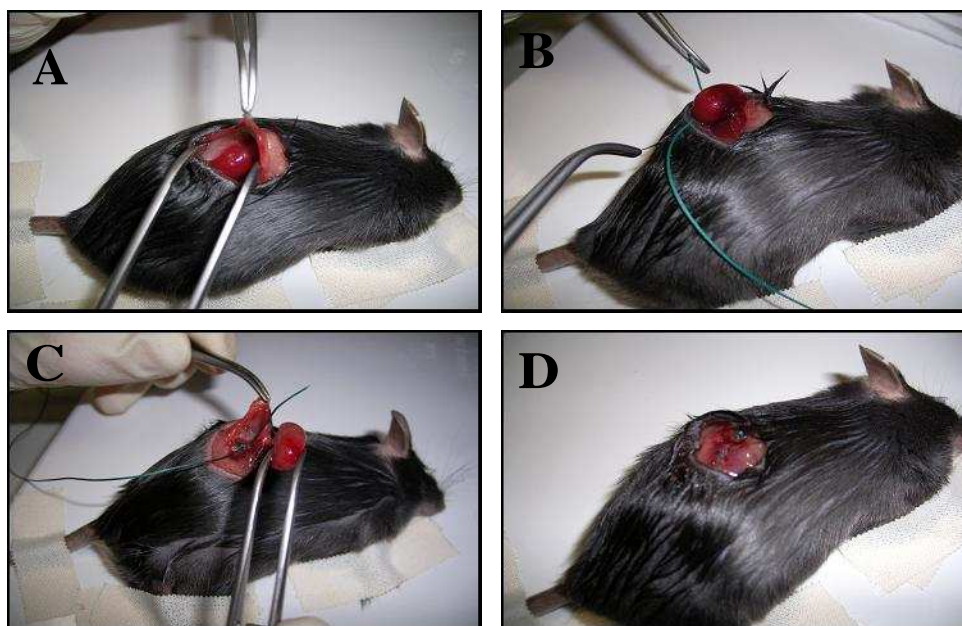


Figure 7: Schematic representation of uninephrectomy

A: Making flank incision.

B: Tying off the kidney's vessels and ureter with silk suture.

C: Excision of the kidney after ligation.

D: Wound closing with silk suture and wound clamps.

This image was kindly provided by Dr. Volha Ninichuk.

3.2.2 Route and rationale of test material administration

The chosen route of administration was subcutaneous, as the animals can tolerate a large number of subcutaneous administrations quite better than numerous intraperitoneal injections. Also, handling is easier and the compound exposure is longer in the circulation by this route.

Test substance and formulation

Spiegelmer Sequence

mNOX-E36 (CCL2 antagonist)	5' GGCGACAUUGGUUGGGCAUGAGGCGA GGCCCUUUGAUGAAUCCGCGGCCA-3'
NOX-A12 (CXCL12 antagonist)	5'-GCGUGGUGUGAUCUAGAUGUAUUGG CUGAUCCUAGUCAGGUACGC-3'
revNOX-A12 (control antagonist)	5'-GCAUGGACUGAUCCUAGUCGGUUA UUAGAUCUAGUGUGGUGCG-3'

To distinguish possible target-specific from unspecific substance class effects, a non-functional spiegelmer with the reverse sequence of NOX-A12 was used. The

Spiegelmers were modified with 40 kDa branched polyethylene glycol (PEG) at the 3'-end (mNOX-E36) or at the 5'-end (NOX-A12 and revNOX-A12). mNOX-E36 and NOX-A12 bind to CCL2 and CXCL12 respectively, with sub-nanomolar affinities. All spiegelmers were dissolved in isotonic 5% glucose solution for administration.

3.2.3 Study design

At the age of 4 months, 1K db/db mice with documented blood glucose levels >11 mmol/L and albumin/creatinine ratios >3 (ratio in age-matched wild-type mice = 0.1) were divided into four groups (n = 10-12) each of these groups received either nil (no injections) or subcutaneous injections of 50 mg/kg NOX-A12, mNOX-E36 or control Spiegelmer in 5% glucose or 5% glucose itself as a vehicle control, on every other day (Figure 8). This dose corresponds to 13.4 mg/kg NOX-A12 or 14.4 mg/kg mNOX-A36 if based on the oligonucleotide part of the molecule as anhydrous free acid. The treatment dose and injection intervals were comparable to our previous db/db mouse studies with similar formulations of Spiegelmers targeting these chemokines. Treatment was continued for 8 weeks.

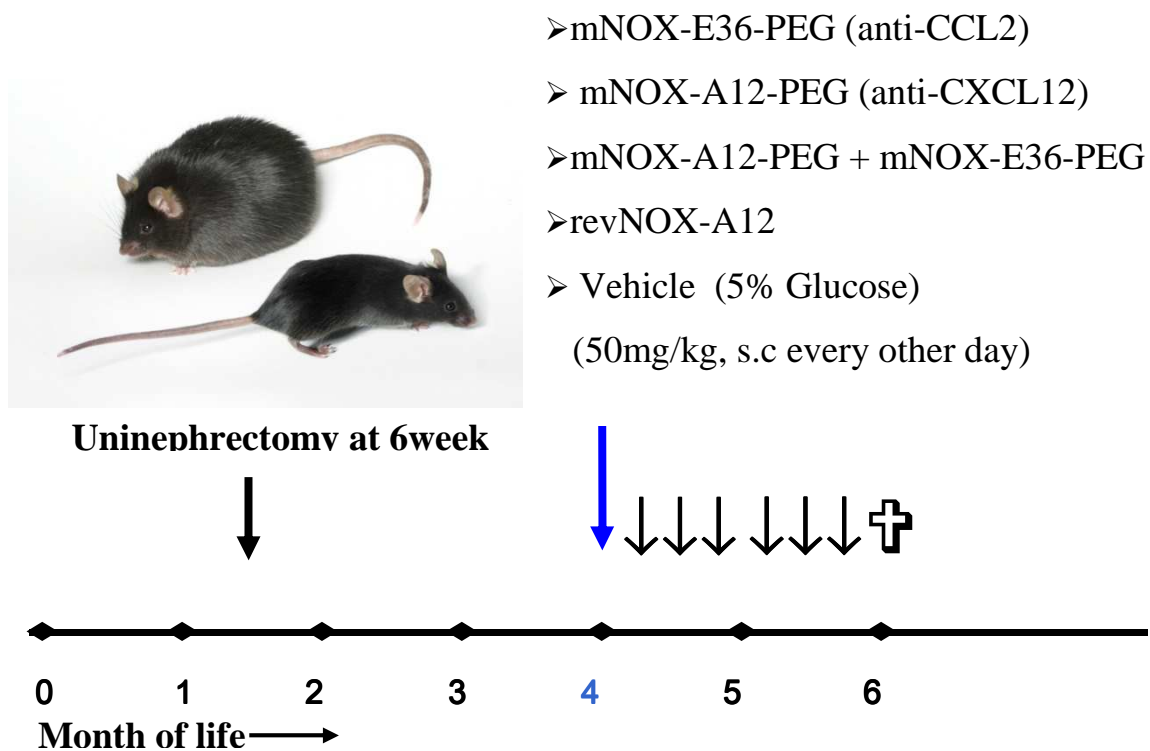


Figure 8: Treatment protocol I

3.2.4 Glomerular filtration rate

5% FITC-inulin was dissolved in two ml of 0.9% NaCl facilitated by heating the solution in boiling water. Mice were anesthetized using isoflurane for approximately 20 seconds. 5% FITC-inulin (3.74 $\mu\text{L/g}$ body weight) was injected retroorbitally under anaesthesia within 10 seconds. Under general anaesthesia, blood was drawn from the retro orbital plexus at 5, 10, 15, 20, 35, 60 and 90 min post administration. Since pH significantly affects FITC fluorescence value, each plasma sample was buffered to pH 7.4, by mixing 10 μL of plasma with 40 μL of 500 mM HEPES (pH 7.4). The titrated samples were then loaded onto a 96-well plate at 50 μL sample/well. Fluorescence was determined with 485 nm excitation, and read at 538 nm emission.

A two-compartment clearance model may be employed for the calculation of GFR. In a two-compartment model used, as depicted in Figure 9, the initial, rapid decay phase represents redistribution of the tracer from the intravascular compartment to the extracellular fluid. Systemic elimination also occurs, but the distribution process is relatively dominant during this initial phase. During the later phase, slower decay in concentration of the tracer systemic clearance of the tracer from the plasma predominates. At any given time (t_X), the plasma concentration of the tracer (Y) equals to $Ae^{-\alpha t} + Be^{-\beta t} + \text{Plateau}$.

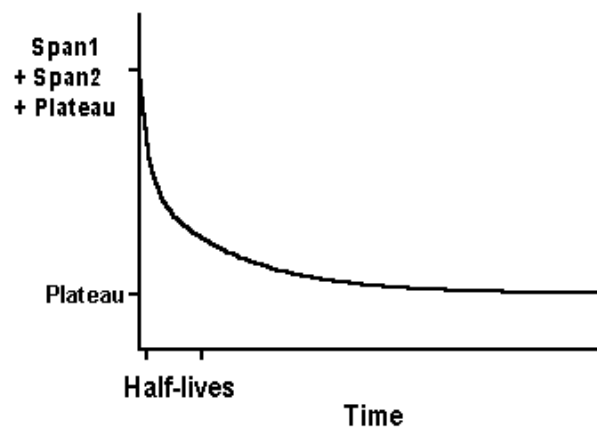


Figure 9: Representation of two phase regression curve

The parameters of above equation could be calculated using a non-linear regression curve-fitting program (GraphPad Prism, GraphPad Software, Inc., San Diego, CA). GFR was calculated using the equation:

$$\text{GFR} = I / (A/\alpha + B/\beta)$$

Where I is the amount of FITC-inulin delivered by the bolus injection; A (Span1) and B (Span2) are the y -intercept values of the two decay rates, and α and β are the decay constants for the distribution and elimination phases, respectively.

Plasma, urine and tissue collection

At 24 weeks of age, after treatment, blood samples were collected under isoflurane anaesthesia. Small blood samples (around 100 μ L) were collected in micro centrifuge tubes containing EDTA (10 μ L of 0.5 M solution per 200 μ L of blood) and plasma was separated by centrifugation at 10,000 rpm for 5 min and stored at -20 °C until used for different cytokine estimations. Urine samples were collected at every alternate week from 16 weeks of age till 24 weeks and stored at -20 °C for further analysis. Tissues were harvested for histopathological evaluation and RNA analysis at the end of the treatment period. All samples were collected 3-4 h after the last Spiegelmer injection.

3.2.5 Plasma CCL2 and CXCL12 ELISA

Plasma chemokines were estimated using commercial ELISA kits following the manufacturer's instructions.

CCL2 ELISA

Protocol (in brief)

- 1) The NUNC 96 well ELISA plate was captured overnight at 4 °C with the capture antibody (1: 250 dilution) in coating buffer (Phosphate buffer, pH 6.5)
- 2) Next day the plates were washed 3 times with the wash buffer (PBS with 0.05% Tween- 20) and blocked with the assay diluent (PBS with 10% FBS) for 1 h.

- 3) Again the wash steps were repeated 3 times followed by addition of standards, samples and sample diluent (blank) into the wells and incubated at RT for 2 h.
- 4) This was followed by 5 washes.
- 5) Then the detection antibody (1:250 dilution) diluted in assay diluent was added and incubated the plate at RT for 1 h.
- 6) The wells were washed again for 7 times and incubated with 100 μ L of TMB substrate (1:1 mixture, A and B) for 10-20 min, followed by addition of 100 μ L 2 N H_2SO_4 .
- 7) The absorbance was read at 450 nm using a spectrophotometer.

CXCL12 ELISA

Plasma levels of CXCL12 were measured using commercial kit from R&D system and the materials provided and used are as follows,

Protocol (in brief)

- 1) To the pre-coated 96 well plate, added 50 μ L of standards, samples and sample diluent (blank) and incubated at RT for 2 h.
- 2) Washed the plate 3 times
- 3) Then incubated the plates for 1 h at RT with conjugated detection antibody diluted in assay diluent.
- 4) Repeated the step2.
- 5) Added 200 μ L of substrate solution and incubated for 10-20 min, followed by addition of 50 μ L of stop solution.
- 6) The absorbance was read at 450 nm using a spectrophotometer.

3.2.6 Urine albumin/creatinine ratio (UACR)

Urine albumin ELISA

Urinary albumin levels were determined using albumin ELISA kit from Bethyl Laboratories following manufacturer's instructions. Generally albumin levels in urine samples from db/db mice were quite high, so urine samples were diluted 1000 times with water before estimation.

Protocol (in brief)

- 1) The NUNC 96 well ELISA plate was captured overnight at 4 °C with the capture antibody (1:100 dilution) in coating buffer (carbonate-bicarbonate pH 9.6)
- 2) Next day the plates were washed 3 times with the wash buffer (Tris, NaCl with 0.05% Tween- 20) and blocked with the blocking solution (Tris, NaCl with 1% BSA, pH 8) for 1 h
- 3) Again the wash steps were repeated 5 times followed by addition of standards, samples and sample diluent (blank) into the wells and incubated at RT for 2 h.
- 4) This was followed by 5 washes.
- 5) Then the HP-conjugated detection antibody (as suggested) diluted in assay diluent was added and incubated the plate at RT for 1 h.
- 6) The wells were washed again for 7 times and incubated with 100 µL of TMB substrate (1:1 mixture, A and B) for 10-20 min until colour reaction developed, followed by addition of 100 µL 2N H₂SO₄.
- 7) The absorbance was read at 450 nm using a spectrophotometer.

Urine creatinine measurement

Urinary creatinine levels were measured using enzymatic reaction (Jaffe' reaction using biochemical kit from Diasys). Urine samples were diluted 5 to 10 times (depending on the expected concentration range) with distilled water. Different dilutions of standard were prepared using the stock provided with the kit. Working monoreagent was prepared by mixing 4 part of reagent 1 (R1) and 1 part of reagent 2 (R2) provided with the kit. 10 µL of each of the diluted samples and standards were added to a 96 well plate with flat bottom (Nunc maxisorb plate). 200 µL of monoreagent was added to each well and absorbance for was read at 490 nm immediately after and 1 (A1) and 2 (A2) min of addition using ELISA plate reader. The change in absorbance (ΔA) was calculated as $\Delta A = [(A2 - A1) \text{ sample or standard}] - [(A2 - A1) \text{ blank}]$. Creatinine content of samples was calculated as:

$$\text{Creatinine (mg/dL)} = \Delta A \text{ sample} / \Delta A \text{ standard} * \text{Concentration of standard (mg/dL)}$$

Urinary albumin to creatinine ratio

Urinary albumin to creatinine ratio was calculated after converting values for albumin and creatinine to similar units (mg/dL). Albumin content for each sample calculated (mg/dL) was divided by creatinine content (mg/dL) for the same sample.

3.2.7 RNA isolation, cDNA preparation and real-time quantitative (RT-PCR)

Renal tissue from each mouse was snap frozen in liquid nitrogen and stored at -80 °C. Real time RT-PCR was performed in pooled samples (5 animals from each group) on a TaqMan ABI 7700 Sequence Detection System using a heat activated TaqDNA polymerase (Amplitaq Gold, PE Biosystems). Controls comprising ddH₂O were negative for target and housekeeper genes. Primers were from Metabion, Martinsried, Germany. From each animal total renal RNA preparation and reverse transcription were performed as described.

Isolation of RNA from tissues

When animals were sacrificed on termination of the study, small parts of tissue from each mouse were preserved in RNA-later and stored at -20 °C until processed for RNA isolation. RNA isolation was carried out using RNA isolation kit. In short, tissues (30 mg) preserved in RNA-later were homogenized using blade homogenizer for 30 s at 14500 rpm in lysis buffer (600 µL) containing β-mercaptoethanol (10 µL/mL). The homogenate was centrifuged at 15000 rpm for 3 min and 350 µL of supernatant was transferred to fresh DEPC-treated tube. To this, equal amount (350 µL) of 70 % ethanol was added and whole mixture was loaded on RNA column and processed for RNA isolation as per the manufacturer's instruction. Isolated RNA was stored at -80 °C until further used.

RNA quantification and purity check

For quantification isolated RNA samples were diluted in DEPC water (2 µL of RNA + 98 µL of DEPC water, 50 times dilution) and absorbance was measured at two wavelengths 260 nm and 280 nm.

Amount of RNA (µg/ µL) = O.D. at 260 nm * 40 * 50 (dilution factor)/ 1000

The ratio of optical densities at 260 nm and 280 nm is an indicator for RNA purity (indicative of protein contamination in the RNA samples). Only samples with a ratio of 1.8 or more were considered to be of acceptable quality.

RNA integrity check

Further quality check (if necessary) was performed using a denaturing RNA gel. In short, 2% Agarose gel with Ethidium-bromide was casted, RNA samples were mixed with RNA loading buffer (4:1 ratio) (Sigma) and were loaded on the gel. Electrophoresis was carried out at constant volt (70-100 V) using MOBS running buffer for 1 h and the gel was read on a gel documentation apparatus under UV lamp. RNA samples showing a single bright band were considered to be of good quality. Loss of RNA integrity could be detected as smear formation in the agarose gel (Figure 10).

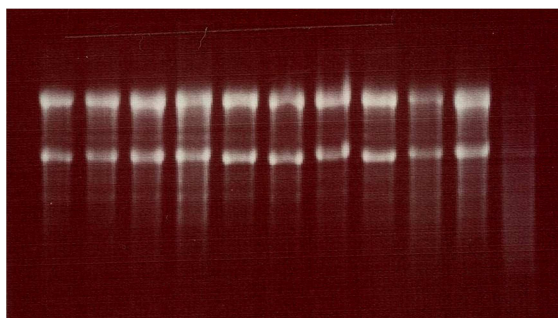


Figure 10: Representative agarose gel for RNA integrity check

cDNA synthesis

The RNA samples isolated according to the procedure detailed above were diluted in DEPC water to a concentration of 1 µg/20 µL. The master mix was made to a volume of 15 µL and added to 2 µg/30 µL RNA samples were taken in separate DEPC treated micro centrifuge tubes which were mixed and placed at 42 °C on a thermal shaker incubator. After 90 min, the cDNA samples were collected and stored at -20 °C until use for real-time RT-PCR analysis.

The master contains the following components: 9 µL of 5x buffer (Invitrogen, Karlsruhe, Germany), 1 µL of 25mM dNTP mixture (Amersham Pharmacia Biotech, Freiburg, Germany), 2 µL of 0.1 M DTT (Invitrogen, Karlsruhe, Germany), 1 µL of 40 U/µL RNasin (Promega, Mannheim, Germany), 0.5 µL of 15 µg/mL linear acrylamide

(Ambion Ltd, Cambridgeshire, UK), 0.5 μ L of Hexanucleotide (Roche, Mannheim, Germany) and 1 μ L of Superscript (Invitrogen, Karlsruhe, Germany) or ddH₂O in case of controls.

Real-time quantitative (TaqMan) RT-PCR

The cDNA samples prepared as described above were diluted 1:10 a dilution for the real-time RT-PCR. The following protocol used for RT-PCR: Pre-incubation was carried out for 5 min at 95 °C to ensure the activation of the polymerase and complete denaturation of cDNA samples. This was followed by amplification for 40 cycles, each comprising of 15 seconds incubation at 95 °C and 45 seconds incubation at 60 °C. For melting curve initial 95 °C for 5 s followed by 65 °C for 1 min with continuous heating was used. The RT-PCR for the reference genes (18S rRNA) was carried out under similar conditions. The CT values were calculated using the Light Cycler 480 and the results were normalized with respective reference gene expression for each sample. In all cases controls consisting of ddH₂O were negative for target or reference genes. All designed SYBR green primers for all genes evaluated were obtained from Metabion (Martinsried, Germany) (Table 6). All gene expression values were normalized using 18s RNA as a house keeping gene. All primers used for amplification were from Metabion (Martinsried, Germany).

3.2.8 *In vitro* studies

Normal renal tissues were obtained from four patients nephrectomized because of renal cell carcinoma, in agreement with the Ethical Committee on human experimentation of the Azienda Ospedaliero-Universitaria Careggi, Florence, Italy. 293 (HEK-293) were purchased from ATCC (Manassas, VA, USA) and cultured as specified by the supplier. The HACAT cell line was a gentle gift of Dr. Rosa Mancina (Florence, Italy). Human renal progenitors were obtained by immune-magnetic sorting for CD133 after depletion of digested total renal cell suspensions for CD45 and podocalyxin, as previously described¹⁸. Primary cultures of human renal progenitors were >99% positive for CD133 and CD24 co-expression, as checked by FACS analysis. Podocyte markers were absent. For podocyte differentiation, cells were treated for 2 days with VRAD medium (vitamin D3, retinoic acid and dexamethasone-supplemented DMEM) as previously

Table 6: Oligonucleotide primers used for SYBR-Green RT-PCR

Target	Primer sequence
CCL2	Reverse : CCTGCTGTTACAGTTGCC
	Forward : ATTGGGATCATCTTGCTGGT
CXCL12	Reverse : TTTCAGATGCTTGACGTTGG
	Forward : GCGCTCTGCATCAGTGAC
TNF	Reverse : AGGGTCTGGGCCATAGAACT
	Forward : CCACCACGCTCTTCTGTCTAC
iNOS	Reverse : TGAAGAAAACCCCTTGTGCT
	Forward : TTCTGTGCTGTCCCAGTGAG
Nephrin (NPHS1)	Reverse : CTCTTTCTACCGCCTCAACG
	Forward : TTAGCAGACACGGACACAGG
Podocin (NPHS2)	Reverse : CAGGAAGCAGATGTCCCAGT
	Forward : TGACGTTCCCTTTTTCCATC
IL-6	Reverse : CCAGAGGAAATTTTCAATAGGC
	Forward : TGATGCACTTGCAGAAAACA
18s RNA	Reverse : AGGGCCTCACTAAACCATCC
	Forward : GCAATTATTCCCCATGAACG

described. Nephrin mRNA quantification was performed assay on demand kits (Applied Biosystems, Warrington, UK)^{20,21}, according to the manufacturer's recommendations and Taq-Man RT-PCR was performed using a 7900HT Real Time PCR System (Taqman, Applied Biosystems) as previously described^{20,21}. To accurately compare samples by means of real-time RT-PCR, identical number of cells (n=10000) were analyzed in all experiments and GAPDH was used to evaluate mRNA quality and integrity.

3.3 Methods part II

3.3.1 Animal studies

Male diabetic C57BLKS db/db mice 5-6 week old were obtained from Taconic (Ry, Denmark) and housed in filter top cages with a 12 h dark/light cycle. All animals had unlimited access to food and water throughout the study duration. At the age of 6 weeks uninephrectomy (1K mice) was performed as described in “Methods part I”. All animal experiments were approved by the local government authorities.

3.3.2 Cat S inhibitor R05461111

RO5461111 (CAS 1252637-46-9) is a competitive inhibitor of the active site of Cat S. The nitril function of RO5461111 allows covalent reversible inhibition of Cat S. It was provided by F. Hoffmann-La Roche, Ltd., Basel, Switzerland. The synthesis and drug development of RO5461111 has been described in WO 2010121918.

3.3.3 Study design

At the age of 4 months, 1K db/db mice with documented blood glucose levels $>11\text{mmol/L}$ and UACR >3 (ratio in age-matched wild-type mice = 0.1) were divided into two groups (n=10-12) and one group fed with food-drug mix contained RO5461111 (87.5 mg/kg, delivering a daily dose of 10 mg/kg body weight) and other group fed with standard food from 16 weeks of age till 24 weeks (Figure 11). Tissues were harvested for histopathological evaluation at the end of the treatment period. Blood and urine samples were obtained at monthly intervals.

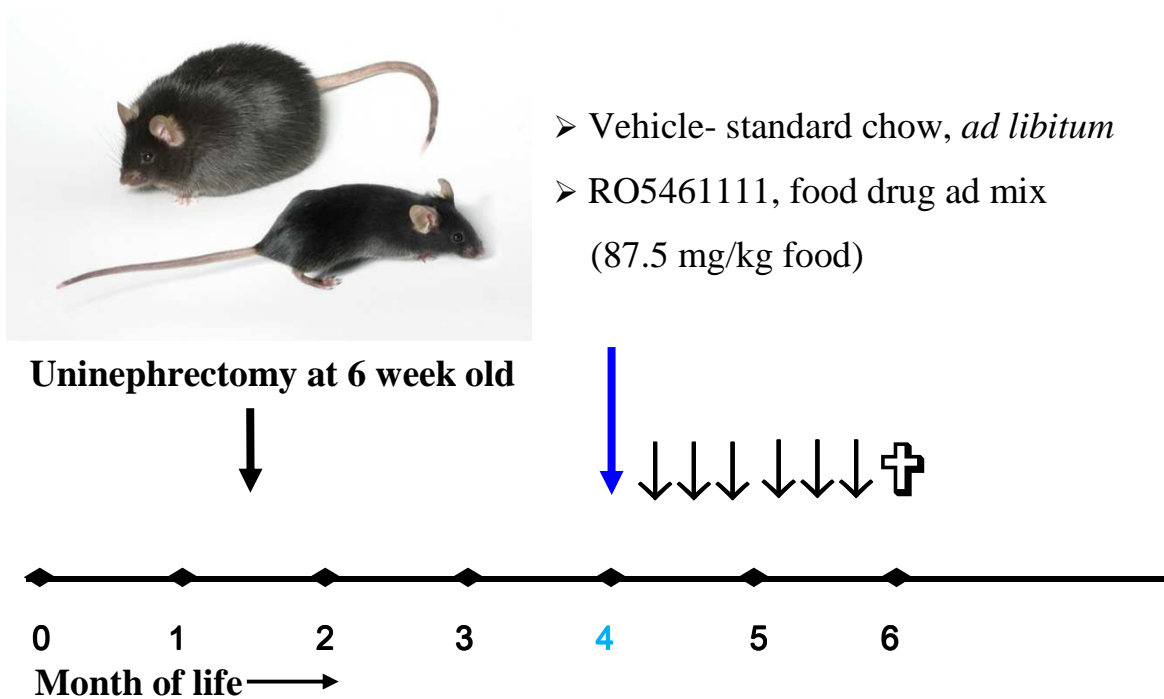


Figure 11: Treatment protocol II

3.3.4 RNA isolation, cDNA preparation and Real-time quantitative (RT-PCR)

The detailed protocols for RNA isolation, cDNA preparation and RT-PCR were explained in “Method section, Part I”. In brief, total RNA from whole kidney was extracted using RNeasy mini extraction kit following the manufacturer’s instructions. 1µg of RNA was transcribed into cDNA using Superscript II. The cDNA was further subjected to real-time PCR using the specific oligonucleotide primers (300 nM, Metabion, Martinsried, Germany) for the genes listed in Table 7. Quantitative detection of mRNA expression was performed using a Light Cycler 480, using SYBR green (SA Biosciences). The mRNA expression values for all genes were normalized to 18s rRNA in the respective cDNA preparations.

Table 7: Oligonucleotide primers used for SYBR-Green RT-PCR

Target	Primer sequence
Cat A	Forward : AGAGCGGTCAGGCCAAGACG Reverse : CGCGGTTCCGGGCATCTCTG
Cat B	Forward : CTGCGCGGGTACTTAGGAGT Reverse : CAGGCAAGAAAGAAGGATCAAG
Cat D	Forward : TTCGTCCTCCTTCGCGATT Reverse : TCCGTCATAGTCCGACGGATA
Cat K	Forward : GCCAGGATGAAAGTTGTATG Reverse : CAGGCGTTGTTCTTATTCC
Cat L	Forward : GTGGACTGTTCTCACGCTCA Reverse : TATCCACGAACCCTGTGTCA
Cat S	Forward : AAGCGGTGTCTATGACGACCC Reverse : GAGTCCCATAGCCAACCACAAG
IL6	Forward : TGATGCACTTGCAGAAAACA Reverse : ACCAGAGGAAATTTTCAATAGGC
TNF alpha	Forward : AGGGTCTGGGCCATAGAACT Reverse : CCACCACGCTCTTCTGTCTAC
iNOS (NOS1)	Forward : TTCTGTGCTGTCCCAGTGAG Reverse : TGAAGAAAACCCCTTGTGCT
eNOS (NOS3)	Forward : TGGGCAACTTGAAGAGTGTGG Reverse : AGAGTTCTGGGGGCTCATCA
Ccl2	Forward : CCTGCTGTTACAGTTGCC Reverse : ATTGGGATCATCTTGCTGGT
Nphs2 (Podocin)	Forward : TGACGTTCCCTTTTTCCATC Reverse : CAGGAAGCAGATGTCCCAGT
Nphs1 (Nephrin)	Forward : TTAGCAGACACGGACACAGG Reverse : CTCTTTCTACCGCCTCAACG
VCAM	Forward : CCGGCATATACGAGTGTGAA Reverse : TCGGGCGAAAATAGTCCTT
ICAM	Forward : GTCACCGTTGTGATCCCTG Reverse : AACAGTTCACCTGCACGGAC
18s	Forward : GCAATTATCCCCATGAACG Reverse : AGGGCCTCACTAAACCATCC

3.3.5 FACS analysis of kidney cells

Flow cytometric analysis of the whole kidney cell preparation was performed on a FACS Calibur flow cytometer from BD Biosciences. In brief, kidneys were mechanically disrupted and incubated in 1x Hanks'balanced salt solution (HBSS) containing 1 mg/mL collagenase type I and 0.1 mg/mL deoxyribonuclease type I for 20 min at 37 °C. After washes, tissues were incubated in 5 ml 2 mmol/L EDTA in 1x HBSS for 20 min at 37°C. The supernatant containing isolated cells was kept on ice and the remaining pellet was incubated in 5 ml of 1 mg/mL collagenase-I in 1x HBSS for 20 min at 37 °C. The suspension was subsequently passed through a 19-gauge, 27-gauge needle, and pooled with the first supernatant from the EDTA incubation. Cells were filtered through a 70- μ m cell strainer and washed twice in PBS. All washing steps were performed in FACS buffer. The renal leukocytes were then characterized by using the following conjugated antibodies: PE anti-CD45, APC anti-CD11b, anti-Gr-1, FITC anti-Ly6C and anti-Ly6G.

In cell culture stimulation experiments, the mouse glomerular endothelial cells (GENCs) were washed with PBS and incubated with binding buffer containing either FITC anti-Annexin V or PE propidium iodide. Apoptotic cells in the supernatants were washed, counted and analysed for the same surface markers mentioned above.

3.3.6 Protein isolation and western blotting

Protein isolation

Proteins from kidney tissue were extracted using RIPA buffer (Sigma, Germany) containing protease inhibitors (Roche, Germany). In brief, part of the kidney tissue stored at -80 °C was homogenized using blade homogenizer for 30 seconds at 4 in RIPA buffer (500 μ L) containing protease inhibitor. The lysates was then maintained at constant agitation for 2 h at 4 °C. The samples were then centrifuged for 20 min at 12000 rpm at 4 °C. Then the supernatant (proteins) was separated into a new tube and the pallet was discarded. Protein estimation was done using Bradford's assay.

Western blotting

After determination of protein concentrations, 50 µg of the protein was mixed with 5x SDS loading buffer (100 mM Tris-HCl, 4% SDS, 20% glycerol, and 0.2% bromophenol blue) for Western blot analysis. Samples were heated at 95 °C for 5 min. Proteins were separated by SDS PAGE and then transferred to a poly-vinylidene difluoride (PVDF) membrane. Non-specific binding to the membrane was blocked for 1 h at room temperature with 5% milk in Tris-buffered saline buffer (TBS, 20 mM Tris-HCl, 150 mM NaCl, and 0.1% Tween 20). The membranes were then incubated overnight at 4 °C with primary antibodies. After washing, the membrane was incubated with respective secondary antibodies in TBS. The signals were visualized by an enhanced chemiluminescence system (Amersham, Buckinghamshire, UK).

3.3.7 Invariant chain assay with mouse splenocytes

Mouse splenocytes were isolated by mechanical teasing of the whole spleen, followed by red blood cell depletion using Triton-X 100 lysis buffer for 30 min and centrifuged at 10,000g for 20 min to remove the cell debris. The supernatants were then loaded onto 10% SDS-PAGE; the proteins were then transferred onto nitrocellulose membrane and incubated with antibody against mouse CD74 antibody (BD biosciences), later incubated with anti-rabbit HP secondary antibody. The membrane was developed with ECL (GE Healthcare, Buckinghamshire, UK).

3.3.8 *In vitro* studies

All cells were cultured as previously described¹⁹⁷. Murine immortalized podocytes were allowed to proliferate in RPMI 1640 medium (GIBCO/ Invitrogen, Paisley, Scotland, UK) containing 10% fetal calf serum, 100 U/ml penicillin, 100 mg/mL streptomycin and 10 U/ml mouse IFN-γ (ImmunoTools, Firesoythe, Germany) at permissive temperature (33 °C), 5% CO₂. Cells were differentiated at non-permissive conditions (37 °C), 5% CO₂ without IFN-γ supplement for 10–14 days. For ECIS experiments, primary podocytes were isolated from mouse glomeruli as described elsewhere. All cells were cultured in RPMI 1640 GlutaMAX™-I medium

supplemented with 10% FBS and 1% of penicillin and streptomycin. TECs were isolated and were grown to confluence in DMEM/F12 media containing 10% fetal calf serum, 1% penicillin–streptomycin, 125 ng/mL prostaglandin E1 (Calbiochem), 25 ng/mL EGF (Sigma), 1.8 µg/mL L-thyroxine (Sigma), 3.38 ng/mL hydrocortisone and 2.5 mg/mL of insulin-transferrin-sodium selenite supplement (I-TSS) (Sigma). All cells were stimulated with different concentration of glucose. HUVECs were stimulated with indicated growth factors and cytokines (R&D Systems) for 24 h. All cells were stimulated in serum free media. Cell-free supernatants were analysed for Cat S secretion by Luminex kit (in-house established).

3.3.9 Electric cell impedance sensing assay (ECIS)

Cat S induced changes in resistance and capacitance of all cells was analyzed using an ECIS device (Applied Biophysics Inc., NY, USA). Briefly, cells were re-suspended in complete media and seeded in eight-well ECIS array plate containing small gold-film electrodes at a density of 100,000 cells/well in a volume of 400 µL media. Both the ECIS arrays and the measurement station were kept in an incubator with high humidity at 37 °C and 5% CO₂. Cell attachment and confluency was monitored in terms of resistance/capacitance at every 30 sec for up to 24 h. Complete mono-layer covering the electrodes was confirmed microscopically prior to stimulation. All cells were then stimulated with different doses of Cat S with or without RO5461111. Capacitance was analyzed for indicated time points at 4000 Hz. All experiments were performed at least twice, every time in duplicates.

3.3.10 *In situ* hybridization

In-situ hybridization was performed using Quantigene View RNA ISH Tissue Assay Kit (Affymetrix / Panomics Solutions). The assay uses proprietary chemistry for the target specific probe sets and branched-DNA signal amplification for detection of specific signal. Specific probe sets for mouse CTSS and F4/80 mRNAs were designed by Affymetrix based on the following sequences: NM_001267695 and NM_021281 for CTSS, NM_010130 for EMR1. Tissue sections of 4 µM prepared from Formalin Fixed Paraffin Embedded (FFPE) mouse kidney tissues were mounted onto micro slides (X-

tra™ Adhesive, Leica) and processed according to manufacturer instructions. Briefly, slides were baked for 1 h at 60 °C (Thermobrite, Abbott Molecular) and fixed in 10% formaldehyde for 1 h at RT. De-paraffinization was achieved using Histo-Clear reagent (National Diagnostics). Pre-hybridization conditions were found to be optimal with 10 min of boiling at 95 °C and 10 min incubation at 40 °C with Protease QF diluted 1/100x. Target probe set hybridization (Type-6 or Type-1 probe sets for blue or red staining respectively) was carried out for 2 h at 40 °C. Hybridized probes were amplified using PreAmplifier Mix QT and Amplifier Mix QT oligonucleotides incubating slides at 40 °C for 25 and 15 min respectively. Slides were then exposed to Label Probe conjugated with alkaline phosphatase (Label Probe 6-AP or 1-AP for blue or red staining respectively) for 15 min at 40 °C and to Fast Blue or Fast Red Substrates at RT for 15 min or at 40 °C for 30 min respectively. When 2-Plex assays were carried-out, incubations with Label Probe 6-AP and Fast Blue Substrate were carried out before incubations with Label Probe 1-AP and Fast Red Substrate. Slides were counterstained with Gill's Hematoxylin stain for 5-10 seconds at RT. After every incubation step, slides were washed 2-3 times in washing solution, PBS or water according to the manufacturer instructions. Imaging was performed under bright field with a Zeiss microscope equipped with an Axiocam MRC camera.

3.3.11 *In vivo* microscopy on the mouse cremaster muscle

The surgical procedure and the technical setup for *in vivo* microscopy on the mouse cremaster muscle have been previously described. For analysing post-ischemic leukocyte responses, the post-capillary vessel segments in a central area of the spread-out cremaster muscle were randomly chosen among those that were at least 150 µm away from neighboring post-capillary venules and did not branch over a distance of at least 150 µm. After having obtained baseline recordings of leukocyte rolling, firm adhesion, and transmigration in all the vessel segments, ischemia was induced by clamping all supplying vessels at the basis of the cremaster muscle using a vascular clamp (Martin, Tuttlingen, Germany). Stagnancy of blood flow was then verified by *in vivo* microscopy. After 30 min of ischemia, the vascular clamp was removed and reperfusion was restored for 160 min. Measurements were repeated at 120 min after onset of reperfusion. For the quantitative analysis of the leukocyte migration

parameters, CapImage software (Dr. Zeintl, Heidelberg, Germany) was used. Rolling leukocytes were defined as those moving slower than the associated blood flow and quantified for 30 s. Firmly, adherent cells were determined as those resting in the associated blood flow for more than 30 s and related to the luminal surface per 100 μm vessel length. Transmigrated cells were counted in regions of interest (ROIs) covering 75 μm on both sides of a vessel over 100 μm vessel length. For measurement of centerline blood flow velocity, green fluorescent microspheres (2 μm diameter; Molecular Probes, Leiden, The Netherlands) were injected via an arterial catheter and their passage through the vessels of interest were recorded. From measured vessel diameters and centerline blood flow velocity, apparent wall shear stress was calculated, assuming a parabolic flow velocity profile over the vessel cross section.

As a measure of microvascular permeability, leakage of FITC dextran (Sigma Aldrich) into the perivascular tissue was analysed. After 130 min of reperfusion, FITC dextran was applied intra-arterially. Fluorescence *in vivo* microscopy measurements were performed 30 min later on five post-capillary vessel segments and the surrounding perivascular tissue. Mean gray values of fluorescence intensity were determined by digital image analysis (Image J) in six randomly selected ROIs (50x50 μm^2), localized ~ 50 μm distant from the venule under investigation. Phenotyping of transmigrated leukocytes was performed on paraffin-embedded tissue sections immunostained with rat-anti-mouse CD45, Ly6G, or F4/80 mAb (Serotec, Oxford, UK) and counterstained with Mayer's hemalaun.

3.3.12 Human studies

Human renal biopsies from patients and controls were collected within the framework of the European Renal cDNA Bank -Kroner-Fresenius Biopsy Bank (ref). Diagnostic renal biopsies were obtained from patients after informed written consent and with approval of the local ethics committees (Die Spezialisierte Unterkommission-SPUK für Innere Medizin, University of Zurich). Total RNA was isolated from micro-dissected samples taken from the tubulo-interstitial compartment. The fragmentation, hybridization, staining and imaging was performed according to the manufacturer's guidelines (Affymetrix). For a detailed description and access to the deposited raw data of the protocol see reference (ref). A single probe-based analysis tool, ChipInspector

(Genomatix Software GmbH, Munich), was used for transcript annotation, total intensity normalization, significance analysis of microarrays and transcript identification based on significantly changed probes (ref). Real-time RT-PCR on biopsies from DN (n=12), and controls (living donors, LD, n= 9) was performed. Reverse transcription and real-time RT-PCR were performed as reported earlier (ref). Pre-developed TaqMan reagents were used for Cat S (CTSS, NM_004079) and the housekeeper gene GAPDH (Applied Biosystems). Data shown are normalized to GAPDH and target gene expression in the control cohort is set as 1. The mRNA expression was analysed by standard curve quantification.

4. Results

4.1 Part I

4.1.1 Plasma CCL2 and CXCL12 levels

To assure Spiegelmer exposure and its biological activity *in vivo*, we determined plasma CCL2 and CXCL12 levels at the beginning and also at the end of the study. Anti-CXCL12 or anti-CCL2 Spiegelmer injections significantly increased the plasma levels of either chemokines in 1K db/db mice (Figure 11). Plasma CCL2 and CXCL12 levels remained undetectable or low in sham-operated db/db mice and vehicle- or control Spiegelmer-treated 1K db/db mice. This is indicating that Spiegelmer antagonists retain their molecular targets in the circulation^{130,155,198}.

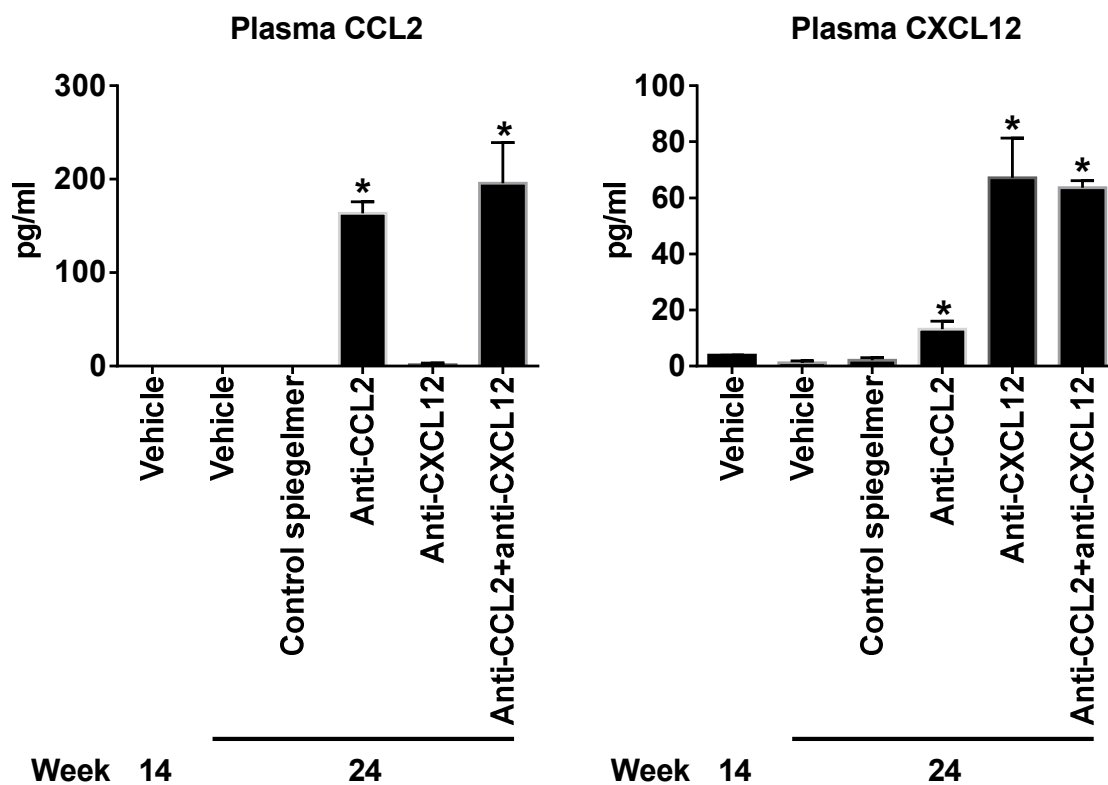
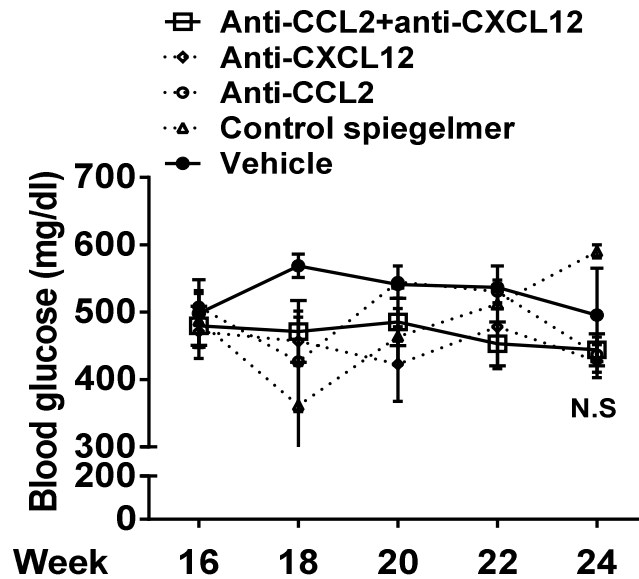


Figure 11: Plasma chemokine levels in Spiegelmer-treated db/db mice. Plasma CCL2 and CXCL12 levels were determined in 14 and 24 week old uninephrectomized db/db mice by ELISA which represent before and after treatment. Data are means \pm SEM. * $p < 0.001$ versus 24 week vehicle group.

4.1.2 Effect of dual blockade on body weight and blood glucose

Treatment with CCL and CXCL12 dual blockade in uninephrectomized db/db mice did not show any significant changes in body weight and blood glucose levels compared to the vehicle-treated mice (Figure 12). This suggests that food *admix* did not influence the physiology of the treated mice.

A



B

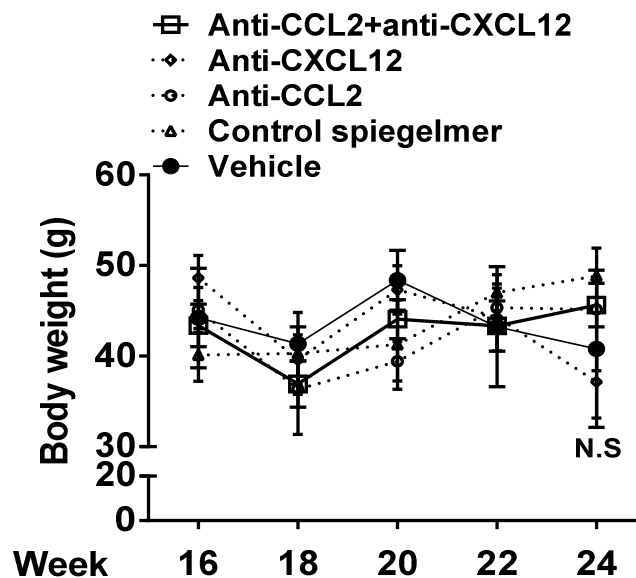


Figure 12: Blood glucose levels and body weight in uninephrectomized db/db mice. (A) Uninephrectomized db/db mice with different treatments were monitored for blood glucose levels and (B) body weight from baseline at 16 weeks until the end of the study at 24 weeks of age. Data are means \pm SEM.

4.1.3 Dual CCL2/CXCL12 blockade has additive effects on glomerulosclerosis in db/db mice

Renal histopathology

Renal histomorphology in 6 months old db/db mice showed moderate glomerulosclerosis as compared to age-matched 2K non-diabetic mice which was aggravated to diffuse glomerulosclerosis by early uninephrectomy of db/db mice. CCL2 as well as CXCL12 inhibition reduced the extent of glomerulosclerosis in uninephrectomized db/db mice to the level of age-matched sham-operated db/db mice while the control Spiegelmer had no effect (Figure 13).

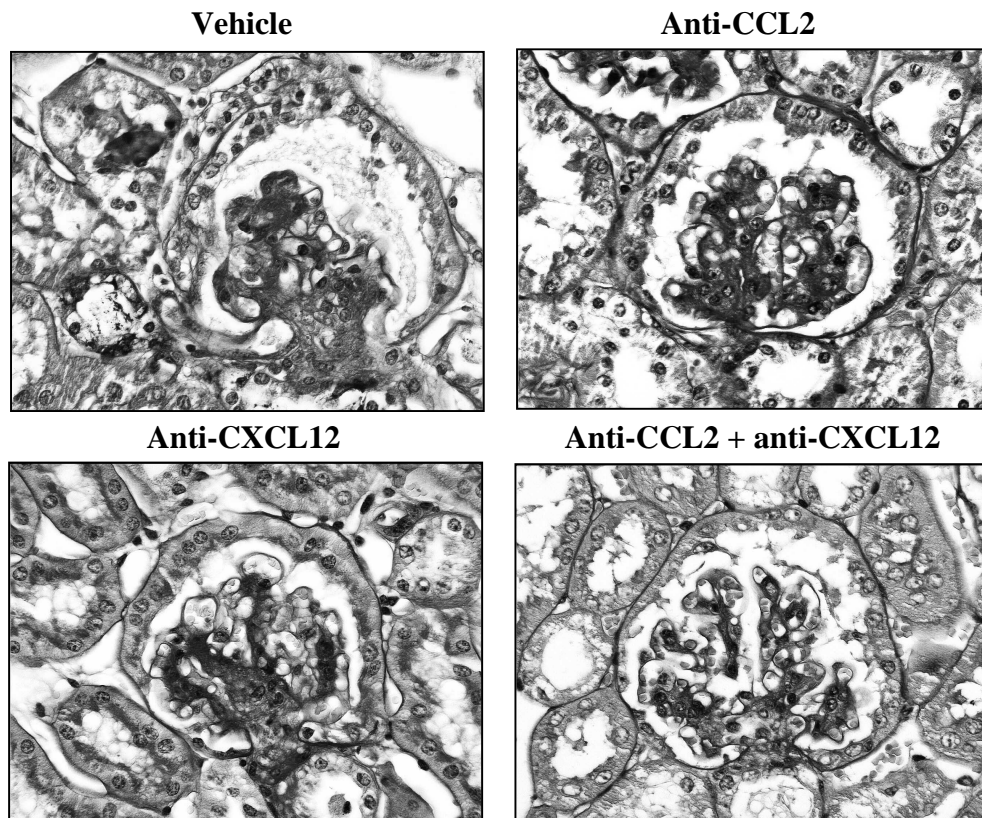


Figure 13: Renal pathology in 6 months old db/db mice. Renal sections from 1K mice of the different treatment groups were stained with periodic acid Schiff (PAS). Stains show representative glomeruli from each group (original magnification 400x).

Glomerulosclerosis

Dual CCL2/CXCL12 blockade improved glomerular pathology with significantly less severe lesions and more normal glomeruli as compared to either of the monotherapies. 1K db/db mice with dual blockade displayed even less glomerular pathology than age-matched 2K db/db mice (Figure 14).

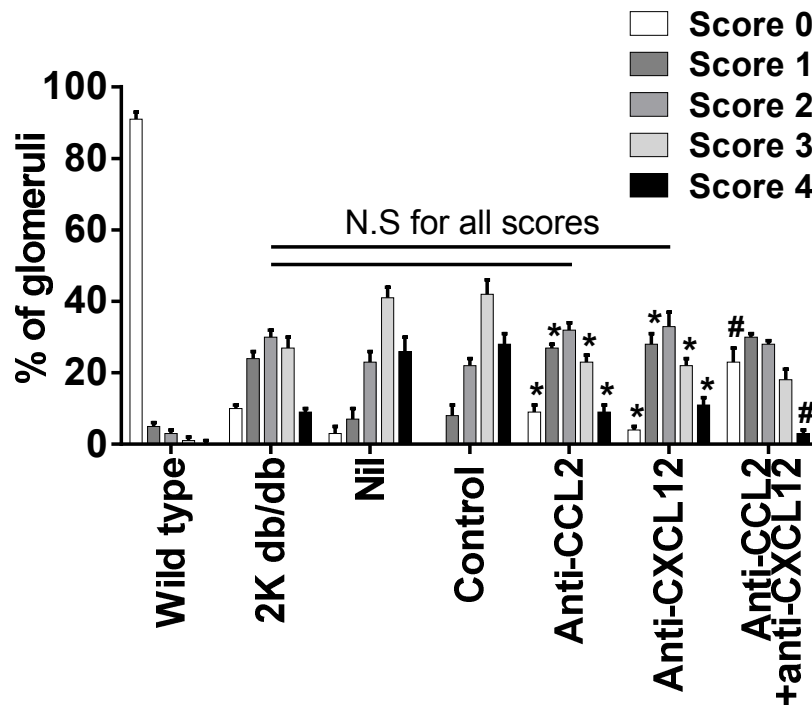


Figure 14: PAS stains from 'Figure 13' were scored for the extent of glomerulosclerosis from 0-4 as described. From each mouse 15 glomeruli from each renal section were graded by that score. The graph illustrates the mean percentage of each score \pm SEM from all mice in each group. Uninephrectomy was associated with a shift towards higher scores of glomerulosclerosis as seen in the control Spiegelmer and vehicle-treated 1K db/db mice. Note that single blockade with either anti(α)-chemokine Spiegelmer significantly reduced the overall scores as compared to control Spiegelmer-treated 1K db/db mice (* $p < 0.05$). Moreover, dual blockade further significantly reduced the percentage of glomeruli with a score 4 and also increased the percentage of glomeruli with a score 1 as compared to either single chemokine blockade ($\dagger p < 0.05$).

4.1.4 Dual CCL2/CXCL12 blockade improves the renal functional parameters and reduces proteinuria in db/db mice

Glomerular function rate

In CKD like DN, the decline in the GFR is associated with progression of the disease over a period due to loss of filtering ability. We therefore determined the GFR by assessing FITC inulin clearance kinetics in all groups of mice. Uninephrectomy was associated with a reduced GFR as compared to a normal GFR of about 350 mL/min in mice. Either CCL2 or CXCL12 blockade significantly increased GFR in 6 months old 1K db/db mice (Figure 15). Dual CCL2/CXCL12 blockade was associated with the highest GFR compared to monotherapies.

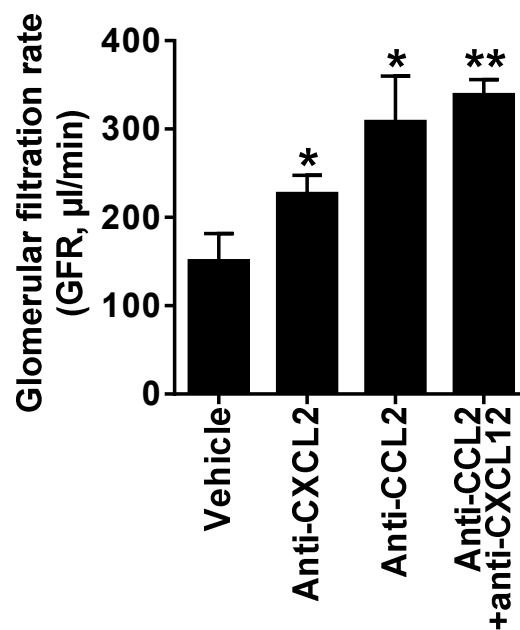


Figure 15: GFR in 6 months old db/db mice. GFR was determined by FITC-inulin clearance kinetics in all groups at the end of the study as described in methods. Note that 1K db/db mice treated with dual chemokine blockade has higher GFR levels. Data are means \pm SEM from at least 6 mice in each group. * $p < 0.05$, ** $p < 0.01$ versus control-Spiegelmer treated 1K db/db mice.

Albumin/creatinine ratio (ACR)

In DN, the progression of kidney disease is associated with increase in ACR, which is an important clinical parameter of glomerular dysfunction. We compared UACR at the beginning and at the end of the treatment course in all groups. CCL2 as well as CXCL12 blockade significantly reduced UACR when compared to control spiegelmer treatment at 6 months (Figure 16). When compared to baseline UACR, CXCL12 as well as dual blockade most effectively prevented proteinuria.

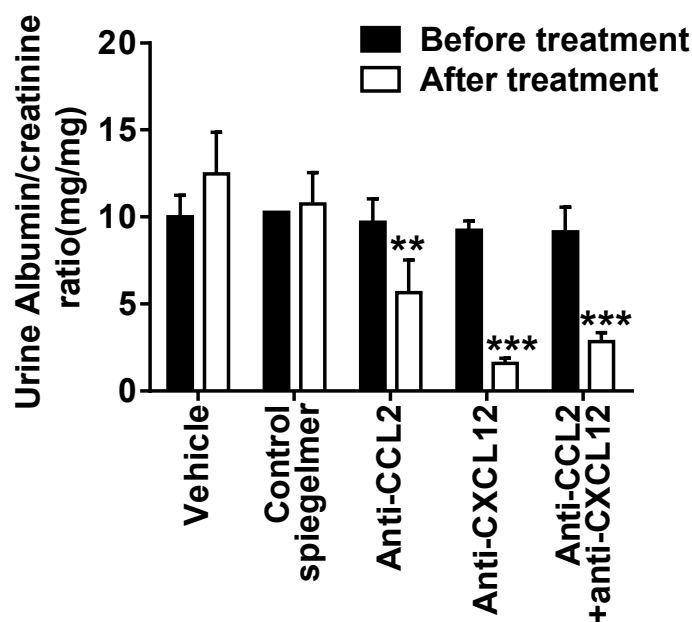


Figure 16: Albuminuria in 6 months old db/db mice. UACR were determined as a functional marker of the glomerular filtration barrier at the initiation (4 months) and termination of treatment (6 months). Data are presented as means \pm SEM from at least 6 mice in each group. ** $p < 0.01$, *** $p < 0.001$ versus control-Spiegelmer treated 1K db/db mice in the respective group.

4.1.5 Dual CCL2/CXCL12 blockade and glomerular cell counts in db/db mice

Ki-67+ proliferating glomerular cells

Glomerular pathology is often related to an altered cell turnover of glomerular cells, for example, mesangial cell proliferation and extracellular matrix accumulation. Therefore, we determined the total numbers of glomerular Ki-67+ proliferating glomerular cell. Total numbers of glomerular cells were determined by counting DAPI

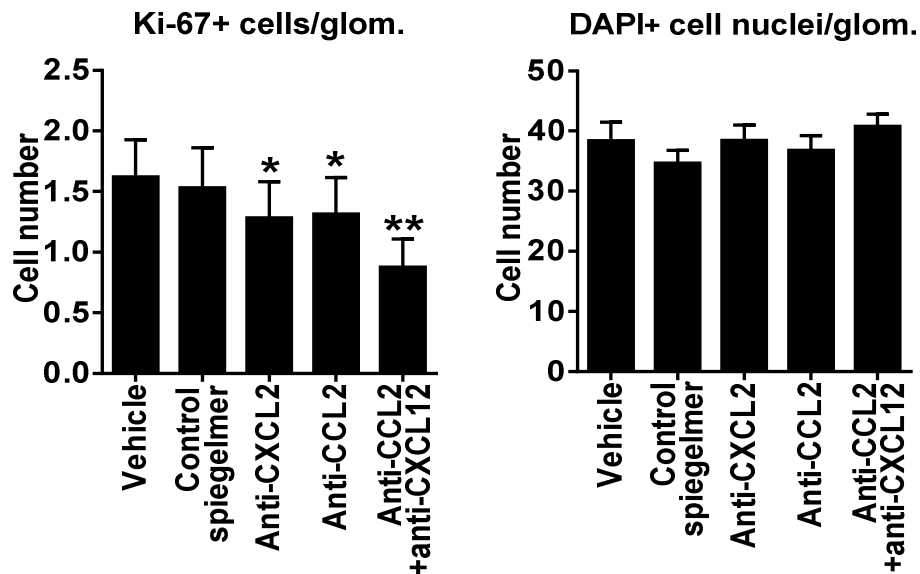


Figure 17: Proliferation of glomerular cells in 1K db/db mice. Renal sections from mice of all groups were stained for the proliferation marker Ki-67 and the numbers of DAPI+ cell nuclei were counted in renal sections from mice of all groups as indicated. The graphs show the mean number of positive cells in 15 glomeruli \pm SEM in sections from 6 months old 1K db/db mice of each group.

* $p < 0.05$, ** $p < 0.01$ versus control Spiegelmer treatment

positive nuclei in glomerular tufts cross sections. None of the interventions significantly affect the total number of cell nuclei in glomerular tufts (Figure 17). The overall numbers of Ki-67+ proliferating cells within glomeruli were low but CCL2 and CXCL12 blockade both significantly reduced their numbers in glomeruli (Figure 17).

4.1.6 CCL2 blockade reduces leukocyte numbers in glomeruli of 1K db/db mice

Chemokine-mediated glomerular pathology in db/db mice can be mediated by leukocyte recruitment^{119,130}. We therefore evaluated the number of glomerular leukocytes by immunostaining for CD45. Significant numbers of CD45 positive leukocytes were detected in glomeruli of vehicle or control Spiegelmer-treated 1K db/db mice (Figure 18). The numbers of glomerular CD45 positive leukocytes were significantly reduced by CCL2 but not by CXCL12 blockade^{130,155}. The numbers of glomerular leukocytes were also reduced with dual chemokine blockade, accordingly (Figure 18).

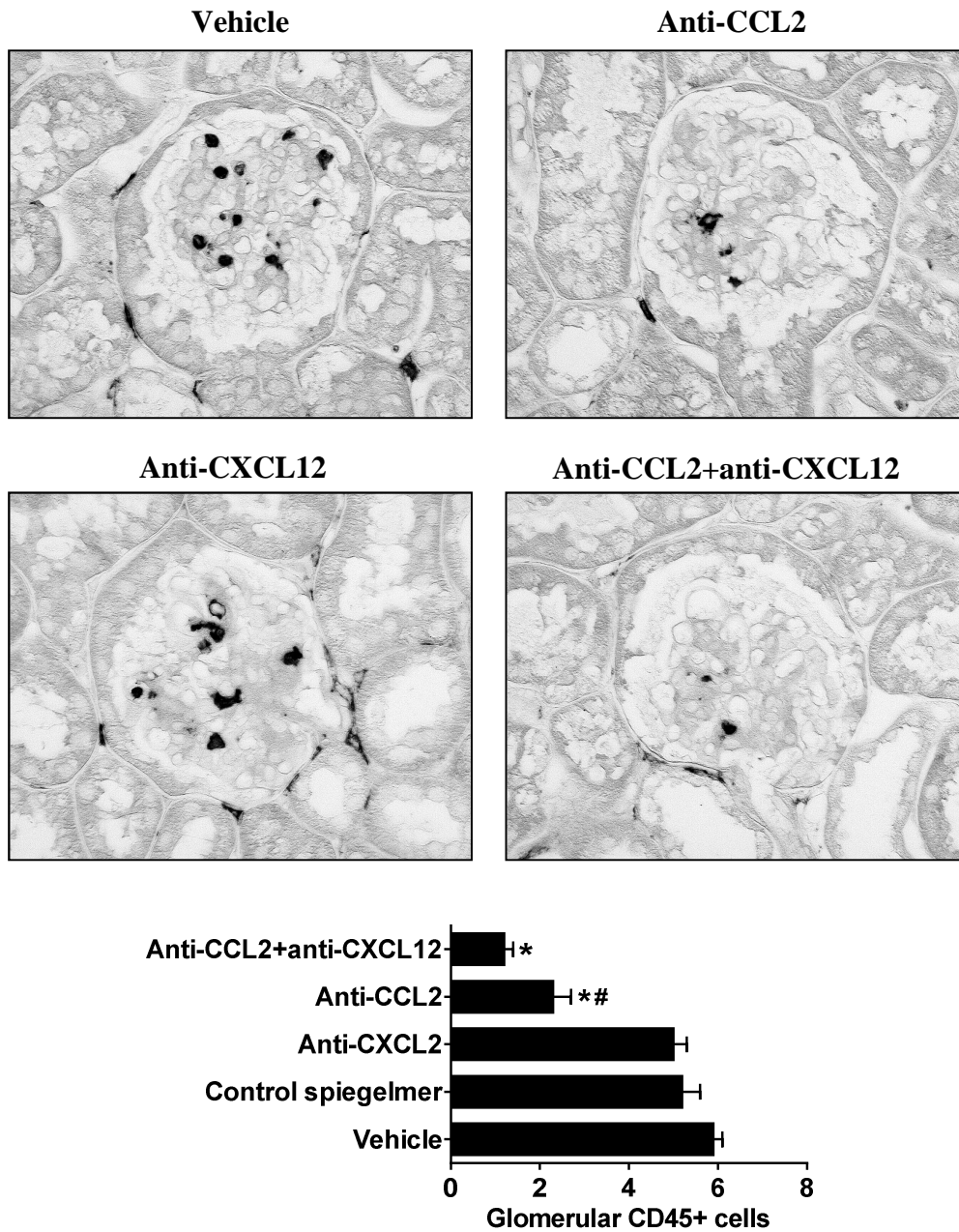


Figure 18: Glomerular leukocyte infiltrates in 1K db/db mice. Renal sections from 1K mice of all treatment groups were stained for CD45 (original magnification 400x). The graph shows the mean number of CD45 positive cells in 15 glomeruli \pm SEM in sections from 6 months old 1K db/db mice of each group. Note that only anti-CCL2 Spiegelmer affected the number of glomerular CD45+ cells (* $p < 0.01$ versus control Spiegelmer, # versus both monotherapies).

4.1.7 Dual CCL2/CXCL12 blockade and renal mRNA expression of proinflammatory and podocyte parameters in db/db mice

We determined the mRNA expression levels of leukocyte- and podocyte-related genes in kidneys of 1K db/db mice. Both antagonists did not significantly alter intrarenal expression of their target gene (Figure 19). However, CCL2 blockade, and not CXCL12 blockade, was associated with lower mRNA levels of iNOS, a parameter of activated macrophages (Figure 19). The cytokine IL-6 showed a trend towards lower levels in all treatment groups. In contrast, CXCL12 blockade increased the mRNA levels of nephrin and podocin, two podocyte parameters, much more than CCL2 blockade. Dual chemokine blockade increased these two podocyte markers most significantly (Figure 20).

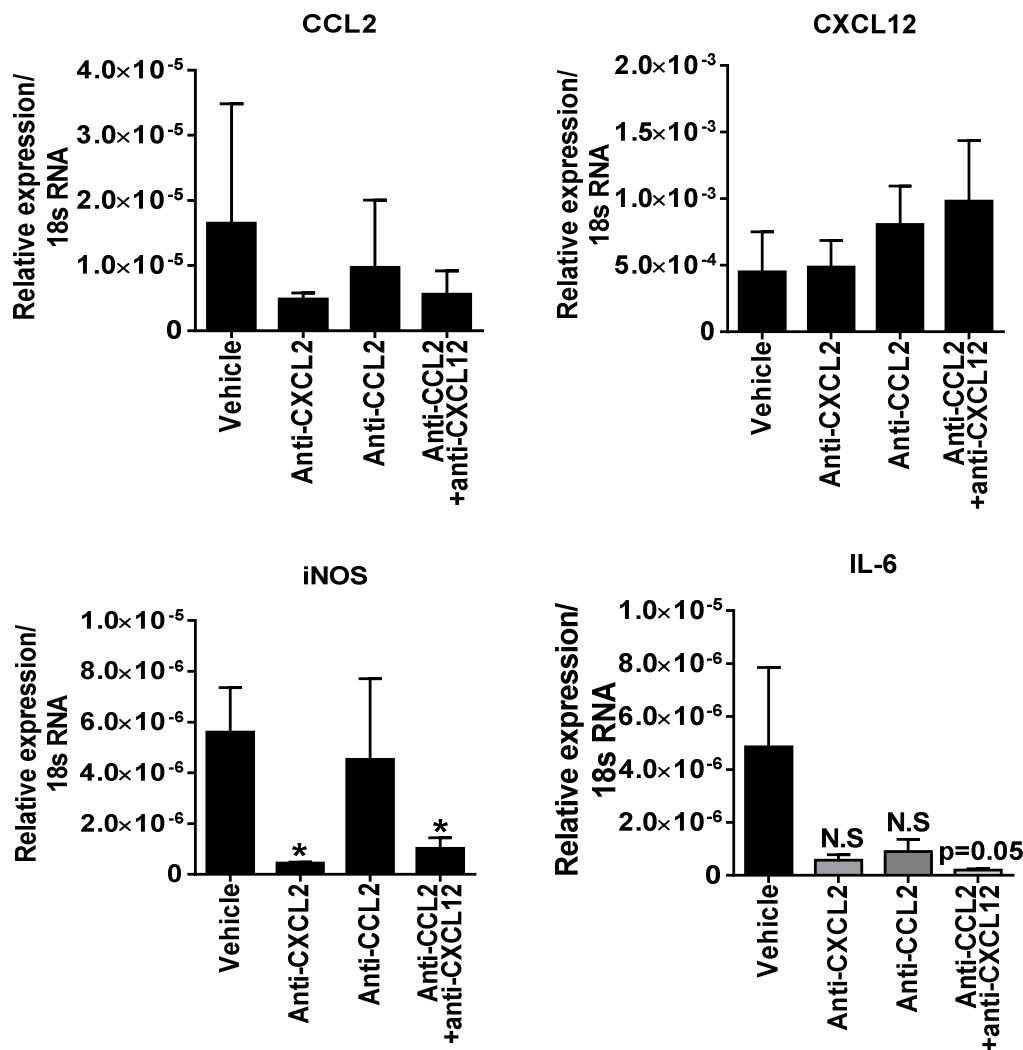


Figure 19: Renal mRNA expression in 1K db/db mice. RNA isolates from kidneys of 1K db/db mice underwent quantitative real-time PCR for a number of genes as indicated. Data are expressed as means of the ratio of the specific mRNA versus that of 18S rRNA \pm SEM. * $p < 0.05$, ** $p < 0.01$, *** $p < 0.001$ versus vehicle).

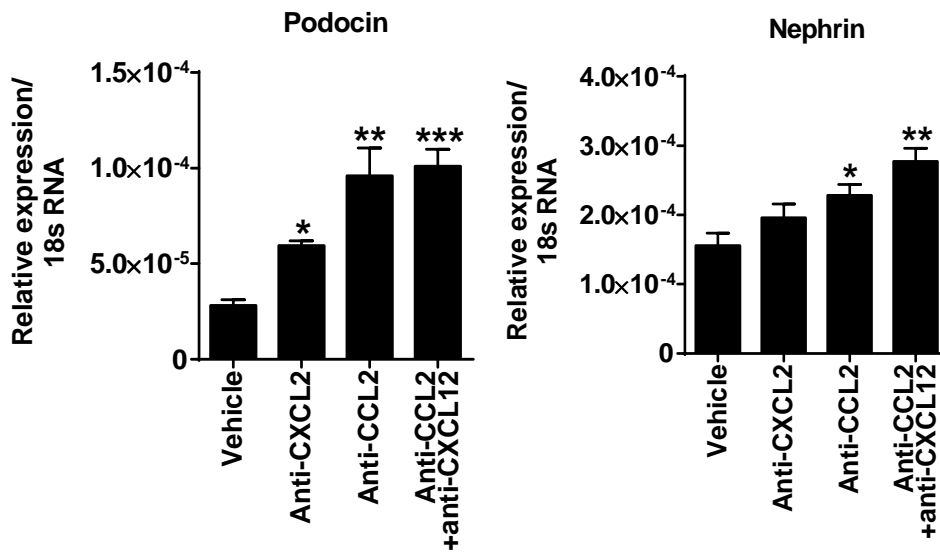


Figure 20: Renal mRNA expression in 1K db/db mice. RNA isolates from kidneys of 1K db/db mice underwent quantitative real-time PCR for a number of genes as indicated. Data are expressed as means of the ratio of the specific mRNA versus that of 18S rRNA \pm SEM. * $p < 0.05$, ** $p < 0.01$, *** $p < 0.001$ versus vehicle).

4.1.8 Dual CCL2/CXCL12 blockade has additive effects on podocyte numbers in db/db mice

We have previously documented that CXCL12 blockade protects 1K db/db mice from podocyte loss, as another marker of glomerular pathology in db/db mice¹⁵⁵. We questioned whether dual chemokine blockade could have additive protective effects on podocytes. Thus, we quantified glomerular podocytes by WT-1 immunostaining in all groups of 1K db/db mice. Compared to an average number of 15-20 WT-1 positive podocytes in murine glomerular cross sections (data not shown) the 6 months old 1K db/db mice revealed only an average of 11 cells per glomerular cross section. CCL2 and particularly CXCL12 blockade both significantly increased glomerular podocyte counts (Figure 21). Interestingly, dual CCL2/CXCL12 blockade showed a small but statistically significant additive effect up to an average of 17 WT-1 positive cells per glomerular cross section (Figure 21).

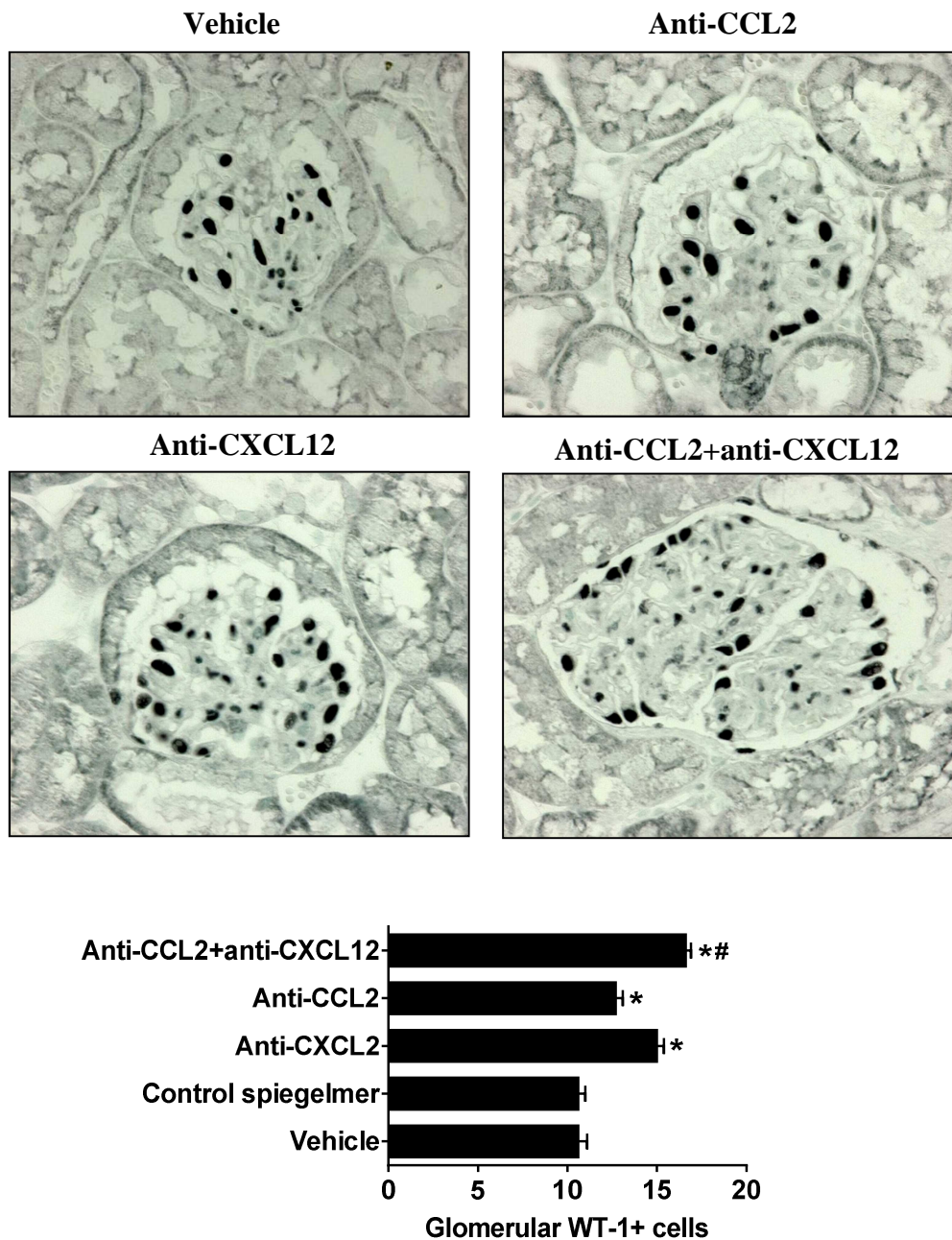


Figure 21: Podocyte numbers in 1K db/db mice. Renal sections from 1K mice of all treatment groups were stained for WT-1 (original magnification 400x). The graph shows the mean number of WT-1 positive cells in 15 glomeruli \pm SEM in sections from 6 months old 1K db/db mice of each group. Note the potent effect of the anti-CXCL12 Spiegelmer on the number of podocytes (* $p < 0.05$ versus control Spiegelmer) and the additive effect of dual blockade versus anti-CXCL12 monotherapy ($\dagger p < 0.05$ versus both monotherapies).

4.1.9 CXCL12 suppresses nephrin *de novo* expression of podocyte progenitors

How does CXCL12 blockade significantly increase podocyte numbers and nephrin expression without any direct effect on podocytes, which we had previously excluded?¹⁵⁵ Given the critical role of CXCL12 in the maintenance of stem cell niches in multi-organ systems, we evaluated the possibility that podocyte-derived CXCL12 may regulate the potential of renal progenitor cells to differentiate toward podocytes. Several groups have recently reported that a subpopulation of parietal epithelial cells (PECs) in glomeruli represent progenitor cells and have the capacity to differentiate into mature podocytes by progressively migrating and differentiating from the urinary pole of the Bowman's capsule toward the glomerular tuft¹⁵⁵⁷⁻¹⁹. We therefore questioned whether CXCL12 serves as a factor that regulates the differentiation of renal progenitor cells towards the podocyte phenotype. We indeed previously reported that¹⁵⁵ culturing human renal progenitors in the VRAD medium over a period of 2 days resulted in their differentiation into podocytes, as demonstrated by novel expression of nephrin, WT-1, synaptopodin, podocin, PDX, and anti-glomerular epithelial protein 1 (GLEPP-1) at both mRNA and protein levels. Since in our *in vivo* models CXCL12 blockade upregulated nephrin expression, in this study we evaluated primary cultures of human renal progenitors, which are already known to express receptors for CXCL12¹⁵⁵, for their potential to up regulate nephrin mRNA expression in presence or absence of this chemokine. The human embryonic kidney epithelial cell line 293 (HEK293) and human keratinocyte cell line (HACAT) were evaluated as additional controls for nephrin mRNA expression before and after treatment with VRAD. As shown in Figure 21A, the effect of VRAD treatment was irrelevant in HEK293 as well as in HACAT cell lines, while it induced a strong up-regulation of nephrin mRNA expression in primary cultures of human renal progenitors, as assessed by quantitative RT-PCR. Of note, adding recombinant CXCL12 suppressed nephrin mRNA up-regulation in a dose-dependent manner (Figure 22A). When CXCL12 was blocked with anti-CXCL12 Spiegelmer, *de novo* mRNA expression of nephrin was no longer compromised, an effect that was not observed with the unspecific control Spiegelmer (Figure 22B).

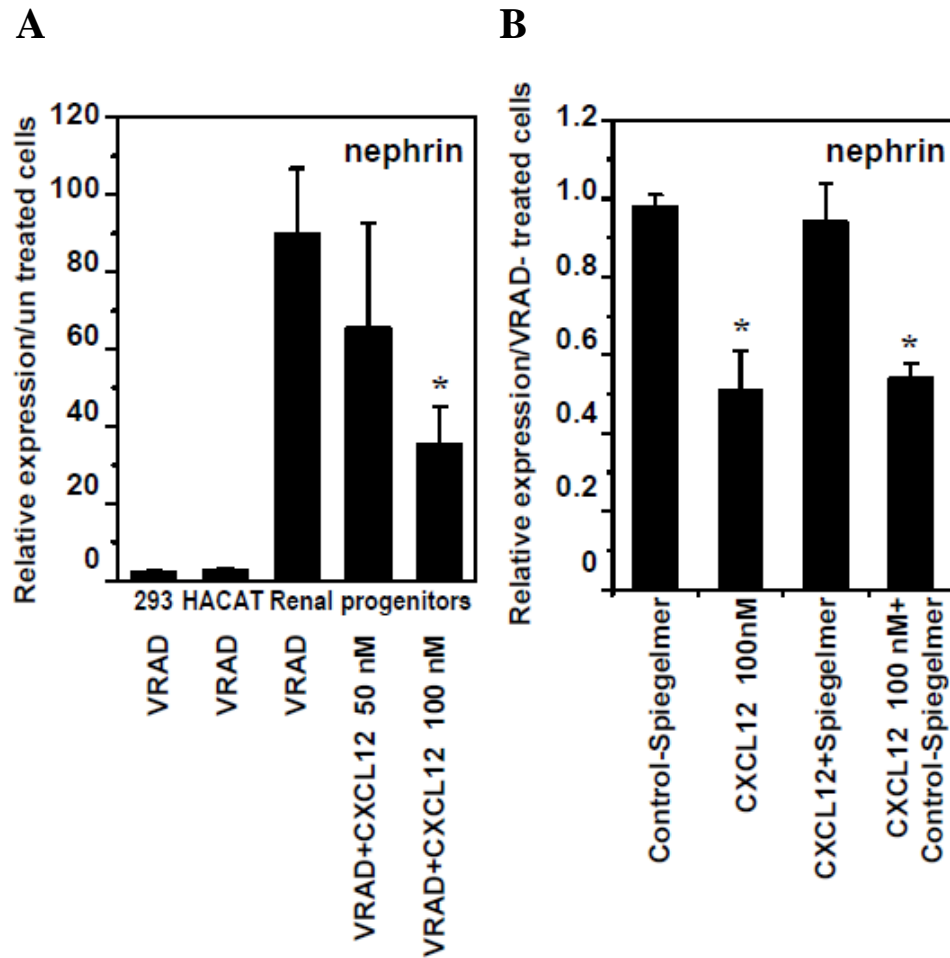


Figure 22: CXCL12 and *de novo* nephrin expression in renal progenitor cells. (A) HEK293, HACAT and human renal progenitors were cultured in VRAD medium as described in methods. Data are expressed as fold increase versus the respective untreated cell type, as assessed in identical number of cells. On human renal progenitors, recombinant CXCL12 was added at different concentrations as indicated and nephrin mRNA expression was determined by real-time RT-PCR. (B) Cells were cultured as before plus adding anti-CXCL12 or control Spiegelmer. Note that only anti-CXCL12 Spiegelmer prevented the CXCL12-mediated suppression of *de novo* nephrin mRNA expression. Data are expressed as fold increase versus VRAD-treated renal progenitors (B), as assessed in identical number of cells. Data in A and B are means \pm SEM. * $p < 0.05$.

4.2 Results part II

4.2.1 Cathepsin S expression in murine and human type 2 diabetic kidney disease

Cat S is associated with the pathophysiology of many inflammatory diseases and its inhibition by small antagonists was shown to be immunosuppressive in several mouse models. Previous studies with other cathepsin inhibitors suggested its protective role in diabetic kidney disease, but, so far, the role of Cat S in DN is unknown.

To study the role of Cat S in the progression of diabetic kidney disease, first we quantified the mRNA expression levels of cysteine Cat A, B, D, K, L and S in all solid organs of wild type BL6 mice. Gene expression profile revealed that Cat S is only found to be consistently expressed at much lower mRNA levels as compared to other Cats, especially in the kidney (Figure 23A). But, when the renal Cat S expression of 6 months old T2D male db/db mice was compared with their wild-type counterparts, a moderate induction was noted for Cats A, D, and S (Figure 23B). Interestingly, early uninephrectomy, which induces hyperfiltration as an accelerating patho-mechanism of glomerulosclerosis in T2D db/db mice, significantly induced Cat S selectively among all other studied Cats both at mRNA (Figure 24A) and protein level (Figure 24B) as compared to age matched controls.

Further, Cat S immunostaining on kidneys from 6 months old T2D male db/db mice displayed strong positivity in epithelial cells of proximal tubuli (Figure 25A). These cells, however, lacked any Cat S mRNA signal by *in situ* hybridization (Figure 25B), implying that filtered Cat S protein gets passively reabsorbed from the glomerular filtrate but is not produced by TECs. *In situ* hybridization displayed Cat S mRNA positivity only in single cells within glomeruli and the tubulointerstitium that co-stain with the mononuclear phagocyte markers F4/80 and CD68 (Figure 25B).

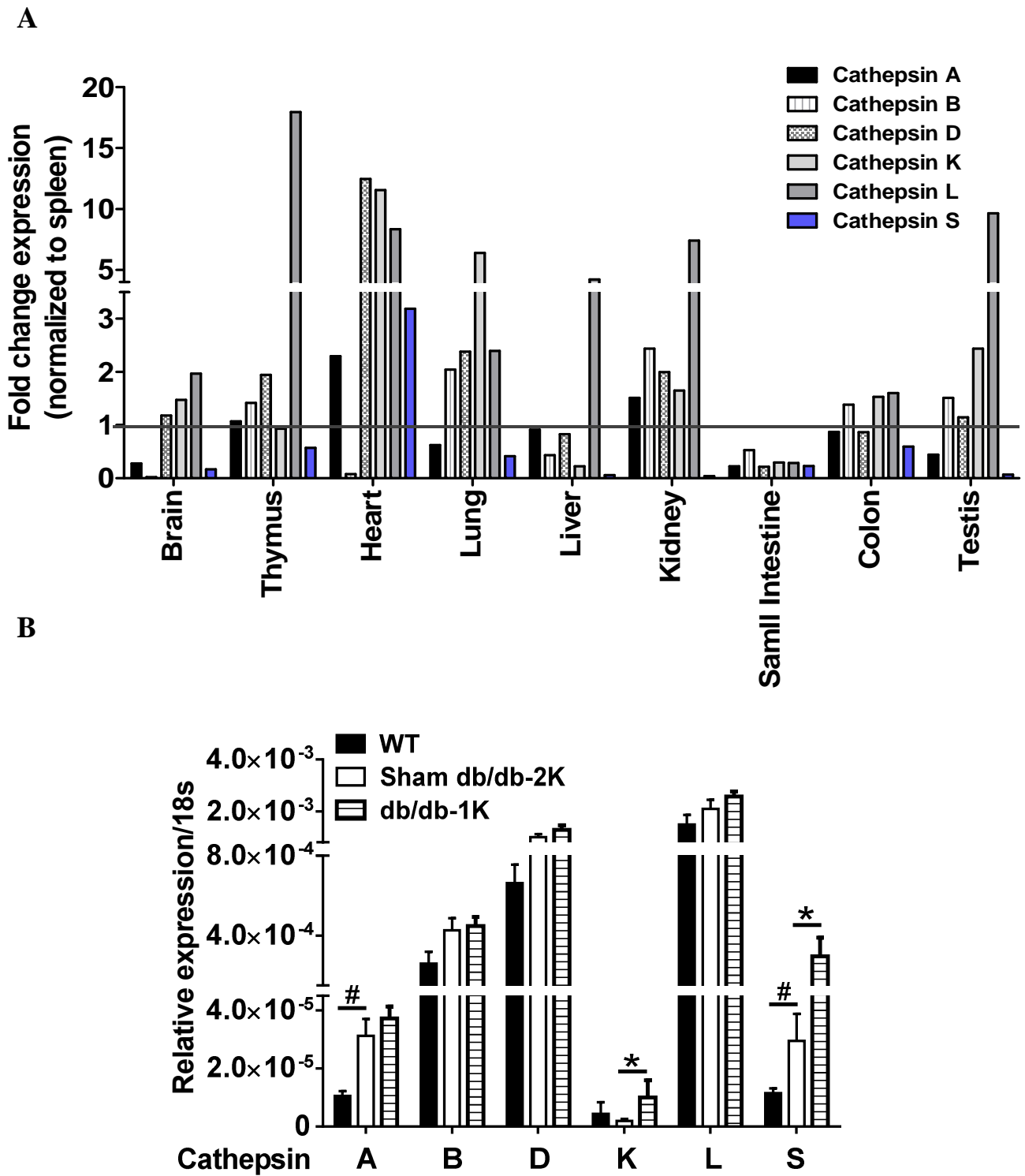
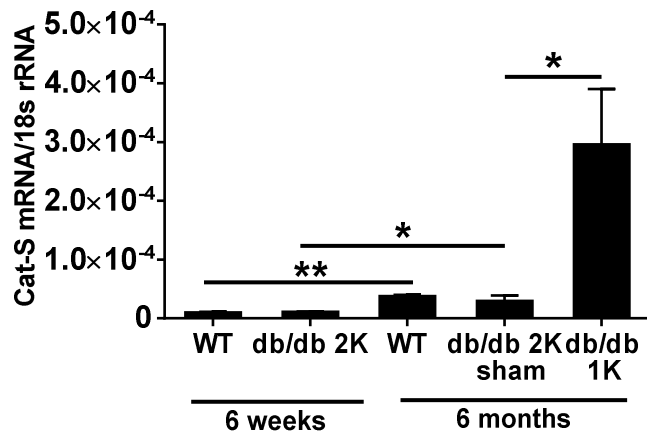


Figure 23: Expression of CCs in kidneys of wild type and db/db mice. (A) mRNA expression pattern of CCs in all solid organs of wild type C57BL6 mice. (B) Differential mRNA expression levels of CCs in kidneys from 6 months old db/db- sham operated and uninephrectomized mice. Age matched WT mice served as a control. Data are expressed as means of the ratio of the specific mRNA versus that of 18S rRNA (n=5-12 mice in each group). * $p < 0.05$ (db/db 1K versus Sham operated mice); # $p < 0.05$ (WT versus Sham operated mice)

A



B

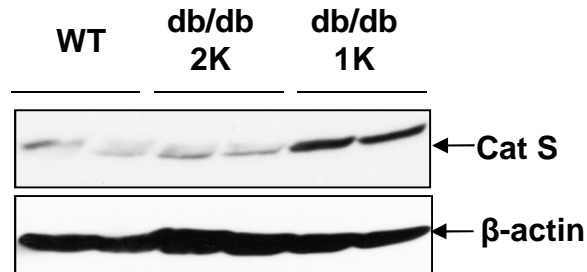


Figure 24: Expression of Cat S. (A) The relative expression of Cat S in kidneys of 6 weeks or 6 months old C57BL6 mice or db/db sham or uninephrectomized mice. (B) Western blot analysis of Cat S levels in kidneys extracts from 6 months old C57BL6 and db/db sham or uninephrectomized mice. Protein loading was corrected for sample protein concentrations and β -actin was used as a control. Data in A are expressed as means of the ratio of the specific mRNA versus that of 18S rRNA. Data in A and B are means \pm SEM of 5-12 mice in each group. * $p < 0.05$, ** $p < 0.01$, *** $p < 0.001$ age matched controls.

To further explore the functional relevance of Cat S in human diabetic kidney disease, we performed both microarray and quantitative real time PCR analysis on micro-dissected kidney tissue samples received from an independent set of 4 and 5 healthy and diseased individuals respectively. Both analysis revealed a 2-3 folds higher Cat S gene expression level at both glomerular and tubular compartments as compared to healthy kidney (Figure 26).

Thus, Cat S expression is selectively induced among other Cats in diabetic kidney disease, which originates to mononuclear macrophage infiltrates. In addition, tubular cells of the mouse kidney are loaded with Cat S protein even under physiological conditions, which suggests that circulating Cat S passes the GFB barrier and gets reabsorbed by proximal TECs. Together, these observations raise many possibilities for the potential role of Cat S in the pathogenesis of DN.

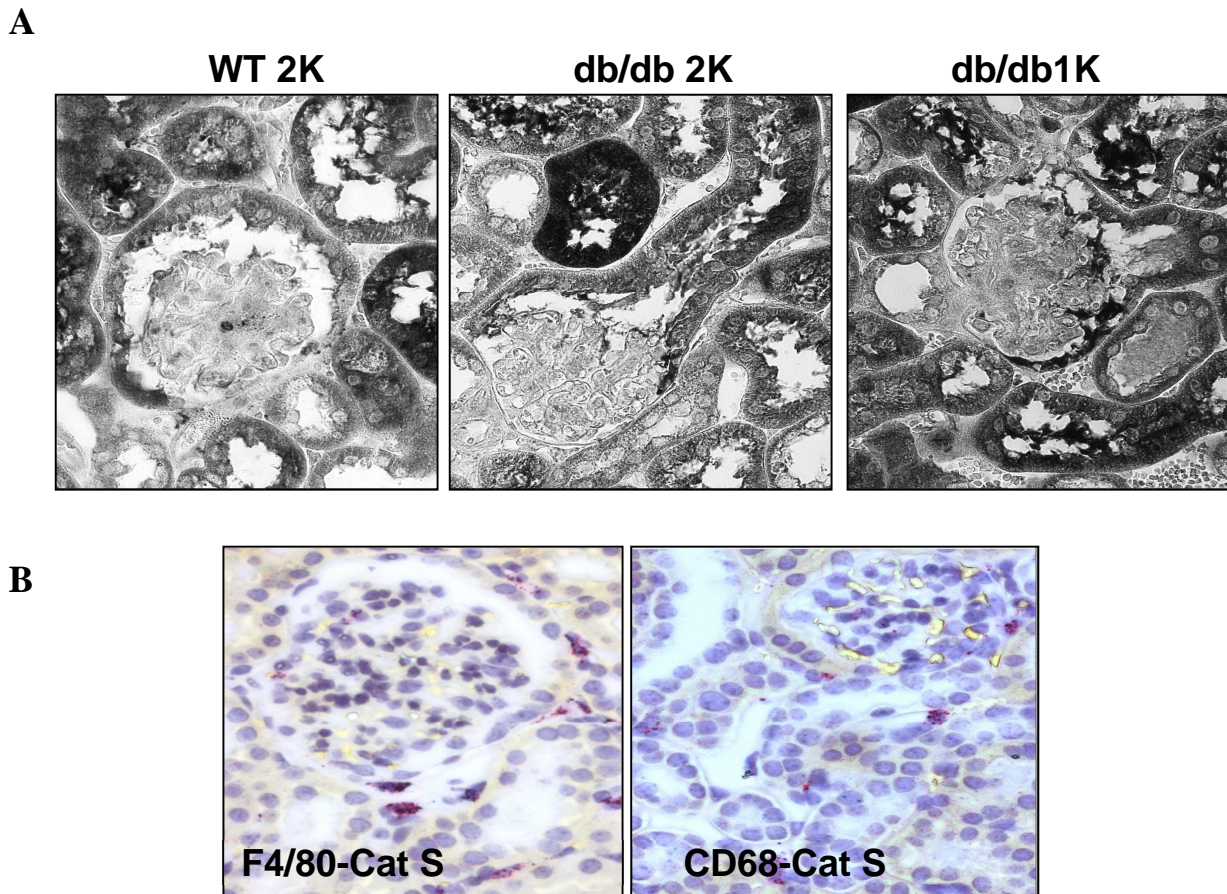


Figure 25: Cat S in-situ hybridization and immunohistochemistry. (A) Kidney sections were prepared for Cat S immunostaining and (B) for in-situ hybridization as described in methods. Cat S mRNA expression is indicated by red colour. Co-staining by either F4/80(macrophages), CD68 (myeloid DCs) is shown in blue colour, respectively. Representative images are shown here at original magnifications of 100x, 200x.

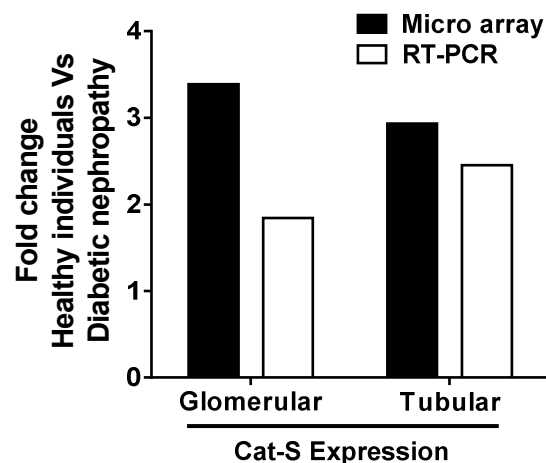


Figure 26: Cathepsin S gene expression in human DN: Microarray and real time PCR analysis were performed on micro-dissected glomeruli and tubulointerstitial compartments from human biopsies tissues of patients with DN (n=5), and controls (living donar, LD, n=7). Gene expression of Cat S gene was significantly upregulated in DN, as compared to controls. Shown are the fold changes of the transcript with the highest probe coverage and quantitative Cat S mRNA expression by real-time RT-PCR. Shown are the fold changes of the expression.

4.2.2 RO5461111 inhibits Cat S activity in db/db mice

To test the functional contribution of Cat S in diabetes, we used the inhibitor RO5461111 (Figure 27A). RO5461111 is a potent and highly selective compound that inhibits human Cat S with an IC_{50} of 0.4 nM and murine Cat S of 0.5 nM. No submicromolar inhibition of any other Cats (Cat B, Cat K, Cat L and Cat V) tested was detected (Table 8). Oral administration of RO5461111 by food admix (87.5 mg/kg of food) to male db/db mice resulted in a dose of 10 mg/kg body weight and resulted in robust lip10 (substrate for Cat S) fragment accumulation in spleens taken at 6 month of age (Figure 27B). RO5461111 bioactivity *in vivo* was also tested by measuring the plasma Cat S activity on Z-VVR-AFC substrate at the beginning and at the end of the study. RO5461111 treatment significantly suppressed the plasma Cat S activity as compared to vehicle-treated mice at 6 month of age and versus baseline activity at treatment initiation at 4 month of age (Figure 27C).

Furthermore, RO5461111 treatment significantly down regulated the kidney Cat S expression at 6 months as evident by real time PCR and western blot (Figure 27D and 27E). Together, RO5461111 is an orally available small molecule Cat S antagonist with favorable pharmacodynamic and pharmacokinetic profiles to efficiently block Cat S over a prolonged period of time in mice (with T2D).

Table 8. *In vitro* enzyme inhibition assay

Cathepsin	IC_{50}
Human Cat S	0.4 nM
Mouse Cat S	0.5 nM
Human Cat K	>25 μ M
Human Cat L	49 μ M
Human Cat B	44 μ M
Human Cat V	1.3 μ M

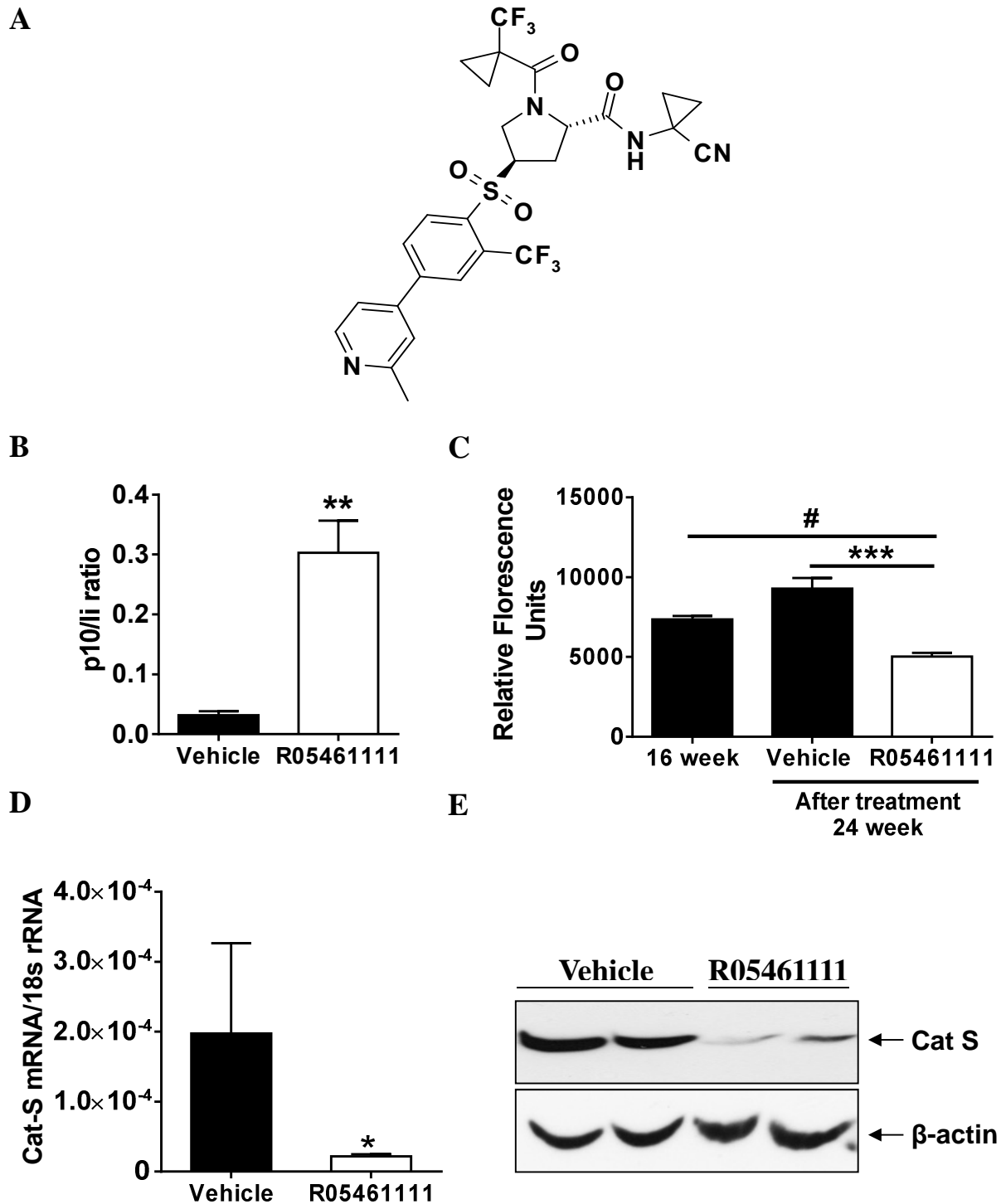


Figure 27: R05461111 selectively inhibits Cat S activity in db/db mice (A) Chemical structure of R05461111. (B) Invariant chain p10 levels were estimated from spleen tissue using western blotting. (C) The plasma Cat S activity was determined using Z-VVR-AFC substrate, before and after treatment at 6 months old and baseline expression at 16weeks old db/db mice. (D) Renal mRNA expression levels of Cat-S in 1K db/db mice were determined by qPCR. (E) Western blot analysis of Cat S protein levels in kidney of 1K db/db mice. Data in D are expressed as mean±SEM of the ratio of the specific mRNA versus that of 18s ribosomal RNA. *p<0.05, **p<0.01, ***p<0.001 versus vehicle group (B, C and D) and #p<0.01 versus 16week old db/db mice (C)

4.2.3 RO5461111 treatment reduces glomerulosclerosis in db/db mice

To test whether pharmacological blockade of Cat S with RO5461111 affects kidney disease in T2D, we fed uninephrectomized 1K db/db mice with either food admix that contained RO5461111 or standard diet. Treatment was continued for 8 weeks from age 4 to 6 months, when kidneys were removed for analysis. RO5461111 treatment significantly reduced the number of glomeruli affected by global glomerulosclerosis and increased the number of unaffected glomeruli as compared to mice fed with control diet (Figure 28A). Together, blockade of Cat S showed an overall improvement in the kidney pathology by reducing the glomerulosclerosis in uninephrectomized db/db mice (Figure 28B).

4.2.4 RO5461111 treatment reduces podocyte loss in db/db mice

Podocytes are an essential part of the GFB and podocyte injury and loss are the patho-mechanistic hallmark of proteinuria and glomerulosclerosis in diabetes²⁶. So, we wondered whether RO5461111 treatment has any protective effect on podocytes loss in the glomeruli of uninephrectomized db/db mice. Therefore, we quantified WT-1 positive cells in glomeruli of both treated and untreated 1K db/db mice at 6 month of age. RO5461111 treatment significantly increased the total numbers of glomerular podocytes (Figure 29A and Figure 29B) and this was associated with a significant increase in the renal mRNA expression levels of the podocyte slit diaphragm-related markers nephrin and podocin (Figure 29C). Together, therapeutic Cat S blockade with RO5461111 significantly prevented podocyte loss in uninephrectomized db/db mice.

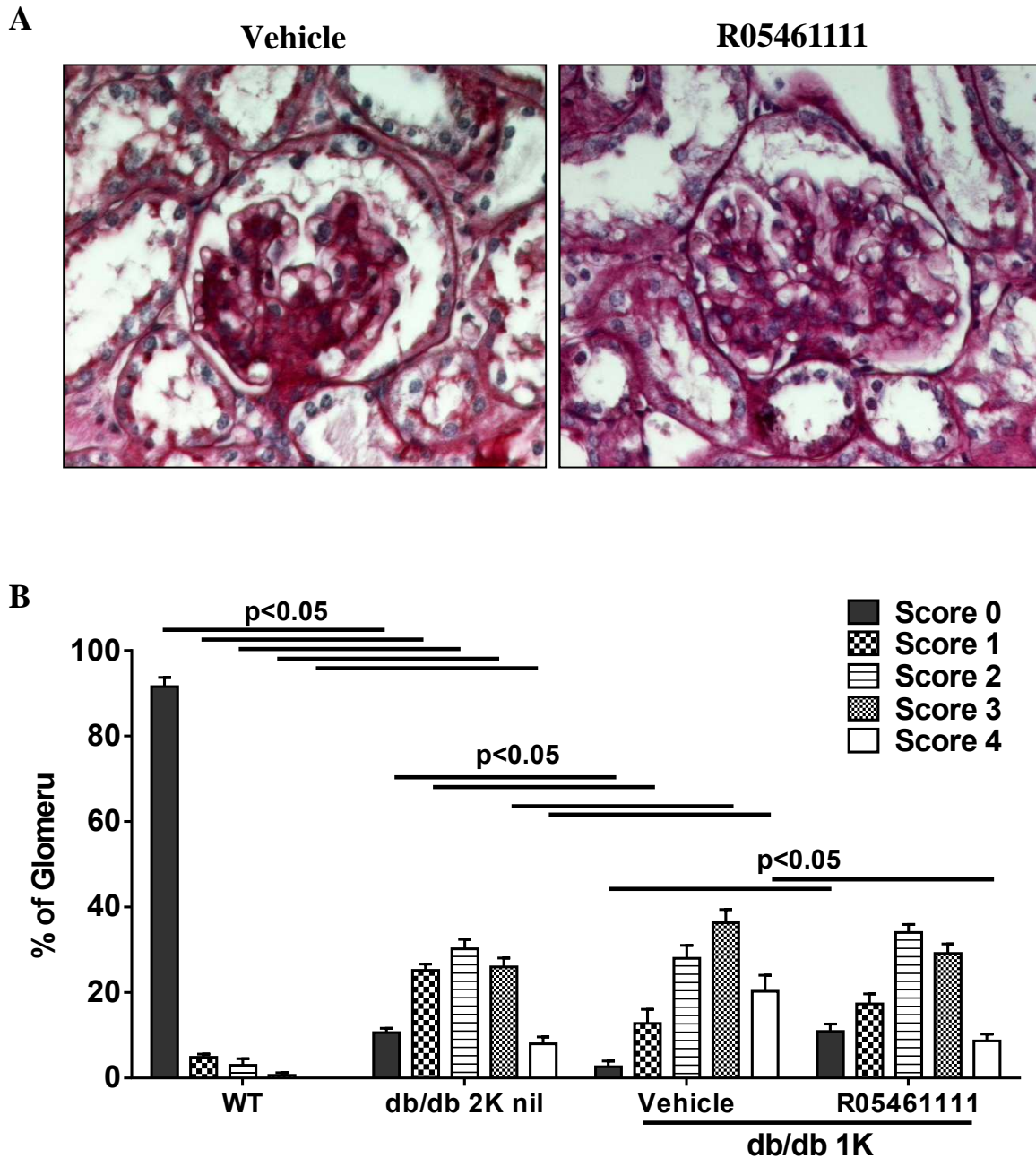


Figure 28:RO5461111 reduces the glomerulosclerosis in 6 month old 1K db/db mice: (A) Renal pathology in 6 months old db/db mice: Kidney sections from both treated and untreated mice were stained with Periodic acid-Schiff (PAS) reagent. Stained images show representative glomeruli from each group (original magnification 400x). (B) PAS sections were scored to analyse the extent of glomerulosclerosis. 15 glomeruli from one renal section were scored by using a semi-quantitative fashion ranging from 0-4 as described in the methods section. Note that uninephrectomy was associated with a shift toward higher scores of glomerulosclerosis as seen in vehicle treated mice, but with RO5461111 treatment the overall scores were significantly reduced. The graph illustrates the mean percentage of each score \pm SEM from all mice in each group. Original magnification, 400x

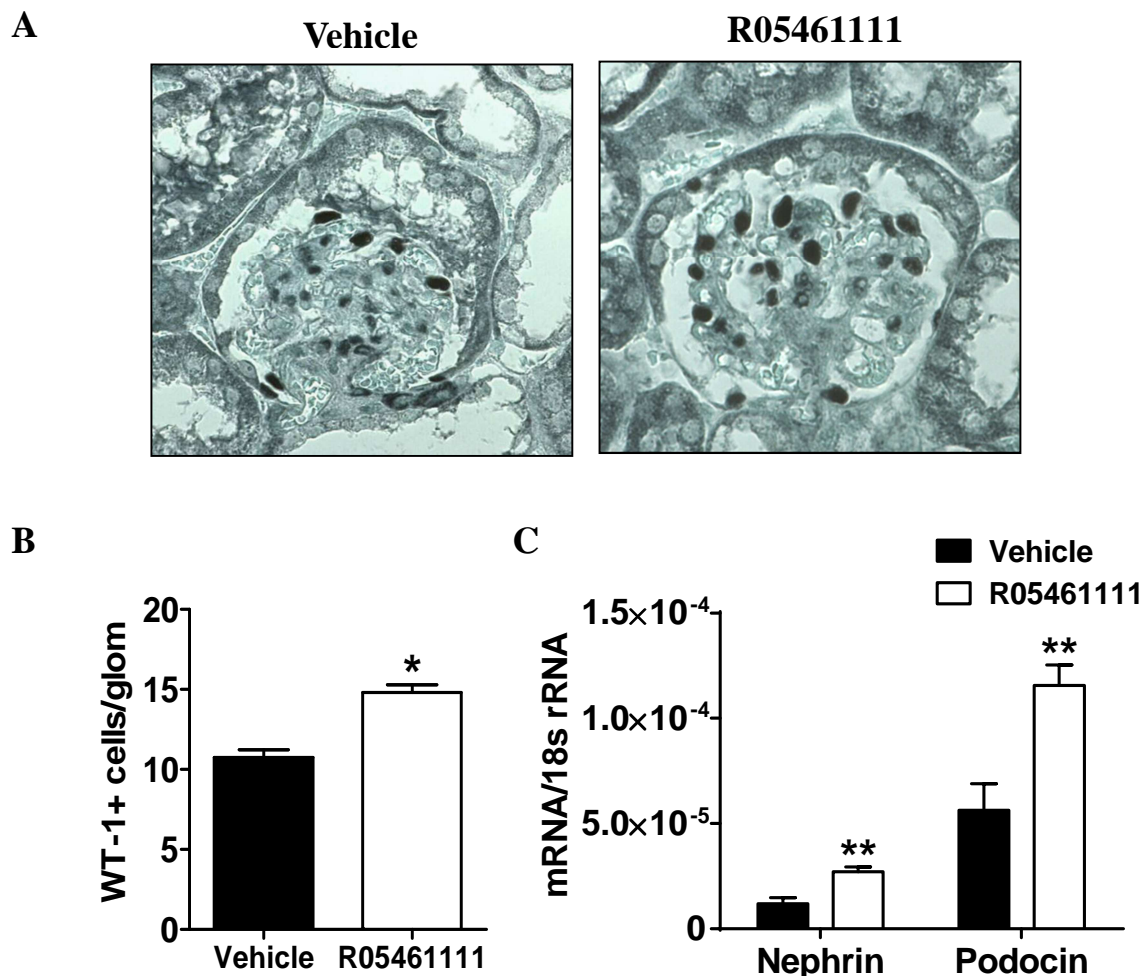


Figure 29: Podocyte numbers in 1K db/db mice. (A) Renal sections from 1K mice of both treatment groups were stained for WT-1. Original magnification, 400x. (B) The graph shows the mean±SEM WT-1 positive cells in 15 glomeruli in sections from 6month-old 1K db/db mice of both treated and untreated groups. (C) Renal mRNA expression in 1K db/db mice. RNA isolates from kidneys of 1K db/db mice underwent quantitative real-time PCR for genes as indicated. Data are expressed as mean±SEM of the ratio of the specific mRNA versus that of 18s ribosomal RNA* p<0.05, ** p<0.01 versus vehicle group

4.2.5 RO5461111 treatment reduces albuminuria in db/db mice

Macroalbuminuria is a clinically important diagnostic and prognostic biomarker of glomerular injury in diabetes. So, we measured UACR at the end of the study in both treated and untreated animals. The beneficial effect of RO5461111 treatment on glomerulosclerosis and podocyte loss was associated with a 60% reduction of albuminuria as compared to the control diet-fed db/db mice (Figure 30).

Together, Cat S blockade with RO5461111 significantly prevented podocyte loss, proteinuria, and glomerulosclerosis in T2D db/db mice.

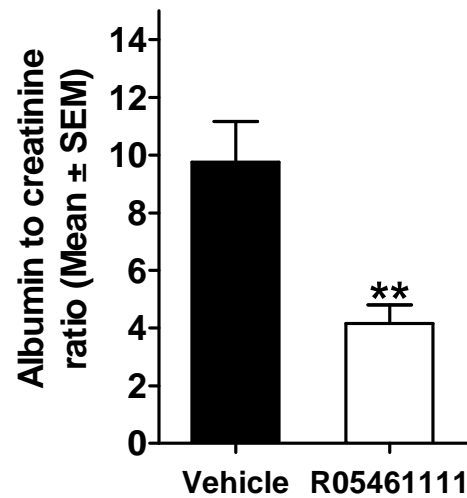


Figure 30: Albuminuria in 6-month-old db/db mice. UACR were determined as a functional parameter of glomerular filtration at the end of the study. Data are given as the mean±SEM from at least eight mice in each group. ** p<0.01 versus vehicle group

4.2.6 Cat S directly injures glomerular endothelial cells rather than podocytes

To confirm the striking effect of Cat S inhibition on podocytes and to observe whether Cat S has direct effect on podocytes *in vitro*, we used the ECIS assay system which allows us to quantify monolayer barrier function by assessing trans-cellular electric capacitance (ref). Surprisingly, increasing doses of recombinant Cat S had no effect on podocytes or other epithelial cell types (Figure 31A and 31B) while the trans-cellular capacitance significantly increased in monolayers of GEnC (Figure 31C). This effect was reversible by RO5461111 co-incubation in a dose-dependent manner (Figure 31C). How does Cat S affect endothelial barrier function? We found that Cat S exposure led to a dose-dependent-detachment of GEnC from culture dishes, a process that could be prevented by RO5461111 co-incubation (Figure 31D). In contrast, podocytes adherence remained unaffected by Cat S. Together, Cat S does not directly impair barrier function or detachment of epithelial cells such as podocytes and TECs, but it leads to a dose-dependent detachment of endothelial cells.

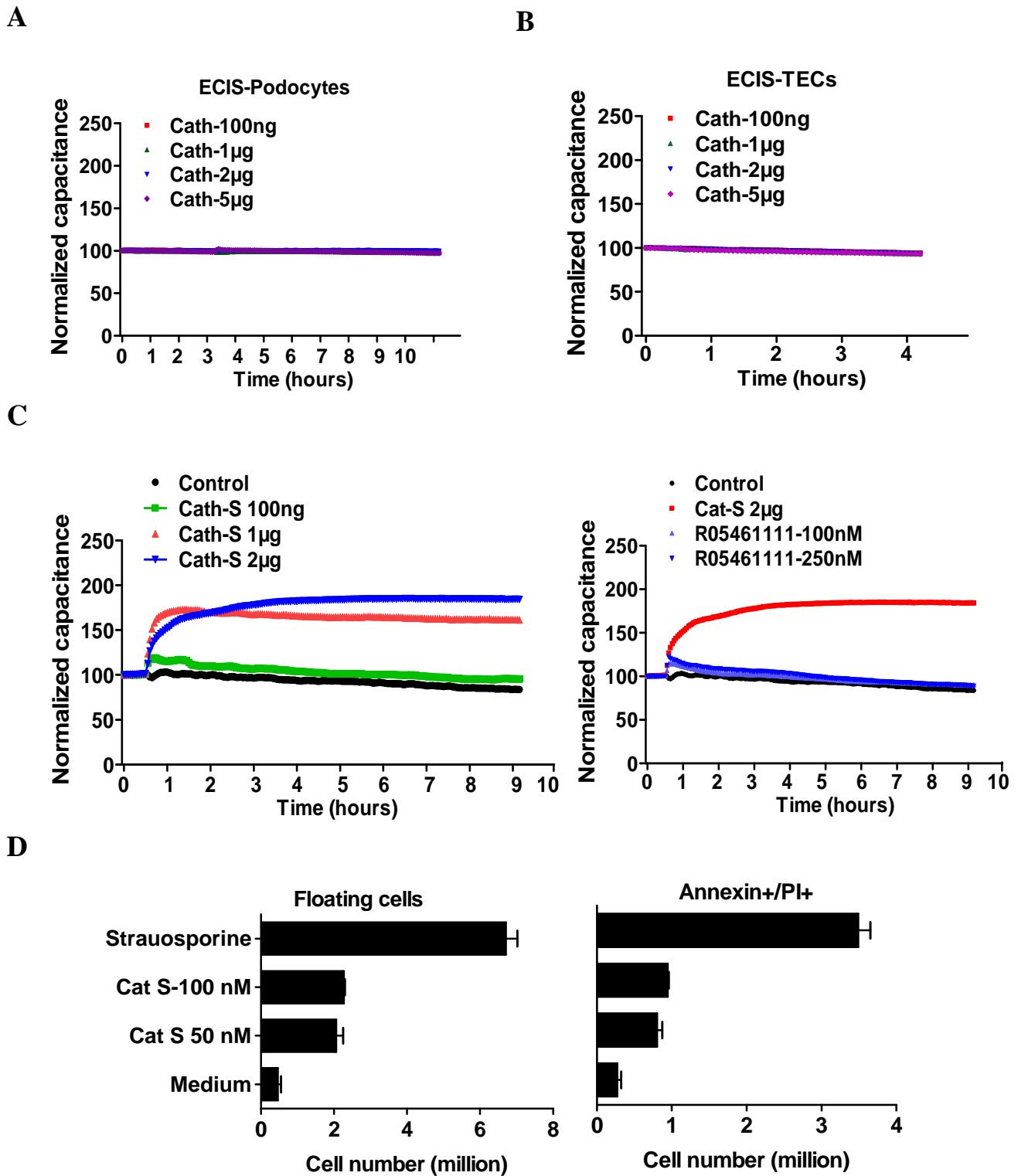


Figure 31: Cat S impairs the endothelial barrier function *in vitro*: (A) Primary murine podocytes, (B) Tubular epithelial cells (TECs) and (C) GEnCs were cultured on ECIS culture ware and grown to confluency. Cells resistance and capacitance were analyzed for indicated time. Observe that Cat S had no effect on of podocytes or epithelial cell types (A and B), while the trans-cellular capacitance significantly increased in monolayers of GEnCs (C). This effect was reversible by RO5461111 co-incubation in a dose-dependent manner (C). (D) FACS analysis was done on floating GEnCs released into media after Cat S stimulation. Data in A and B are expressed as normalized resistance or capacitance \pm SEM for three independent experiments. Data in C are represented as total cell number in millions. * $p < 0.05$, ** $p < 0.01$ versus control medium

4.2.7 RO5461111 reduces oxidative stress-induced vascular permeability *in vivo*

Oxidative stress is a major element of endothelial dysfunction in diabetes that contributes to diabetes complications such as diabetic glomerulosclerosis. To test whether Cat S is a mediator of oxidative stress-related endothelial dysfunction, we performed M. cremaster *in vivo* microscopy upon local ischemia and monitored leukocyte recruitment and FITC-dextran leakage from the intravascular compartment into the interstitial space (as an *in vivo* model of endothelial activation and barrier dysfunction). RO5461111 treatment significantly reduced the trans- endothelial migration of leukocytes as well as the extravasation of dextran from the microvasculature (Figures 32A-C). In addition, studies have reported that mice lack in eNOS gene (endothelial nitric oxide synthase) developed the DN. To confirm the treatment effect on endothelial vasculature in db/db mice, we measured the mRNA expression levels of endothelial damage markers, VCAM, ICAM and eNOS in kidneys of both treated and untreated mice at 6 month old. RO5461111 treatment significantly down regulated VCAM, but not ICAM as compared to vehicle fed mice (Figure 32D). Interestingly, eNOS expression was moderately upregulated in treatment group, indicating that RO5461111 treatment restored the endothelial vasculature (Figure 32D). Thus, Cat S mediates oxidative-stress induced microvascular permeability. As proteinuria is a biomarker of endothelial dysfunction in diabetes, the Cat S-dependent albuminuria in db/db mice should relate to this phenomenon.

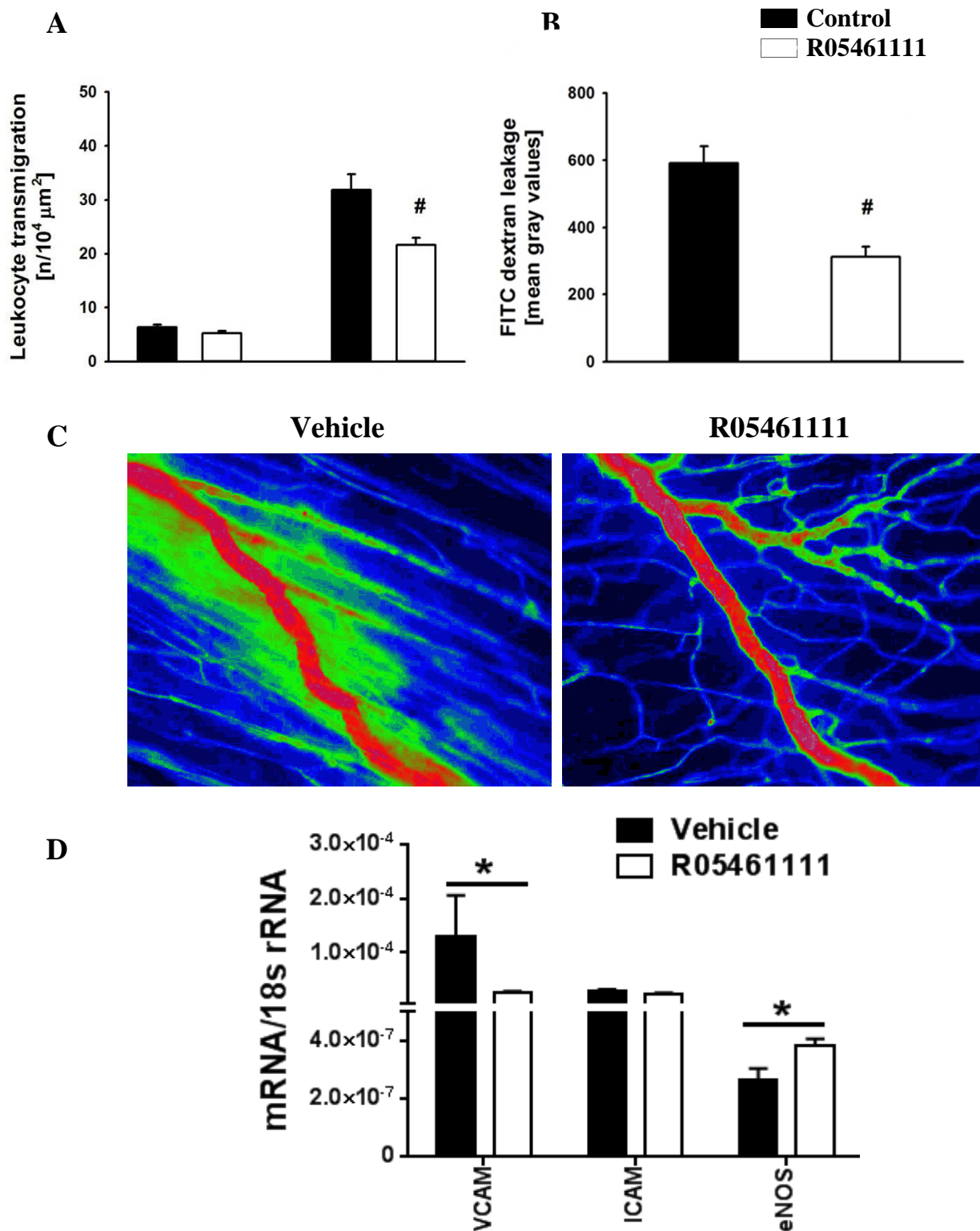


Figure 32: *In vivo* microscopy of cremaster muscles. *In vivo* microscopy was performed on cremaster muscle post-capillary venules as described in methods. (A) Leukocyte trans-endothelial migration was determined 130min after reperfusion. (B) Microvascular FITC-dextran leakage was determined 30min after dextran injection, i.e 130min after reperfusion. (C) Representative images illustrate the increase of vascular dextran permeability with (right) or without inhibitor (left image). (D) Renal mRNA expression of ED markers in 1K db/db mice. RNA isolates from kidneys of 1K db/db mice underwent quantitative real-time PCR for genes as indicated. Data are expressed as mean±SEM of the ratio of the specific mRNA versus that of 18s ribosomal RNA. Data in A B and D are means ± SEM. # $p < 0.05$ versus vehicle.

4.2.8 Cat S blockade reduces glomerular leukocyte recruitment and inflammation in db/db mice with T2D

Chemokine mediated leukocyte infiltrates play a key role in renal vascular inflammation in diabetes mellitus, and promote DN by local production of pro-inflammatory mediators. Given the role of Cat S in leukocyte extravasation through activated endothelia, we speculated that Cat S would also promote glomerular leukocyte recruitment and glomerular inflammation. Flowcytometric analysis of renal cell suspensions prepared from uninephrectomized 1K db/db mice at the end of the study showed that RO5461111 treatment had significantly reduced intrarenal CD45+ leukocyte infiltrates, half of them each being neutrophils and Ly6C+ mononuclear phagocytes (Figure 33).

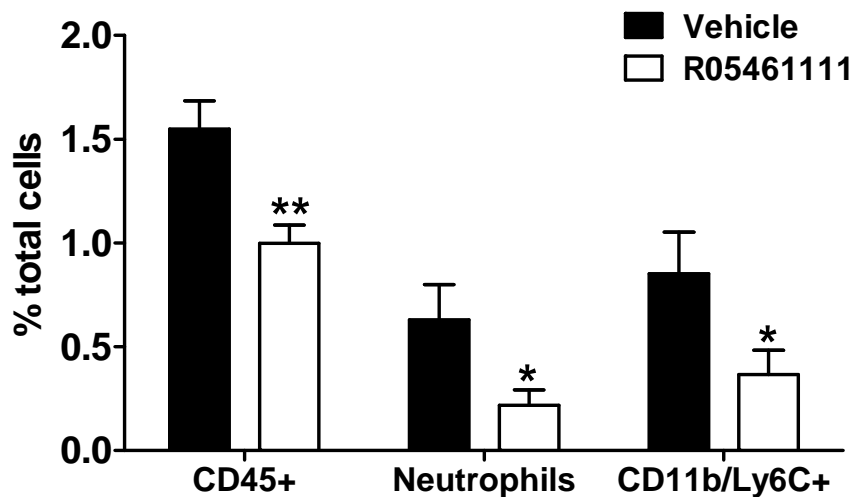


Figure 33: FACS analysis of whole kidney cells for CD45 positive leukocytes, Ly6C and 7/4 double positive neutrophils and CD11b and Ly6C double positive macrophages. For each sample 50,000 events were counted. Graphs represent the mean percentage of events for each group. Data represented are mean \pm SEM (n =5-7), * p<0.05, * p<0.001 versus vehicle treated group.

Infiltrating glomerular macrophages are hallmark of renal vascular inflammation, and their accumulation is a characteristic feature of DN. We therefore evaluated the number of glomerular macrophages on kidney sections stained for Mac2 (Figure 34A). Immunostaining revealed that RO5461111 treatment had significantly reduced the numbers of glomerular as well as interstitial macrophages compared to wild type and sham-operated db/db mice (Figure 34A and 34B).

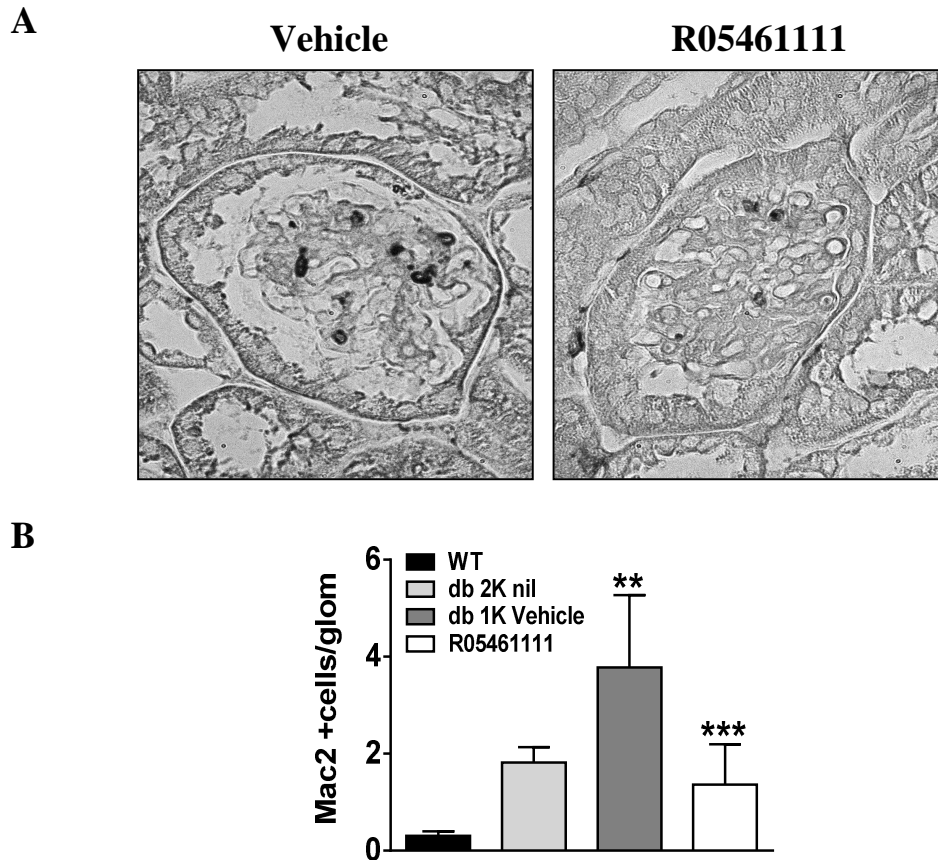


Figure 34: (A) Renal sections from both treated and untreated mice were stained for Mac2. (original magnification x400). Values are shown as number of positive cells in 15 glomeruli. (B) The representative graphs show the number of Mac2 positive cells from each group. Note that all inflammatory leukocyte numbers were reduced in treatment group. *** $p < 0.001$ versus vehicle treated group, # $p < 0.01$, db 2K vs vehicle

We further determined the mRNA expression levels of proinflammatory and macrophage activation markers in kidneys of 6months old 1K db/db mice. In correlation with less macrophage number, RO5461111 treatment significantly reduced the renal mRNA expression levels of proinflammatory cytokines, IL-6 and TNF and macrophage related markers, iNOS and CCL2 (Figure 35).

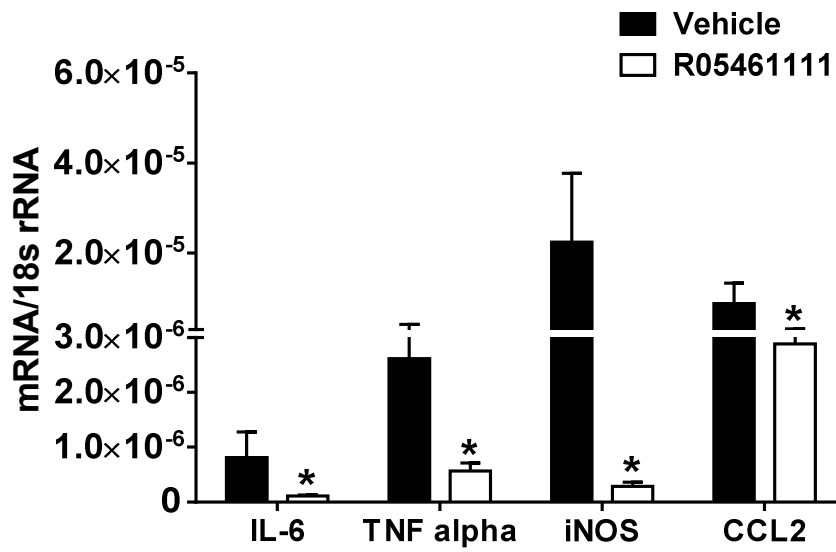


Figure 35: Renal mRNA expression in 1K db/db mice. RNA isolates from kidneys of 1K db/db mice underwent quantitative real-time PCR for genes as indicated. Data are expressed as mean \pm SEM of the ratio of the specific mRNA versus that of 18s ribosomal RNA. * p<0.05 versus vehicle group

Together, Cat S-driven endothelial dysfunction involves an increased microvascular permeability, which includes leukocyte transmigration and blockade of Cat S reduced renal leukocyte recruitment and inflammation in db/db mice with T2D.

5. Discussion

5.1 Chemokine blockade in diabetic nephropathy

DN is a leading cause of CKD¹⁶. It is well accepted that, inflammation plays a crucial role in promoting the development and progression of DN. Numerous pathomechanisms including increased local expression of growth factors and inflammatory mediators are known to induce DN²⁰. The majority of chemokines belongs to the latter group of factors because pro-inflammatory chemokines promote tissue inflammation and remodelling by recruiting and activating immune cells in DN like in other types of kidney diseases^{50,52,199}. For example, targeted deletion or inhibition of CCL2 and their receptor CCR2 prevented the glomerulosclerosis by blocking macrophage recruitment to glomeruli of mice with T1 and T2D^{118,119}. Moreover, recent studies from our laboratory have shown that delayed onset of CCL2 blockade was able to prevent diabetic glomerulosclerosis by preventing glomerular macrophage recruitment in late-stage DN of uninephrectomized db/db mice with type 2 diabetes¹³⁰.

In addition, a subgroup of the chemokine super family, known as ‘homeostatic’ chemokines, displays functions independent of tissue inflammation⁷⁶. For example, blockade of CXCL12 prevented diabetic glomerulosclerosis which was independent of glomerular macrophage recruitment, but a profound effect on podocyte counts and proteinuria was documented¹⁵⁵. Therefore, we hypothesized that dual blockade of both chemokines; compared to monotherapies of either CCL2 or CXCL12 antagonists, might have beneficial effects in an accelerated mouse model of DN.

Data of the present study confirm our previous reports on CCL2 blockade with Spiegelmers in the same experimental set up. In the present as well as in the previous studies CCL2 blockade resulted in a 50-60% reduction of glomerular leukocytes, which entirely represent macrophages in the db/db mouse model setup¹³⁰. These findings are consistent with data from models of T1D and T2D in *Ccl2*-deficient mice or with CCR2 blockade in 1K db/db mice^{118,119}. CCR2+ macrophages belong to the proinflammatory (M1) phenotype that contribute to intrarenal inflammation and tissue damage via the release of ROS or cytokines like TNF- α . As such anti-CCL2-Spiegelmer-treated 1K db/db mice revealed lower numbers of glomerular leukocytes which were associated with lower intra-renal mRNA levels of iNOS, IL-6 or TNF- α at the end of the study. Consistent with our previous findings the protection from glomerulosclerosis with

CCL2 blockade correlated with some lower levels of proteinuria and a higher GFR¹³⁰. Thus, CCL2 blockade prevents the progression of DN by interfering with macrophage-driven glomerular inflammation.

The present study also reconfirms our previous data on CXCL12 blockade in this model¹⁵⁵. It was interesting that NOX-A12 prevented the progression of glomerulosclerosis in 1K db/db mice without affecting glomerular leukocyte counts indicating that the homeostatic chemokine CXCL12 is not involved in glomerular leukocyte recruitment. We had recently reported that CXCL12 is rather constitutively expressed in podocytes¹⁵⁵. CXCL12 blockade increased podocyte numbers in 1K db/db mice also in the present study. Furthermore, CXCL12 blockade increased the renal mRNA expression levels of nephrin and podocin, two podocyte slit membrane-related proteins that serve as markers of podocyte differentiation²⁰⁰. Podocyte damage is an important pathomechanism promoting the progression of diabetic glomerulosclerosis and seems to result from various triggers that foster podocyte dedifferentiation and podocyte apoptosis²⁰¹.

Till now, it remains unclear whether the beneficial effect of CXCL12 blockade on podocyte numbers relates to a protective effect on podocyte death or detachment or are rather due to enhanced podocyte regeneration from local podocyte progenitors, e.g. from PECs^{48,202}. The latter concept may be more likely because, CXCL12 blockade also mobilizes hematopoietic progenitor cells from the bone marrow²⁰³⁻²⁰⁵. Moreover, in recent years, several studies have clearly demonstrated the existence of renal progenitor system (both glomerular and tubular) in the kidney^{48,202,206,207} (Figure 36). These studies have demonstrated that the renal progenitors which are localized between vascular and urinary pole express both progenitor and podocyte markers, which proliferate and differentiate to generate novel podocytes²⁰⁶. In addition, inhibition of Notch signalling enhanced renal progenitor growth and increased podocyte numbers in experimental models of FSGS⁴⁷. By using *in vivo* multi-photon microscopy, Peterdi *et.al.* have demonstrated that, renal progenitors replaced the lost podocytes in rat models of PAN nephritis²⁰⁸. Consistent with these studies, our *in vitro* studies demonstrated that CXCL12 suppressed the induced maturation of renal progenitors towards podocytes as documented by inhibition of *de novo* nephrin expression. This effect was specific to

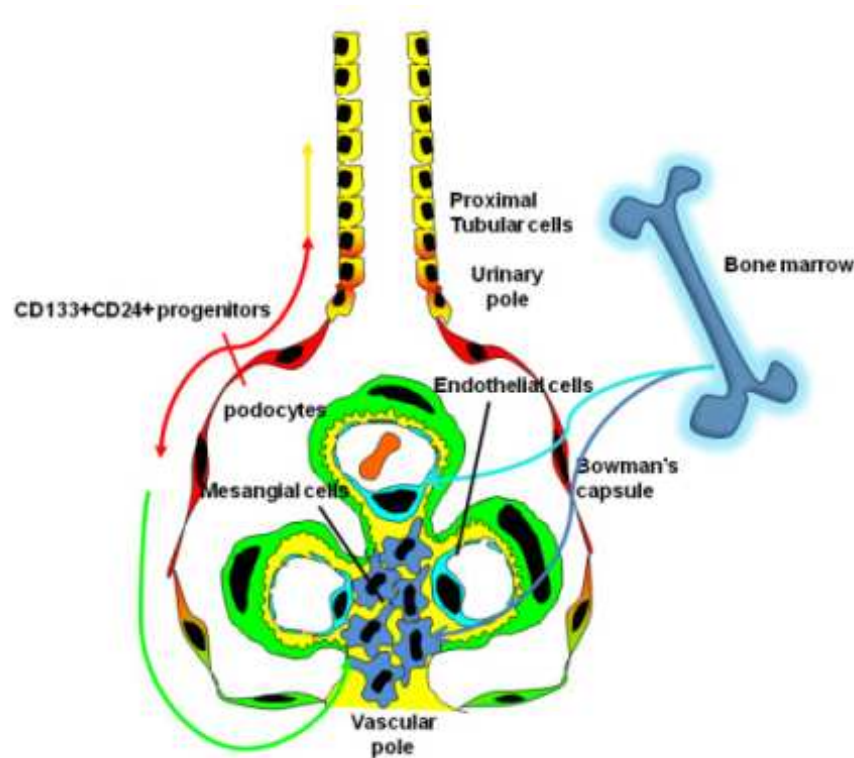


Figure 36: Representative diagram for kidney regeneration by different types of renal and extrarenal progenitors. CD24+CD133+ renal progenitors (red) are localized at the urinary pole and are in close contiguity with podocytes (green) at one extremity (the vascular stalk) and with tubular renal cells (yellow) at the other extremity. A transitional cell population (red/green) displays features of either renal progenitors (red) or podocytes (green) and localizes between the urinary pole and the vascular pole. At the vascular stalk of the glomerulus, the transitional cells are localized in close continuity with cells that lack progenitor markers, but exhibit the podocyte markers and the phenotypic features of differentiated podocytes (green). On the opposite side, at the urinary pole, transitional cells (red/yellow) with a mixed phenotype between tubular cells (yellow) and progenitor cells (red). The direction of differentiation is indicated by the arrows. Adapted from Romagnani *et.al.* 2013²⁰⁶

renal progenitors and was not observed in other epithelial cells. Our *in vitro* finding that CXCL12 blockade reverts this inhibitory effect on nephrin expression may correspond to our *in vivo* observation where CXCL12 blockade increased renal nephrin mRNA expression and podocyte numbers. Thus, CXCL12 blockade may enhance renal progenitors differentiation toward the podocyte lineage, thus enhancing podocyte regeneration.

One could thus hypothesize that dual blockade with anti-CCL2- and anti-CXCL12-Spiegelmers could lead to Spiegelmer-Spiegelmer interaction effects like complex formation or additive off-target effects. However, the plasma chemokine level analysis confirmed that dual blockade does not significantly affect the biological activity of each Spiegelmer in terms of binding to its natural target (in the plasma). This observation is consistent with the finding that 1K db/db mice with dual blockade

recapitulate the biological effects of single blockade. For example, 1K db/db mice treated with dual blockade displayed the reduction of glomerular leukocytes and a trend towards lower iNOS and TNF- α expression to the same extent as seen with CCL2 blockade. In addition, dual blockade also increased podocyte numbers and nephrin or podocin mRNA expression to the same extent as seen with CXCL12 blockade only. As a result the combination of these blockades was more potent than single blockade in preventing diffuse glomerulosclerosis as evidenced by significantly less glomeruli with global glomerulosclerosis and significantly more normal glomeruli. This additive therapeutic effect was less prominent for GFR and proteinuria because CXCL12 blockade by itself already had a profound effect on these two functional endpoints. Together, these data first document that chemokine antagonist combinations hold a potential for additive preventive effects on (diabetic) glomerulosclerosis when the individual chemokine targets mediate different pathomechanisms in the specific disease process, i.e. inflammation and renal progenitor differentiation toward the podocyte lineage.

There are some limitations to the conclusions drawn from the present two studies.

1. Based on previous studies in our laboratory, only a single dose of Spiegelmers (50 mg/kg body weight) was used. But it might be possible that higher doses are even more effective.
2. This study lacks supporting evidence from human experiments. However, Anti-CCL2 Spiegelmer (NOX-E36) is already in Phase IIa clinical trials to treat the diabetic kidney disease, whereas, NOX-A12 entered phase IIa clinical trials to treat multiple myeloma. (www.noxxon.com)

5.2 Cathepsin S inhibition in diabetic nephropathy

In this study, we have demonstrated that Cat S plays an important role in the progression of DN and inhibition of Cat S with R05461111 offers protection from the development of kidney disease in T2D. To the best of our knowledge, this is the first study that investigated the role of Cat S in the pathogenesis of DN.

Patients with diabetes and atherosclerosis have higher Cat S plasma levels and the elastolytic properties of Cat S contribute to macro vascular complications and mortality^{184-186,209,210}. However, the functional role of Cat S in microvascular diabetes

complications is not yet explored. We had hypothesized that Cat S contributes to kidney disease in T2D. Our studies confirm that Cat S localizes to the diabetic kidney and that Cat S inhibition with R05461111 reduces proteinuria, podocyte loss, and glomerulosclerosis in db/db mice. Additional *in vitro* and *in vivo* experiments suggest that Cat S contributes to endothelial dysfunction (ED), which is a central pathomechanism in microvascular complications of diabetes.

Cat S mRNA expression in the healthy mouse kidney was low as determined by RT-PCR and *in situ* hybridization, but immunostaining revealed strong positivity, especially in tubules, which was consistent in mice and humans. This implies that circulating Cat S protein is filtered and passively reabsorbed in the renal tubules. However, advanced DN was associated with a significant increase in renal Cat S mRNA expression, which we could not properly localize by in-situ hybridization, most likely due to a lack of sensitivity of the method. Cat S immunostaining of mouse and human kidneys with advanced DN displayed increased positivity in all compartments and in vascular endothelial cells and infiltrating leukocytes, respectively. It is of note that therapeutic Cat S inhibition drastically reduced renal Cat S mRNA and protein expression, wherein the reduction in protein expression was much more pronounced, implying that the inhibition of systemic Cat S expression reduces the amount of renal deposition of Cat S protein. However, also the reduction of proteinuria may account for this effect.

Cat S inhibition has a potent protective effect on proteinuria and podocyte loss and, to a lesser extent, on glomerulosclerosis. Podocyte loss is the central pathomechanism of DN progression as loss of podocytes cannot easily be replaced so that glomerular scarring progressively contributes to the loss of renal function¹⁹. We have identified Cat S-related biological effects that contribute to disease progression, i.e. ED and renal inflammation that were abrogated by therapeutic Cat S inhibition.

ED has been implicated as a potential and central pathomechanism for both diabetic and non-diabetic renal vascular complications²¹¹. As shown in figure 37, various factors of the diabetic milieu contribute to the development of ED which finally leads to DN. Microalbuminuria, a clinically important diagnostic and prognostic biomarker of glomerular injury, is now thought to be an early biomarker of ED, as increased vascular permeability leads to albumin leakage from the glomerular capillaries into the urine²¹² (Figure 38). In fact, micro-albuminuria is not always a

predictor of progressive DN but rather of cardiovascular complications in diabetes as well as in the non-diabetic population²¹³⁻²¹⁶. ED involves several alterations of normal endothelial cell functions, including increased oxidative stress²¹⁷.

Our *in vivo* microscopy studies document that Cat S is a mediator of vascular permeability upon oxidative stress. Cat S inhibition significantly improved microvascular permeability of FITC-dextran, a finding that may explain the reduction of proteinuria with Cat S inhibition in T2D db/db mice. Our *in vitro* studies document that Cat S specifically and dose-dependently increases endothelial cell monolayer permeability by inducing endothelial cell detachment and death, an effect that was not found with podocytes or other epithelial cells. But Cat S toxicity on endothelial cells

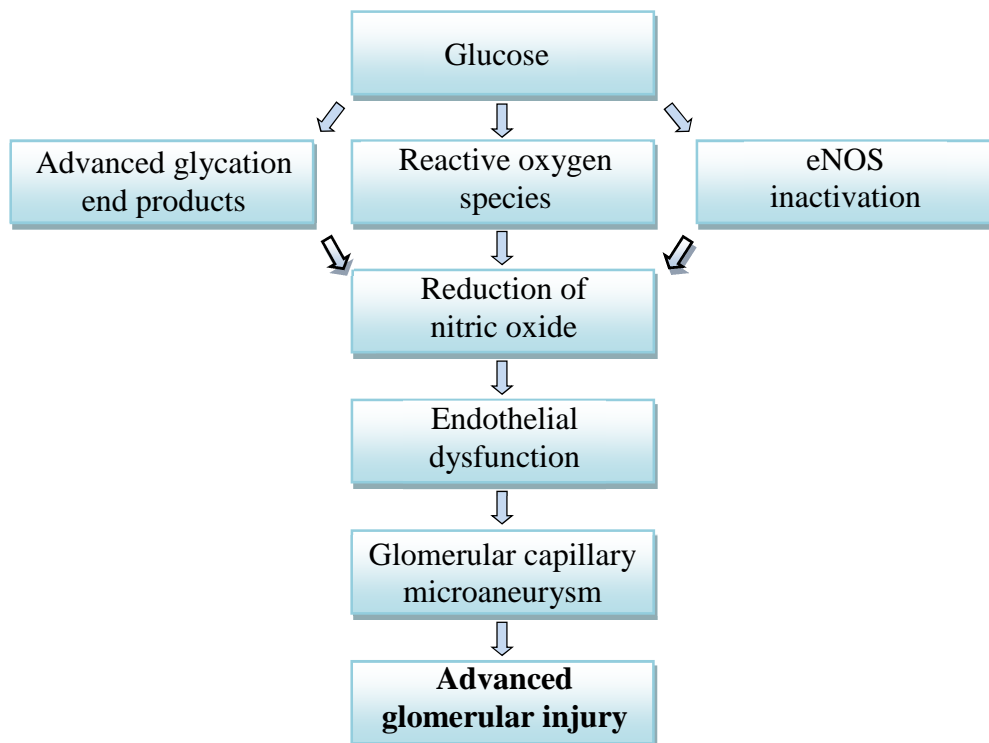


Figure 37: Factors that contribute to the development of endothelial dysfunction in patients with diabetes. Factors including reactive oxygen species, eNOS inactivation and advanced glycation end products contribute to a reduction in the levels of nitric oxide in the endothelium, which in turn leads to endothelial dysfunction. Abbreviation: eNOS, endothelial nitric oxide synthase. Adapted and modified from Nakagawa, T. *et.al.* 2010²¹²

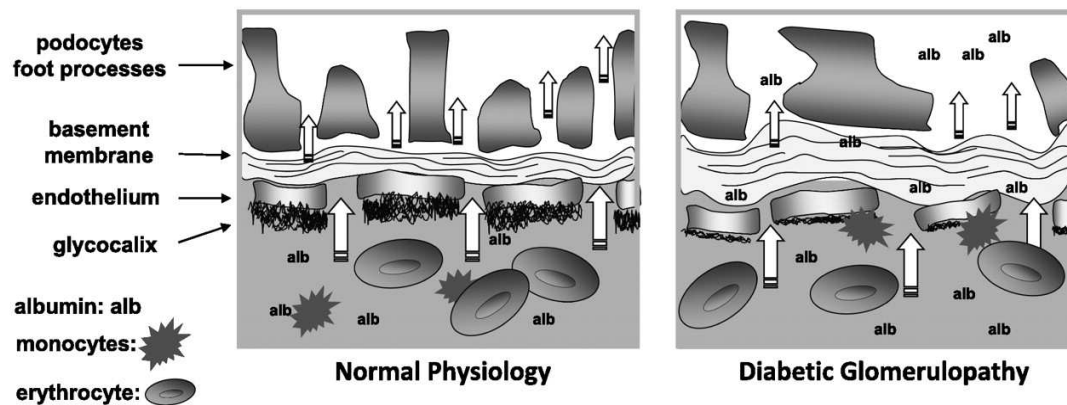


Figure 38: Schematic representation of the relative changes occurring at GFB. Various factors released during the early stages of diabetic glomerulopathy damages the endothelial fenestrations which increases the vascular permeability leading to albumin leakage. Adapted from Karalliedde J, *et. al.* 2011²¹¹

in vivo is less severe, probably due to the presence of protease inhibitors^{210,218}. Vice versa, decreased levels of cystatin C are associated with progressive cardiovascular disease by increasing the vascular activity of cysteine proteases²¹⁹.

ED in DN is further associated with reduced eNOS expression²¹⁷, which is now thought to be an important pathophysiological link between ED and the functional and histopathological alterations in DN²¹². In fact, db/db mice show impaired eNOS activation along the progression of DN and restoring eNOS activity reduced the albuminuria as a marker of improved ED²²⁰. Also Cat S inhibition increased renal eNOS expression, which was associated with less proteinuria and protection from glomerulosclerosis in T2D db/db mice. These findings suggest that circulating Cat S and potentially local production of Cat S contribute to ED in diabetes, which manifests as increased microvascular permeability (proteinuria) and progressive glomerulosclerosis, the latter, for example, being driven by less eNOS production. Cat S inhibition has the potential to reverse these pathomechanisms in T2D db/db mice. Finally, neo-angiogenesis is another consequence of ED that contributes to the microvascular complications of diabetes, which is driven by Cat S²²¹.

Tissue remodeling in DN is also driven by local inflammation involving intrarenal cytokine and chemokine production and the recruitment of pro-inflammatory and pro-fibrotic macrophages that amplify the inflammatory response and produce pro-

fibrotic mediators, respectively^{212,222}. ED supports this process by endothelial cell activation, luminal expression of adhesion molecules and chemokines that support macrophage recruitment⁵⁰. Cat S has the potential to modulate this inflammatory component of vascular disease as activated macrophages produce Cat S and contribute to vascular remodeling in atherosclerosis and vascular inflammation^{169,186,189}. In fact, our data are consistent with this concept, as Cat S inhibition reduced intrarenal expression of VCAM and ICAM as well as renal leukocyte recruitment and the expression of pro-inflammatory mediators such as IL-6, TNF- α , iNOS, and CCL2. The significant reduction of intrarenal Cat S protein expression correlated with the lower number of leukocytes in db/db mice treated with RO5461111, suggesting that infiltrating leukocytes are a major source of Cat S production inside the diabetic kidney. This would be consistent with the strong Cat S staining intensity in infiltrating leukocytes into the renal interstitium in patients with advanced DN, which were not seen to the same extent in the mouse model.

Together, Cat S inhibition is protective on kidney disease in T2D db/db mice. Our data suggest that Cat S is a mediator of ED, which implies microvascular permeability and inflammation, both driving tissue remodeling, i.e. progressive glomerulosclerosis. We conclude that Cat S is a mediator also of microvascular diabetes complications, which adds onto its known pathogenic role in macro-vascular disease. This implies that Cat S inhibition, for example with RO5461111, could elicit protective effects on vascular complications in diabetes²²³. However, there are some limitations to the conclusions drawn from this study.

1. Only a fixed dose of Cat S inhibitor RO5461111 (10 mg/kg body weight) was used throughout the study. But it might be possible that higher doses are even more effective.
2. It might be possible that blockade of Cat S lead to different results in other disease models. However, clinical trials with other Cat S inhibitors were shown to be more effective and safe in patients with Rheumatoid Arthritis.

6. Summary and conclusion

CCL2/MCP-1 and CXCL12/SDF-1 both contribute to glomerulosclerosis in type 2 diabetic mice, yet through different mechanisms. CCL2 mediates macrophage-related inflammation while CXCL12 contributes to podocyte loss. Antagonism of CCL2 and its receptor CCR2 are currently under phase III clinical trials for the treatment of diabetic kidney disease, whereas CXCL12 inhibition was also shown to be protective in various mouse models including, T2D. Dual blockade was significantly more effective than monotherapies in preventing glomerulosclerosis. CCL2 blockade reduced glomerular leukocyte counts and renal iNOS or IL-6 mRNA expression. CXCL12 blockade rather maintained podocyte numbers and renal nephrin and podocin mRNA expression. Consistently, CXCL12 blockade suppressed nephrin mRNA up regulation in primary cultures of human renal progenitors induced to differentiate towards the podocyte lineage. All aforementioned parameters were significantly improved in the dual blockade group which also suppressed proteinuria and was associated with the highest levels of GFR. Blood glucose levels and body weight were identical in all treatment groups. Together, dual blockade of CCL2 and CXCL12 found to be superior compared to single blockade in preventing the progression of diabetic glomerulosclerosis because both approaches target different disease pathomechanisms, i.e. inflammation and progenitor differentiation towards the podocyte lineage. Thus, dual CCL2/CXCL12 blockade could be a novel strategy to more efficiently prevent glomerulosclerosis in T2D.

Cat S is an elastolytic cysteine protease, known to drive vascular wall degeneration, a process that is independently associated with progressive vascular disease and all-cause mortality in patients with chronic kidney disease. Previous studies have shown that Cat inhibition was protective in various animal models of kidney diseases. In addition, Cat S inhibition was evolved as a novel therapeutic target in inflammatory and vascular disorders, but the pathogenic role of Cat S in kidney remodelling and progression of DN is not explored. Treatment with the orally available specific Cat S antagonist RO5461111 from month 4-6 of age significantly reduced albuminuria, podocyte loss, and glomerulosclerosis in association with lower glomerular and tubulointerstitial macrophage infiltrates as well as pro-inflammatory cytokines. In addition RO5461111 significantly lowered the mRNA expression of adhesion molecules, VCAM and ICAM and restored eNOS expression. *In vitro* studies

with glomerular endothelial cells have documented a toxic effect of Cat S on endothelial cells in terms of viability, detachment, and permeability. *In vivo* microscopy studies revealed that cathepsin S inhibition with RO5461111 improved oxidative stress-induced microvascular permeability. Together, Cat S is a circulating mediator of endothelial dysfunction driving albuminuria and progressive kidney disease in T2D and Cat S blockade with R05461111 could be a novel therapeutic strategy to prevent the progression of DN and diabetes associated complications.

7. Zusammenfassung und Fazit

CCL2/MCP-1 und CXCL12/SDF-1 sind beide an der Entwicklung der Glomerulosklerose im Rahmen von Typ 2 Diabetes beteiligt, dies aber durch unterschiedliche Mechanismen. CCL2 mediiert durch Makrophagen vermittelte Entzündungen wohingegen CXCL12 zum Podozytenverlust beiträgt. Die Antagonisten von CCL2 und seinem Rezeptor CCR2 befinden sich momentan in der Phase III der Zulassung (klinische Studien) für diabetische Nierenerkrankungen, zudem wurde auch gezeigt, dass CXCL12 Inhibierung einen protektiven Effekt in verschiedenen Mausmodellen zeigt, inklusive T2D. Es zeigte sich, dass durch eine duale Blockade eine signifikante Verbesserung der Glomerulosklerose nachweisbar war. Die CCL2 Blockade führte zu einer verminderten renalen Leukozyteninfiltration und ebenso zu einer verringerten renalen Expression von iNOS sowie IL-6 mRNA. Blockade von CXCL12 führte zu einem geringeren Schwund an Podozyten und renalem Nephlin sowie Podocin mRNA Expression. Alle genannten Parameter waren in der dualen Blockade signifikant verbessert, außerdem konnte eine verminderte Proteinurie und eine höhere glomeruläre Filtrationsrate nachgewiesen werden. Blutzuckerwerte zeigten keine Unterschiede in den verschiedenen Gruppen. Zusammenfassend ergibt sich daraus folgendes: eine gekoppelte Blockade von CCL2 und CXCL12 ist einer Blockade der einzelnen Komponenten überlegen. Dies zeigt sich in der Prävention der Progression der diabetischen Glomerulosklerose. Eine duale Blockade von CCL2 und CXCL12 könnte eine neue effizientere Therapie darstellen um bei Patienten mit einem T2D eine Glomerulosklerose zu verhindern.

Cathepsin S ist eine Cystein-Protease, die durch Proteolyse elastischer Fasern Gefäße degeneriert. Ein Prozess der mit dem Fortschreiten vaskulärer Erkrankungen in Verbindung gebracht wird, die auch begleitend bei chronischen Nierenerkrankungen auftritt. Studien bestätigen dass Cathepsin Inhibition zu einer Verbesserung in Tiermodellen mit Nierenerkrankungen führt. Zusätzlich wurde CatS als ein neuer therapeutischer Ansatzpunkt für entzündliche und vaskuläre Veränderungen bestätigt. Jedoch ist die Rolle von CatS im Bereich des „Nieren-remodelling“ und der Progression von diabetischer Nephropathie bisher nicht untersucht. Hierzu wurde ein spezifischer CatS Antagonist RO5461111 an Mäuse obiger Linie in einem Alter von vier bis sechs Monaten oral verabreicht. RO5461111 reduzierte signifikant die mRNA Expression des

Adhäsionsmoleküls VCAM und stellte die eNOS mRNA Expression wieder her. *In vitro* Studien mit glomerulären Endothelzellen zeigten einen toxischen Effekt von CatS, der sich hinsichtlich der Funktionsfähigkeit, Ablösung und Durchlässigkeit der Zellen darstellte. Mikroskopische *in vivo* Untersuchungen zeigten das eine CatS Inhibition mit RO546111 zu einer Verringerung des oxidativen Stresses führt und dadurch eine geringere microvaskuläre Permeabilität auftritt. Das Resume aus dem obigen ist, dass CatS ein im Blut zirkulierender Mediator für endotheliale Dysfunktion ist. CatS vermittelt Albuminurie und fortschreitende Nierenpathologie in T2D. R0546111 könnte als Antagonist von CatS ein neues Therapeutikum darstellen um die Progression der diabetischen Nephropathie zu mindern und den durch T2D vermittelte Komplikationen zu behandeln.

8. References

1. Levey, A.S. & Coresh, J. Chronic kidney disease. *Lancet* **379**, 165-180 (2012).
2. Levey, A.S., Tangri, N. & Stevens, L.A. Classification of chronic kidney disease: a step forward. *Annals of internal medicine* **154**, 65-67 (2011).
3. Levey, A.S., Astor, B.C., Stevens, L.A. & Coresh, J. Chronic kidney disease, diabetes, and hypertension: what's in a name? *Kidney international* **78**, 19-22 (2010).
4. Ju, W., Smith, S. & Kretzler, M. Genomic biomarkers for chronic kidney disease. *Translational research : the journal of laboratory and clinical medicine* **159**, 290-302 (2012).
5. Vehaskari, V.M. Genetics and CKD. *Advances in chronic kidney disease* **18**, 317-323 (2011).
6. Kottgen, A. Genome-wide association studies in nephrology research. *American journal of kidney diseases : the official journal of the National Kidney Foundation* **56**, 743-758 (2010).
7. Fabrizi, F., Messa, P., Basile, C. & Martin, P. Hepatic disorders in chronic kidney disease. *Nature reviews. Nephrology* **6**, 395-403 (2010).
8. Lucas, G.M., *et al.* Chronic kidney disease incidence, and progression to end-stage renal disease, in HIV-infected individuals: a tale of two races. *The Journal of infectious diseases* **197**, 1548-1557 (2008).
9. Zimmet, P., Alberti, K.G. & Shaw, J. Global and societal implications of the diabetes epidemic. *Nature* **414**, 782-787 (2001).
10. Stoycheff, N., *et al.* Nephrotic syndrome in diabetic kidney disease: an evaluation and update of the definition. *American journal of kidney diseases : the official journal of the National Kidney Foundation* **54**, 840-849 (2009).
11. Alberti, K.G. & Zimmet, P.Z. Definition, diagnosis and classification of diabetes mellitus and its complications. Part 1: diagnosis and classification of diabetes mellitus provisional report of a WHO consultation. *Diabetic medicine : a journal of the British Diabetic Association* **15**, 539-553 (1998).
12. Atkinson, M.A. & Eisenbarth, G.S. Type 1 diabetes: new perspectives on disease pathogenesis and treatment. *Lancet* **358**, 221-229 (2001).
13. Expert Committee on the, D. & Classification of Diabetes, M. Report of the Expert Committee on the Diagnosis and Classification of Diabetes Mellitus. *Diabetes care* **23 Suppl 1**, S4-19 (2000).
14. Scully, T. Diabetes in numbers. *Nature* **485**, S2-3 (2012).
15. Koster, I., Huppertz, E., Hauner, H. & Schubert, I. Direct costs of diabetes mellitus in Germany - CoDiM 2000-2007. *Experimental and clinical endocrinology & diabetes : official journal, German Society of Endocrinology [and] German Diabetes Association* **119**, 377-385 (2011).
16. Remuzzi, G., Schieppati, A. & Ruggenti, P. Clinical practice. Nephropathy in patients with type 2 diabetes. *The New England journal of medicine* **346**, 1145-1151 (2002).
17. Remuzzi, G., Macia, M. & Ruggenti, P. Prevention and treatment of diabetic renal disease in type 2 diabetes: the BENEDICT study. *Journal of the American Society of Nephrology : JASN* **17**, S90-97 (2006).
18. Levey, A.S., *et al.* Definition and classification of chronic kidney disease: a position statement from Kidney Disease: Improving Global Outcomes (KDIGO). *Kidney international* **67**, 2089-2100 (2005).
19. Qian, Y., Feldman, E., Pennathur, S., Kretzler, M. & Brosius, F.C., 3rd. From fibrosis to sclerosis: mechanisms of glomerulosclerosis in diabetic nephropathy. *Diabetes* **57**, 1439-1445 (2008).
20. Navarro-Gonzalez, J.F., Mora-Fernandez, C., Muros de Fuentes, M. & Garcia-Perez, J. Inflammatory molecules and pathways in the pathogenesis of diabetic nephropathy. *Nature reviews. Nephrology* **7**, 327-340 (2011).
21. Kim, Y.H., *et al.* Podocyte depletion and glomerulosclerosis have a direct relationship in the PAN-treated rat. *Kidney international* **60**, 957-968 (2001).
22. Mundel, P. & Shankland, S.J. Podocyte biology and response to injury. *Journal of the American Society of Nephrology : JASN* **13**, 3005-3015 (2002).
23. Tryggvason, K., Patrakka, J. & Wartiovaara, J. Hereditary proteinuria syndromes and mechanisms of proteinuria. *The New England journal of medicine* **354**, 1387-1401 (2006).
24. Zenker, M., Machuca, E. & Antignac, C. Genetics of nephrotic syndrome: new insights into molecules acting at the glomerular filtration barrier. *Journal of molecular medicine* **87**, 849-857 (2009).
25. Shah, S.N., He, C.J. & Klotman, P. Update on HIV-associated nephropathy. *Current opinion in nephrology and hypertension* **15**, 450-455 (2006).

26. Matsusaka, T., *et al.* Podocyte injury damages other podocytes. *Journal of the American Society of Nephrology : JASN* **22**, 1275-1285 (2011).
27. Haraldsson, B., Nystrom, J. & Deen, W.M. Properties of the glomerular barrier and mechanisms of proteinuria. *Physiological reviews* **88**, 451-487 (2008).
28. Chen, Y.M. & Miner, J.H. Glomerular basement membrane and related glomerular disease. *Translational research : the journal of laboratory and clinical medicine* **160**, 291-297 (2012).
29. Pagtalunan, M.E., *et al.* Podocyte loss and progressive glomerular injury in type II diabetes. *The Journal of clinical investigation* **99**, 342-348 (1997).
30. Stieger, N., Worthmann, K. & Schiffer, M. The role of metabolic and haemodynamic factors in podocyte injury in diabetes. *Diabetes/metabolism research and reviews* **27**, 207-215 (2011).
31. Steffes, M.W., Schmidt, D., McCrery, R., Basgen, J.M. & International Diabetic Nephropathy Study, G. Glomerular cell number in normal subjects and in type 1 diabetic patients. *Kidney international* **59**, 2104-2113 (2001).
32. Cook, H.T. Focal segmental glomerulosclerosis in IgA nephropathy: a result of primary podocyte injury? *Kidney international* **79**, 581-583 (2011).
33. Wiggins, R.C. The spectrum of podocytopathies: a unifying view of glomerular diseases. *Kidney international* **71**, 1205-1214 (2007).
34. Wharram, B.L., *et al.* Podocyte depletion causes glomerulosclerosis: diphtheria toxin-induced podocyte depletion in rats expressing human diphtheria toxin receptor transgene. *Journal of the American Society of Nephrology : JASN* **16**, 2941-2952 (2005).
35. Kerjaschki, D. Caught flat-footed: podocyte damage and the molecular bases of focal glomerulosclerosis. *The Journal of clinical investigation* **108**, 1583-1587 (2001).
36. Vakifahmetoglu, H., Olsson, M. & Zhivotovsky, B. Death through a tragedy: mitotic catastrophe. *Cell death and differentiation* **15**, 1153-1162 (2008).
37. Greka, A. & Mundel, P. Cell biology and pathology of podocytes. *Annual review of physiology* **74**, 299-323 (2012).
38. Vitale, I., Galluzzi, L., Castedo, M. & Kroemer, G. Mitotic catastrophe: a mechanism for avoiding genomic instability. *Nature reviews. Molecular cell biology* **12**, 385-392 (2011).
39. Lasagni, L., Lazzeri, E., Shankland, S.J., Anders, H.J. & Romagnani, P. Podocyte mitosis - a catastrophe. *Current molecular medicine* (2012).
40. Castedo, M., *et al.* Cell death by mitotic catastrophe: a molecular definition. *Oncogene* **23**, 2825-2837 (2004).
41. Galluzzi, L., *et al.* Molecular definitions of cell death subroutines: recommendations of the Nomenclature Committee on Cell Death 2012. *Cell death and differentiation* **19**, 107-120 (2012).
42. Ianzini, F. & Mackey, M.A. Spontaneous premature chromosome condensation and mitotic catastrophe following irradiation of HeLa S3 cells. *International journal of radiation biology* **72**, 409-421 (1997).
43. Menon, M.C., Chuang, P.Y. & He, C.J. The glomerular filtration barrier: components and crosstalk. *International journal of nephrology* **2012**, 749010 (2012).
44. Macconi, D., *et al.* Podocyte repopulation contributes to regression of glomerular injury induced by ACE inhibition. *The American journal of pathology* **174**, 797-807 (2009).
45. Ryu, M., *et al.* Plasma leakage through glomerular basement membrane ruptures triggers the proliferation of parietal epithelial cells and crescent formation in non-inflammatory glomerular injury. *The Journal of pathology* (2012).
46. Remuzzi, G., Benigni, A. & Remuzzi, A. Mechanisms of progression and regression of renal lesions of chronic nephropathies and diabetes. *The Journal of clinical investigation* **116**, 288-296 (2006).
47. Lasagni, L., *et al.* Notch activation differentially regulates renal progenitors proliferation and differentiation toward the podocyte lineage in glomerular disorders. *Stem cells* **28**, 1674-1685 (2010).
48. Appel, D., *et al.* Recruitment of podocytes from glomerular parietal epithelial cells. *Journal of the American Society of Nephrology : JASN* **20**, 333-343 (2009).
49. Navarro, J.F. & Mora, C. Role of inflammation in diabetic complications. *Nephrology, dialysis, transplantation : official publication of the European Dialysis and Transplant Association - European Renal Association* **20**, 2601-2604 (2005).
50. Galkina, E. & Ley, K. Leukocyte recruitment and vascular injury in diabetic nephropathy. *Journal of the American Society of Nephrology : JASN* **17**, 368-377 (2006).
51. Shikata, K. & Makino, H. Role of macrophages in the pathogenesis of diabetic nephropathy. *Contributions to nephrology*, 46-54 (2001).

52. Ruster, C. & Wolf, G. The role of chemokines and chemokine receptors in diabetic nephropathy. *Frontiers in bioscience : a journal and virtual library* **13**, 944-955 (2008).
53. Alexandraki, K., *et al.* Inflammatory process in type 2 diabetes: The role of cytokines. *Annals of the New York Academy of Sciences* **1084**, 89-117 (2006).
54. Sassy-Prigent, C., *et al.* Early glomerular macrophage recruitment in streptozotocin-induced diabetic rats. *Diabetes* **49**, 466-475 (2000).
55. Ikezumi, Y., Hurst, L.A., Masaki, T., Atkins, R.C. & Nikolic-Paterson, D.J. Adoptive transfer studies demonstrate that macrophages can induce proteinuria and mesangial cell proliferation. *Kidney international* **63**, 83-95 (2003).
56. Guler, S., *et al.* Plasma soluble intercellular adhesion molecule 1 levels are increased in type 2 diabetic patients with nephropathy. *Hormone research* **58**, 67-70 (2002).
57. Park, C.W., *et al.* High glucose-induced intercellular adhesion molecule-1 (ICAM-1) expression through an osmotic effect in rat mesangial cells is PKC-NF-kappa B-dependent. *Diabetologia* **43**, 1544-1553 (2000).
58. Basta, G., *et al.* Advanced glycation end products activate endothelium through signal-transduction receptor RAGE: a mechanism for amplification of inflammatory responses. *Circulation* **105**, 816-822 (2002).
59. Onozato, M.L., Tojo, A., Goto, A. & Fujita, T. Radical scavenging effect of gliclazide in diabetic rats fed with a high cholesterol diet. *Kidney Int* **65**, 951-960 (2004).
60. Chow, F.Y., Nikolic-Paterson, D.J., Ozols, E., Atkins, R.C. & Tesch, G.H. Intercellular adhesion molecule-1 deficiency is protective against nephropathy in type 2 diabetic db/db mice. *Journal of the American Society of Nephrology : JASN* **16**, 1711-1722 (2005).
61. Lim, A.K., *et al.* Antibody blockade of c-fms suppresses the progression of inflammation and injury in early diabetic nephropathy in obese db/db mice. *Diabetologia* **52**, 1669-1679 (2009).
62. Lim, A.K. & Tesch, G.H. Inflammation in diabetic nephropathy. *Mediators of inflammation* **2012**, 146154 (2012).
63. Locati, M. & Murphy, P.M. Chemokines and chemokine receptors: biology and clinical relevance in inflammation and AIDS. *Annual review of medicine* **50**, 425-440 (1999).
64. Belperio, J.A., *et al.* CXC chemokines in angiogenesis. *Journal of leukocyte biology* **68**, 1-8 (2000).
65. Hogaboam, C.M., Steinhauser, M.L., Chensue, S.W. & Kunkel, S.L. Novel roles for chemokines and fibroblasts in interstitial fibrosis. *Kidney international* **54**, 2152-2159 (1998).
66. Mantovani, A., Bonecchi, R. & Locati, M. Tuning inflammation and immunity by chemokine sequestration: decoys and more. *Nature reviews. Immunology* **6**, 907-918 (2006).
67. Rossi, D. & Zlotnik, A. The biology of chemokines and their receptors. *Annual review of immunology* **18**, 217-242 (2000).
68. Bacon, K., *et al.* Chemokine/chemokine receptor nomenclature. *Journal of interferon & cytokine research : the official journal of the International Society for Interferon and Cytokine Research* **22**, 1067-1068 (2002).
69. Bazan, J.F., *et al.* A new class of membrane-bound chemokine with a CX3C motif. *Nature* **385**, 640-644 (1997).
70. Murphy, P.M., *et al.* International union of pharmacology. XXII. Nomenclature for chemokine receptors. *Pharmacological reviews* **52**, 145-176 (2000).
71. Zlotnik, A. & Yoshie, O. Chemokines: a new classification system and their role in immunity. *Immunity* **12**, 121-127 (2000).
72. Rovai, L.E., Herschman, H.R. & Smith, J.B. The murine neutrophil-chemoattractant chemokines LIX, KC, and MIP-2 have distinct induction kinetics, tissue distributions, and tissue-specific sensitivities to glucocorticoid regulation in endotoxemia. *Journal of leukocyte biology* **64**, 494-502 (1998).
73. Xia, Y. & Frangogiannis, N.G. MCP-1/CCL2 as a therapeutic target in myocardial infarction and ischemic cardiomyopathy. *Inflammation & allergy drug targets* **6**, 101-107 (2007).
74. Yoshie, O., Imai, T. & Nomiyama, H. Novel lymphocyte-specific CC chemokines and their receptors. *Journal of leukocyte biology* **62**, 634-644 (1997).
75. Forster, R., *et al.* CCR7 coordinates the primary immune response by establishing functional microenvironments in secondary lymphoid organs. *Cell* **99**, 23-33 (1999).
76. Moser, B., Wolf, M., Walz, A. & Loetscher, P. Chemokines: multiple levels of leukocyte migration control. *Trends in immunology* **25**, 75-84 (2004).
77. Meurens, F., *et al.* Expression of mucosal chemokines TECK/CCL25 and MEC/CCL28 during fetal development of the ovine mucosal immune system. *Immunology* **120**, 544-555 (2007).

78. Cyster, J.G. Chemokines and cell migration in secondary lymphoid organs. *Science* **286**, 2098-2102 (1999).
79. Lomize, A.L., Pogozheva, I.D. & Mosberg, H.I. Structural organization of G-protein-coupled receptors. *Journal of computer-aided molecular design* **13**, 325-353 (1999).
80. Kelvin, D.J., *et al.* Chemokines and serpentine: the molecular biology of chemokine receptors. *Journal of leukocyte biology* **54**, 604-612 (1993).
81. Godessart, N. Chemokine receptors: attractive targets for drug discovery. *Annals of the New York Academy of Sciences* **1051**, 647-657 (2005).
82. Borroni, E.M., *et al.* The chemoattractant decoy receptor D6 as a negative regulator of inflammatory responses. *Biochemical Society transactions* **34**, 1014-1017 (2006).
83. Pease, J.E. Tails of the unexpected - an atypical receptor for the chemokine RANTES/CCL5 expressed in brain. *British journal of pharmacology* **149**, 460-462 (2006).
84. Allen, S.J., Crown, S.E. & Handel, T.M. Chemokine: receptor structure, interactions, and antagonism. *Annual review of immunology* **25**, 787-820 (2007).
85. Butcher, E.C. & Picker, L.J. Lymphocyte homing and homeostasis. *Science* **272**, 60-66 (1996).
86. Springer, T.A. Traffic signals for lymphocyte recirculation and leukocyte emigration: the multistep paradigm. *Cell* **76**, 301-314 (1994).
87. Shaw, S.K., *et al.* Coordinated redistribution of leukocyte LFA-1 and endothelial cell ICAM-1 accompany neutrophil transmigration. *The Journal of experimental medicine* **200**, 1571-1580 (2004).
88. Dwir, O., Grabovsky, V. & Alon, R. Selectin avidity modulation by chemokines at subsecond endothelial contacts: a novel regulatory level of leukocyte trafficking. *Ernst Schering Research Foundation workshop*, 109-135 (2004).
89. Proudfoot, A.E., *et al.* Glycosaminoglycan binding and oligomerization are essential for the in vivo activity of certain chemokines. *Proceedings of the National Academy of Sciences of the United States of America* **100**, 1885-1890 (2003).
90. Johnatty, R.N., *et al.* Cytokine and chemokine regulation of proMMP-9 and TIMP-1 production by human peripheral blood lymphocytes. *Journal of immunology* **158**, 2327-2333 (1997).
91. Xia, P., *et al.* Characterization of vascular endothelial growth factor's effect on the activation of protein kinase C, its isoforms, and endothelial cell growth. *The Journal of clinical investigation* **98**, 2018-2026 (1996).
92. Wiedermann, C.J., *et al.* Monocyte haptotaxis induced by the RANTES chemokine. *Current biology : CB* **3**, 735-739 (1993).
93. Gewirtz, A.M., *et al.* Chemokine regulation of human megakaryocytopoiesis. *Blood* **86**, 2559-2567 (1995).
94. Koch, A.E., *et al.* Interleukin-8 as a macrophage-derived mediator of angiogenesis. *Science* **258**, 1798-1801 (1992).
95. Baggiolini, M., Moser, B. & Clark-Lewis, I. Interleukin-8 and related chemotactic cytokines. The Giles Filley Lecture. *Chest* **105**, 95S-98S (1994).
96. Lane, B.R., *et al.* Interleukin-8 and growth-regulated oncogene alpha mediate angiogenesis in Kaposi's sarcoma. *Journal of virology* **76**, 11570-11583 (2002).
97. Arenberg, D.A., *et al.* Epithelial-neutrophil activating peptide (ENA-78) is an important angiogenic factor in non-small cell lung cancer. *The Journal of clinical investigation* **102**, 465-472 (1998).
98. Luster, A.D., Unkeless, J.C. & Ravetch, J.V. Gamma-interferon transcriptionally regulates an early-response gene containing homology to platelet proteins. *Nature* **315**, 672-676 (1985).
99. Farber, J.M. HuMig: a new human member of the chemokine family of cytokines. *Biochemical and biophysical research communications* **192**, 223-230 (1993).
100. Arenberg, D.A., *et al.* Interferon-gamma-inducible protein 10 (IP-10) is an angiostatic factor that inhibits human non-small cell lung cancer (NSCLC) tumorigenesis and spontaneous metastases. *The Journal of experimental medicine* **184**, 981-992 (1996).
101. Hensbergen, P.J., *et al.* The CXCR3 targeting chemokine CXCL11 has potent antitumor activity in vivo involving attraction of CD8+ T lymphocytes but not inhibition of angiogenesis. *Journal of immunotherapy* **28**, 343-351 (2005).
102. Kuna, P., *et al.* RANTES, a monocyte and T lymphocyte chemotactic cytokine releases histamine from human basophils. *Journal of immunology* **149**, 636-642 (1992).
103. Luster, A.D. Chemokines regulate lymphocyte homing to the intestinal mucosa. *Gastroenterology* **120**, 291-294 (2001).
104. Viola, A. & Luster, A.D. Chemokines and their receptors: drug targets in immunity and inflammation. *Annual review of pharmacology and toxicology* **48**, 171-197 (2008).

105. Panee, J. Monocyte Chemoattractant Protein 1 (MCP-1) in obesity and diabetes. *Cytokine* **60**, 1-12 (2012).
106. Van Coillie, E., Van Damme, J. & Opdenakker, G. The MCP/eotaxin subfamily of CC chemokines. *Cytokine & growth factor reviews* **10**, 61-86 (1999).
107. Gruden, G., *et al.* Mechanical stretch induces monocyte chemoattractant activity via an NF-kappaB-dependent monocyte chemoattractant protein-1-mediated pathway in human mesangial cells: inhibition by rosiglitazone. *Journal of the American Society of Nephrology : JASN* **16**, 688-696 (2005).
108. Segerer, S., Nelson, P.J. & Schlondorff, D. Chemokines, chemokine receptors, and renal disease: from basic science to pathophysiologic and therapeutic studies. *Journal of the American Society of Nephrology : JASN* **11**, 152-176 (2000).
109. Rovin, B.H., Yoshimura, T. & Tan, L. Cytokine-induced production of monocyte chemoattractant protein-1 by cultured human mesangial cells. *Journal of immunology* **148**, 2148-2153 (1992).
110. Tesch, G.H., *et al.* Monocyte chemoattractant protein-1 promotes macrophage-mediated tubular injury, but not glomerular injury, in nephrotoxic serum nephritis. *The Journal of clinical investigation* **103**, 73-80 (1999).
111. Viedt, C. & Orth, S.R. Monocyte chemoattractant protein-1 (MCP-1) in the kidney: does it more than simply attract monocytes? *Nephrology, dialysis, transplantation : official publication of the European Dialysis and Transplant Association - European Renal Association* **17**, 2043-2047 (2002).
112. Segerer, S., *et al.* Expression of the chemokine monocyte chemoattractant protein-1 and its receptor chemokine receptor 2 in human crescentic glomerulonephritis. *Journal of the American Society of Nephrology : JASN* **11**, 2231-2242 (2000).
113. Vielhauer, V., *et al.* Obstructive nephropathy in the mouse: progressive fibrosis correlates with tubulointerstitial chemokine expression and accumulation of CC chemokine receptor 2- and 5-positive leukocytes. *Journal of the American Society of Nephrology : JASN* **12**, 1173-1187 (2001).
114. Grandaliano, G., *et al.* MCP-1 and EGF renal expression and urine excretion in human congenital obstructive nephropathy. *Kidney international* **58**, 182-192 (2000).
115. Eardley, K.S., *et al.* The relationship between albuminuria, MCP-1/CCL2, and interstitial macrophages in chronic kidney disease. *Kidney international* **69**, 1189-1197 (2006).
116. Morii, T., *et al.* Association of monocyte chemoattractant protein-1 with renal tubular damage in diabetic nephropathy. *Journal of diabetes and its complications* **17**, 11-15 (2003).
117. Chiarelli, F., *et al.* Circulating monocyte chemoattractant protein-1 and early development of nephropathy in type 1 diabetes. *Diabetes care* **25**, 1829-1834 (2002).
118. Chow, F.Y., *et al.* Monocyte chemoattractant protein-1 promotes the development of diabetic renal injury in streptozotocin-treated mice. *Kidney international* **69**, 73-80 (2006).
119. Chow, F.Y., *et al.* Monocyte chemoattractant protein-1-induced tissue inflammation is critical for the development of renal injury but not type 2 diabetes in obese db/db mice. *Diabetologia* **50**, 471-480 (2007).
120. Wada, T., *et al.* Intervention of crescentic glomerulonephritis by antibodies to monocyte chemotactic and activating factor (MCAF/MCP-1). *Faseb J* **10**, 1418-1425 (1996).
121. Ruiz-Ortega, M., *et al.* Angiotensin II participates in mononuclear cell recruitment in experimental immune complex nephritis through nuclear factor-kappa B activation and monocyte chemoattractant protein-1 synthesis. *Journal of immunology* **161**, 430-439 (1998).
122. Ihm, C.G., *et al.* A high glucose concentration stimulates the expression of monocyte chemotactic peptide 1 in human mesangial cells. *Nephron* **79**, 33-37 (1998).
123. Kato, S., *et al.* Renin-angiotensin blockade lowers MCP-1 expression in diabetic rats. *Kidney international* **56**, 1037-1048 (1999).
124. Amann, B., Tinzmann, R. & Angelkort, B. ACE inhibitors improve diabetic nephropathy through suppression of renal MCP-1. *Diabetes care* **26**, 2421-2425 (2003).
125. Han, S.Y., *et al.* Spironolactone prevents diabetic nephropathy through an anti-inflammatory mechanism in type 2 diabetic rats. *Journal of the American Society of Nephrology : JASN* **17**, 1362-1372 (2006).
126. Takaishi, H., Taniguchi, T., Takahashi, A., Ishikawa, Y. & Yokoyama, M. High glucose accelerates MCP-1 production via p38 MAPK in vascular endothelial cells. *Biochemical and biophysical research communications* **305**, 122-128 (2003).

127. Lee, E.Y., *et al.* The monocyte chemoattractant protein-1/CCR2 loop, inducible by TGF-beta, increases podocyte motility and albumin permeability. *American journal of physiology. Renal physiology* **297**, F85-94 (2009).
128. Jefferson, J.A., Alpers, C.E. & Shankland, S.J. Podocyte biology for the bedside. *American journal of kidney diseases : the official journal of the National Kidney Foundation* **58**, 835-845 (2011).
129. Tarabra, E., *et al.* Effect of the monocyte chemoattractant protein-1/CC chemokine receptor 2 system on nephrin expression in streptozotocin-treated mice and human cultured podocytes. *Diabetes* **58**, 2109-2118 (2009).
130. Ninichuk, V., *et al.* Late onset of Ccl2 blockade with the Spiegelmer mNOX-E36-3'PEG prevents glomerulosclerosis and improves glomerular filtration rate in db/db mice. *The American journal of pathology* **172**, 628-637 (2008).
131. Balabanian, K., *et al.* The chemokine SDF-1/CXCL12 binds to and signals through the orphan receptor RDC1 in T lymphocytes. *The Journal of biological chemistry* **280**, 35760-35766 (2005).
132. Crump, M.P., *et al.* Solution structure and basis for functional activity of stromal cell-derived factor-1; dissociation of CXCR4 activation from binding and inhibition of HIV-1. *The EMBO journal* **16**, 6996-7007 (1997).
133. Nagasawa, T., Kikutani, H. & Kishimoto, T. Molecular cloning and structure of a pre-B-cell growth-stimulating factor. *Proceedings of the National Academy of Sciences of the United States of America* **91**, 2305-2309 (1994).
134. Broxmeyer, H.E. Chemokines in hematopoiesis. *Current opinion in hematology* **15**, 49-58 (2008).
135. Bleul, C.C., Fuhlbrigge, R.C., Casasnovas, J.M., Aiuti, A. & Springer, T.A. A highly efficacious lymphocyte chemoattractant, stromal cell-derived factor 1 (SDF-1). *The Journal of experimental medicine* **184**, 1101-1109 (1996).
136. Aiuti, A., Webb, I.J., Bleul, C., Springer, T. & Gutierrez-Ramos, J.C. The chemokine SDF-1 is a chemoattractant for human CD34+ hematopoietic progenitor cells and provides a new mechanism to explain the mobilization of CD34+ progenitors to peripheral blood. *The Journal of experimental medicine* **185**, 111-120 (1997).
137. Colobran, R., Pujol-Borrell, R., Armengol, M.P. & Juan, M. The chemokine network. I. How the genomic organization of chemokines contains clues for deciphering their functional complexity. *Clinical and experimental immunology* **148**, 208-217 (2007).
138. Loetscher, P. & Moser, B. Homing chemokines in rheumatoid arthritis. *Arthritis research* **4**, 233-236 (2002).
139. De Klerck, B., *et al.* Pro-inflammatory properties of stromal cell-derived factor-1 (CXCL12) in collagen-induced arthritis. *Arthritis research & therapy* **7**, R1208-1220 (2005).
140. Balabanian, K., *et al.* Role of the chemokine stromal cell-derived factor 1 in autoantibody production and nephritis in murine lupus. *Journal of immunology* **170**, 3392-3400 (2003).
141. Meiron, M., Zohar, Y., Anunu, R., Wildbaum, G. & Karin, N. CXCL12 (SDF-1alpha) suppresses ongoing experimental autoimmune encephalomyelitis by selecting antigen-specific regulatory T cells. *The Journal of experimental medicine* **205**, 2643-2655 (2008).
142. O'Boyle, G., Mellor, P., Kirby, J.A. & Ali, S. Anti-inflammatory therapy by intravenous delivery of non-heparan sulfate-binding CXCL12. *FASEB journal : official publication of the Federation of American Societies for Experimental Biology* **23**, 3906-3916 (2009).
143. Yano, T., Liu, Z., Donovan, J., Thomas, M.K. & Habener, J.F. Stromal cell derived factor-1 (SDF-1)/CXCL12 attenuates diabetes in mice and promotes pancreatic beta-cell survival by activation of the prosurvival kinase Akt. *Diabetes* **56**, 2946-2957 (2007).
144. Schober, A., Knarren, S., Lietz, M., Lin, E.A. & Weber, C. Crucial role of stromal cell-derived factor-1alpha in neointima formation after vascular injury in apolipoprotein E-deficient mice. *Circulation* **108**, 2491-2497 (2003).
145. Togel, F., Isaac, J., Hu, Z., Weiss, K. & Westenfelder, C. Renal SDF-1 signals mobilization and homing of CXCR4-positive cells to the kidney after ischemic injury. *Kidney Int* **67**, 1772-1784 (2005).
146. Stokman, G., *et al.* SDF-1 provides morphological and functional protection against renal ischaemia/reperfusion injury. *Nephrology, dialysis, transplantation : official publication of the European Dialysis and Transplant Association - European Renal Association* **25**, 3852-3859 (2010).
147. Takabatake, Y., *et al.* The CXCL12 (SDF-1)/CXCR4 axis is essential for the development of renal vasculature. *Journal of the American Society of Nephrology : JASN* **20**, 1714-1723 (2009).

148. Ding, M., *et al.* Loss of the tumor suppressor Vhlh leads to upregulation of Cxcr4 and rapidly progressive glomerulonephritis in mice. *Nature medicine* **12**, 1081-1087 (2006).
149. Tachibana, K., *et al.* The chemokine receptor CXCR4 is essential for vascularization of the gastrointestinal tract. *Nature* **393**, 591-594 (1998).
150. Ara, T., Tokoyoda, K., Okamoto, R., Koni, P.A. & Nagasawa, T. The role of CXCL12 in the organ-specific process of artery formation. *Blood* **105**, 3155-3161 (2005).
151. Vielhauer, V., Anders, H.J. & Schlondorff, D. Chemokines and chemokine receptors as therapeutic targets in lupus nephritis. *Seminars in nephrology* **27**, 81-97 (2007).
152. Kryczek, I., Wei, S., Keller, E., Liu, R. & Zou, W. Stroma-derived factor (SDF-1/CXCL12) and human tumor pathogenesis. *American journal of physiology. Cell physiology* **292**, C987-995 (2007).
153. Rempel, S.A., Dudas, S., Ge, S. & Gutierrez, J.A. Identification and localization of the cytokine SDF1 and its receptor, CXC chemokine receptor 4, to regions of necrosis and angiogenesis in human glioblastoma. *Clinical cancer research : an official journal of the American Association for Cancer Research* **6**, 102-111 (2000).
154. Petruzzello-Pellegrini, T.N., *et al.* The CXCR4/CXCR7/SDF-1 pathway contributes to the pathogenesis of Shiga toxin-associated hemolytic uremic syndrome in humans and mice. *The Journal of clinical investigation* **122**, 759-776 (2012).
155. Sayyed, S.G., *et al.* Podocytes produce homeostatic chemokine stromal cell-derived factor-1/CXCL12, which contributes to glomerulosclerosis, podocyte loss and albuminuria in a mouse model of type 2 diabetes. *Diabetologia* **52**, 2445-2454 (2009).
156. Turk, V., Turk, B. & Turk, D. Lysosomal cysteine proteases: facts and opportunities. *The EMBO journal* **20**, 4629-4633 (2001).
157. Turk, V., *et al.* Cysteine cathepsins: from structure, function and regulation to new frontiers. *Biochimica et biophysica acta* **1824**, 68-88 (2012).
158. Choi, K.Y., Swierczewska, M., Lee, S. & Chen, X. Protease-activated drug development. *Theranostics* **2**, 156-178 (2012).
159. Berdowska, I. Cysteine proteases as disease markers. *Clinica chimica acta; international journal of clinical chemistry* **342**, 41-69 (2004).
160. Mason, R.W. Emerging functions of placental cathepsins. *Placenta* **29**, 385-390 (2008).
161. Dubin, G. Proteinaceous cysteine protease inhibitors. *Cellular and molecular life sciences : CMLS* **62**, 653-669 (2005).
162. Lecaille, F., Kaleta, J. & Bromme, D. Human and parasitic papain-like cysteine proteases: their role in physiology and pathology and recent developments in inhibitor design. *Chemical reviews* **102**, 4459-4488 (2002).
163. Drake, F.H., *et al.* Cathepsin K, but not cathepsins B, L, or S, is abundantly expressed in human osteoclasts. *The Journal of biological chemistry* **271**, 12511-12516 (1996).
164. Wex, T., *et al.* Human cathepsin W, a cysteine protease predominantly expressed in NK cells, is mainly localized in the endoplasmic reticulum. *Journal of immunology* **167**, 2172-2178 (2001).
165. Linnevers, C., Smeekens, S.P. & Bromme, D. Human cathepsin W, a putative cysteine protease predominantly expressed in CD8+ T-lymphocytes. *FEBS letters* **405**, 253-259 (1997).
166. Bromme, D., Li, Z., Barnes, M. & Mehler, E. Human cathepsin V functional expression, tissue distribution, electrostatic surface potential, enzymatic characterization, and chromosomal localization. *Biochemistry* **38**, 2377-2385 (1999).
167. Mohamed, M.M. & Sloane, B.F. Cysteine cathepsins: multifunctional enzymes in cancer. *Nature reviews. Cancer* **6**, 764-775 (2006).
168. Cheng, X.W., *et al.* Increased expression of elastolytic cysteine proteases, cathepsins S and K, in the neointima of balloon-injured rat carotid arteries. *The American journal of pathology* **164**, 243-251 (2004).
169. Sukhova, G.K., *et al.* Deficiency of cathepsin S reduces atherosclerosis in LDL receptor-deficient mice. *The Journal of clinical investigation* **111**, 897-906 (2003).
170. Reiser, J., Adair, B. & Reinheckel, T. Specialized roles for cysteine cathepsins in health and disease. *The Journal of clinical investigation* **120**, 3421-3431 (2010).
171. Nakagawa, T.Y., *et al.* Impaired invariant chain degradation and antigen presentation and diminished collagen-induced arthritis in cathepsin S null mice. *Immunity* **10**, 207-217 (1999).
172. Driessen, C., Lennon-Dumenil, A.M. & Ploegh, H.L. Individual cathepsins degrade immune complexes internalized by antigen-presenting cells via Fcγ receptors. *European journal of immunology* **31**, 1592-1601 (2001).
173. Martinon, F., Mayor, A. & Tschopp, J. The inflammasomes: guardians of the body. *Annual review of immunology* **27**, 229-265 (2009).

174. Sever, S., *et al.* Proteolytic processing of dynamin by cytoplasmic cathepsin L is a mechanism for proteinuric kidney disease. *The Journal of clinical investigation* **117**, 2095-2104 (2007).
175. Shechter, P., Boner, G. & Rabkin, R. Tubular cell protein degradation in early diabetic renal hypertrophy. *Journal of the American Society of Nephrology : JASN* **4**, 1582-1587 (1994).
176. Schaefer, L., Han, X., Gretz, N. & Schaefer, R.M. Alterations of cathepsins B, H and L in proximal tubules from polycystic kidneys of the Han:SPRD rat. *Kidney international* **50**, 424-431 (1996).
177. Reiser, J., *et al.* Podocyte migration during nephrotic syndrome requires a coordinated interplay between cathepsin L and alpha3 integrin. *The Journal of biological chemistry* **279**, 34827-34832 (2004).
178. Van Den Berg, J.G., *et al.* Interleukin-4 and -13 promote basolateral secretion of H(+) and cathepsin L by glomerular epithelial cells. *American journal of physiology. Renal physiology* **282**, F26-33 (2002).
179. Bauer, Y., *et al.* Identification of cathepsin L as a potential sex-specific biomarker for renal damage. *Hypertension* **57**, 795-801 (2011).
180. Kirschke, H., Wiederanders, B., Bromme, D. & Rinne, A. Cathepsin S from bovine spleen. Purification, distribution, intracellular localization and action on proteins. *The Biochemical journal* **264**, 467-473 (1989).
181. Hsing, L.C., *et al.* Roles for cathepsins S, L, and B in insulinitis and diabetes in the NOD mouse. *Journal of autoimmunity* **34**, 96-104 (2010).
182. Liuzzo, J.P., Petanceska, S.S., Moscatelli, D. & Devi, L.A. Inflammatory mediators regulate cathepsin S in macrophages and microglia: A role in attenuating heparan sulfate interactions. *Molecular medicine* **5**, 320-333 (1999).
183. Hall, A., *et al.* Structural basis for different inhibitory specificities of human cystatins C and D. *Biochemistry* **37**, 4071-4079 (1998).
184. Jobs, E., *et al.* Association between serum cathepsin S and mortality in older adults. *JAMA : the journal of the American Medical Association* **306**, 1113-1121 (2011).
185. Liu, J., *et al.* Lysosomal cysteine proteases in atherosclerosis. *Arteriosclerosis, thrombosis, and vascular biology* **24**, 1359-1366 (2004).
186. Lutgens, S.P., Cleutjens, K.B., Daemen, M.J. & Heeneman, S. Cathepsin cysteine proteases in cardiovascular disease. *FASEB journal : official publication of the Federation of American Societies for Experimental Biology* **21**, 3029-3041 (2007).
187. Gupta, S., Singh, R.K., Dastidar, S. & Ray, A. Cysteine cathepsin S as an immunomodulatory target: present and future trends. *Expert opinion on therapeutic targets* **12**, 291-299 (2008).
188. Lee-Dutra, A., Wiener, D.K. & Sun, S. Cathepsin S inhibitors: 2004-2010. *Expert opinion on therapeutic patents* **21**, 311-337 (2011).
189. de Nooijer, R., *et al.* Leukocyte cathepsin S is a potent regulator of both cell and matrix turnover in advanced atherosclerosis. *Arteriosclerosis, thrombosis, and vascular biology* **29**, 188-194 (2009).
190. Pan, L., *et al.* Cathepsin S deficiency results in abnormal accumulation of autophagosomes in macrophages and enhances Ang II-induced cardiac inflammation. *PloS one* **7**, e35315 (2012).
191. Buhling, F., *et al.* Expression of cathepsins B, H, K, L, and S during human fetal lung development. *Developmental dynamics : an official publication of the American Association of Anatomists* **225**, 14-21 (2002).
192. Ward, C., *et al.* Antibody targeting of cathepsin S inhibits angiogenesis and synergistically enhances anti-VEGF. *PloS one* **5**(2010).
193. Luhe, A., Hildebrand, H., Bach, U., Dinger, T. & Ahr, H.J. A new approach to studying ochratoxin A (OTA)-induced nephrotoxicity: expression profiling in vivo and in vitro employing cDNA microarrays. *Toxicological sciences : an official journal of the Society of Toxicology* **73**, 315-328 (2003).
194. Breyer, M.D., *et al.* Mouse models of diabetic nephropathy. *Journal of the American Society of Nephrology : JASN* **16**, 27-45 (2005).
195. Brosius, F.C., 3rd, *et al.* Mouse models of diabetic nephropathy. *Journal of the American Society of Nephrology : JASN* **20**, 2503-2512 (2009).
196. Klussmann, S., Nolte, A., Bald, R., Erdmann, V.A. & Furste, J.P. Mirror-image RNA that binds D-adenosine. *Nat Biotechnol* **14**, 1112-1115 (1996).
197. Allam, R., *et al.* Histones from dying renal cells aggravate kidney injury via TLR2 and TLR4. *Journal of the American Society of Nephrology : JASN* **23**, 1375-1388 (2012).
198. Kulkarni, O., *et al.* Spiegelmer inhibition of CCL2/MCP-1 ameliorates lupus nephritis in MRL-(Fas)lpr mice. *Journal of the American Society of Nephrology : JASN* **18**, 2350-2358 (2007).

199. Tesch, G.H. MCP-1/CCL2: a new diagnostic marker and therapeutic target for progressive renal injury in diabetic nephropathy. *American journal of physiology. Renal physiology* **294**, F697-701 (2008).
200. Mazzinghi, B., *et al.* Essential but differential role for CXCR4 and CXCR7 in the therapeutic homing of human renal progenitor cells. *The Journal of experimental medicine* **205**, 479-490 (2008).
201. Sayyed, S.G., *et al.* An orally active chemokine receptor CCR2 antagonist prevents glomerulosclerosis and renal failure in type 2 diabetes. *Kidney international* **80**, 68-78 (2011).
202. Ronconi, E., *et al.* Regeneration of glomerular podocytes by human renal progenitors. *Journal of the American Society of Nephrology : JASN* **20**, 322-332 (2009).
203. Peled, A., *et al.* Dependence of human stem cell engraftment and repopulation of NOD/SCID mice on CXCR4. *Science* **283**, 845-848 (1999).
204. Avecilla, S.T., *et al.* Chemokine-mediated interaction of hematopoietic progenitors with the bone marrow vascular niche is required for thrombopoiesis. *Nat Med* **10**, 64-71 (2004).
205. Sugiyama, T., Kohara, H., Noda, M. & Nagasawa, T. Maintenance of the hematopoietic stem cell pool by CXCL12-CXCR4 chemokine signaling in bone marrow stromal cell niches. *Immunity* **25**, 977-988 (2006).
206. Romagnani, P. & Remuzzi, G. Renal progenitors in non-diabetic and diabetic nephropathies. *Trends in endocrinology and metabolism: TEM* **24**, 13-20 (2013).
207. Lindgren, D., *et al.* Isolation and characterization of progenitor-like cells from human renal proximal tubules. *The American journal of pathology* **178**, 828-837 (2011).
208. Peti-Peterdi, J. & Sipos, A. A high-powered view of the filtration barrier. *Journal of the American Society of Nephrology : JASN* **21**, 1835-1841 (2010).
209. Aikawa, E., *et al.* Arterial and aortic valve calcification abolished by elastolytic cathepsin S deficiency in chronic renal disease. *Circulation* **119**, 1785-1794 (2009).
210. Lafarge, J.C., Naour, N., Clement, K. & Guerre-Millo, M. Cathepsins and cystatin C in atherosclerosis and obesity. *Biochimie* **92**, 1580-1586 (2010).
211. Karalliedde, J. & Gnudi, L. Endothelial factors and diabetic nephropathy. *Diabetes care* **34 Suppl 2**, S291-296 (2011).
212. Nakagawa, T., *et al.* Endothelial dysfunction as a potential contributor in diabetic nephropathy. *Nature reviews. Nephrology* **7**, 36-44 (2011).
213. Dinneen, S.F. & Gerstein, H.C. The association of microalbuminuria and mortality in non-insulin-dependent diabetes mellitus. A systematic overview of the literature. *Archives of internal medicine* **157**, 1413-1418 (1997).
214. Ruggerenti, P., *et al.* Measurable urinary albumin predicts cardiovascular risk among normoalbuminuric patients with type 2 diabetes. *Journal of the American Society of Nephrology : JASN* **23**, 1717-1724 (2012).
215. Ninomiya, T., *et al.* Albuminuria and kidney function independently predict cardiovascular and renal outcomes in diabetes. *Journal of the American Society of Nephrology : JASN* **20**, 1813-1821 (2009).
216. Hillege, H.L., *et al.* Urinary albumin excretion predicts cardiovascular and noncardiovascular mortality in general population. *Circulation* **106**, 1777-1782 (2002).
217. Pober, J.S., Min, W. & Bradley, J.R. Mechanisms of endothelial dysfunction, injury, and death. *Annual review of pathology* **4**, 71-95 (2009).
218. Cox, J.M., *et al.* Determination of cathepsin S abundance and activity in human plasma and implications for clinical investigation. *Analytical biochemistry* **430**, 130-137 (2012).
219. Shi, G.P., *et al.* Cystatin C deficiency in human atherosclerosis and aortic aneurysms. *The Journal of clinical investigation* **104**, 1191-1197 (1999).
220. Cheng, H., Wang, H., Fan, X., Pauksakon, P. & Harris, R.C. Improvement of endothelial nitric oxide synthase activity retards the progression of diabetic nephropathy in db/db mice. *Kidney international* **82**, 1176-1183 (2012).
221. Shi, G.P., *et al.* Deficiency of the cysteine protease cathepsin S impairs microvessel growth. *Circulation research* **92**, 493-500 (2003).
222. Tuttle, K.R. Linking metabolism and immunology: diabetic nephropathy is an inflammatory disease. *Journal of the American Society of Nephrology : JASN* **16**, 1537-1538 (2005).
223. Thurmond, R.L., Sun, S., Karlsson, L. & Edwards, J.P. Cathepsin S inhibitors as novel immunomodulators. *Current opinion in investigational drugs* **6**, 473-482 (2005).

9. Abbreviations

ACE	angiotensin converting enzyme
AGEs	advanced glycation end products
Ang II	angiotensin II
AT1R	angiotensin II type 1 receptor
AT2R	angiotensin II type 2 receptor
BM	basement membrane
BSA	bovine serum albumin
cDNA	complementary DNA
Cat(s)	cathepsin(s)
CCL	chemokine C-C motif ligand
CCR	chemokine C-C motif receptor
CXCL	chemokine C-X-C motif ligand
CXCR	chemokine C-X-C motif receptor
CX3CR	chemokine C-X3-C motif receptor
CKD	chronic kidney disease
CT	cycle threshold
DARC	duffy antigen receptor for chemokines
ddH ₂ O	double distilled water
DEPC	diethyl pyrocarbonate
DM	diabetes mellitus
DMEM	Dulbecco's modified Eagle's medium
DMSO	dimethyl sulfoxide
DN	diabetic nephropathy
<i>et al.</i>	<i>et al.</i> = and others
eNOS	endothelial nitric oxide synthase
ECM	extracellular matrix
ED	endothelial dysfunction
EDTA	ethylenediaminetetra-acetic acid
ELISA	Enzyme-Linked Immunosorbent Assay
ESRD	end-stage renal disease
FACS	fluorescence activated cell sorting
FCS	fetal calf serum
FITC	fluorescein iso-thiocyanate
GBM	glomerular basement membrane
GEnC	glomerular endothelial cell line
GFR	glomerular filtration rate
GPCR	G protein-coupled receptor
HE	hematoxylin-Eosin
HIV	human immunodeficiency virus
hpf	high-power-field
h/hrs	hour/hours
ICAM-1	intercellular adhesion molecule-1
i.e.	id est = in other words
IL	interleukin
IL-8	interleukin-8
IFN- γ	interferon- γ
IP-10	interferon inducible protein-10
kDa	kilo dalton

K/DOQI	kidney disease outcomes quality initiative
MCP	monocyte chemoattractant protein
min	minute/min
MIP	macrophage inflammatory protein
mL/min	milliliter/minute
M/MØ	monocytes / macrophages
mNOX-E36	anti-CCL2 Spiegelmer
mNOX-A12	anti-CXCL12 Spiegelmer
mRNA	messenger ribonucleic acid
NADPH	nicotinamide adenine dinucleotide phosphate
NF-κB	nuclear factor-κB
NO	nitric oxide
NOS	nitric oxide synthase
O.D.	optical density
PAS	periodic acid Schiff
PBS	phosphate buffered saline
PCR	polymerase chain reaction
PKC	protein kinase C
RANTES	regulated on activation normal T cell expressed and secreted
RAS	renin angiotensin system
revNOX-A12	control Spiegelmer for NOX-A12
RNA	ribonucleic acid
RNase	ribonuclease
ROS	reactive oxygen species
RPM	revolutions per minute
RPMI Medium	cell culture medium
rRNA	ribosomal ribonucleic acid
RT	room temperature
RT-PCR	real-time reverse transcription-polymerase chain reaction
s	second
STZ	streptozotocin
T1D	type 1 diabetes
T2D	type 2 diabetes
TECs	tubular epithelial cells
TGF-β	transforming growth factor-β
Th1	T helper cell type 1
TNF-α	tumor necrosis factor-α
TZDs	thiazolidinediones
UACR	urinary albumin creatinine ratio
UUO	unilateral urethral obstruction
VCAM-1	vascular cell adhesion molecule-1
VEGF	vascular endothelial growth factor
vs	versus
v/v	volume/volume
WT	wild type
WT-1	wilms tumor 1
1K	1 kidney
2K	2 kidneys

10. Appendix

FACS buffer

Sterile DPBS	500 mL
Sodium azide	500 mg (0.1%)
BSA	1 g (0.2%)

10X HBSS (Hank's Balanced Saline Solution) without Ca, Mg

For 1000 mL:

KCl	4 g
KH ₂ PO ₄	0.6 g
NaCl	80 g
Na ₂ HPO ₄ ·2H ₂ O	0.621 g

Dissolve in 1000 mL and autoclave.

DNase stock solution (1 mg/mL)

DNase (type III) 15000 U/6 mg (Sigma D5025)
 To prepare 1 mg/mL solution, add 6 ml of 50% (w/v) Glycerol in 20 mM Tris-HCl (pH 7.5), 1 mM MgCl₂.
 Can be kept at -20 °C for several weeks.
 Caution: Solution is stable only for 1 week at 4 °C.

Collagenase / DNase solution

1 mg/mL Collagenase, 0.1 mg/mL DNase in 1X HBSS (with Ca, Mg)
 For 10 mL:
 Collagenase (type I) (Sigma C0130) 10 mg
 1 mg/mL DNase stock solution 1 mL
 HBSS (with Ca, Mg) 9 mL
 To be pre-heated in 37 °C water bath before use.
 Caution: Prepare freshly every time (Stable only for few days)

Citrate buffer 10X

110 mM Sodiumcitrate in ddH₂O
 Adjust pH 6.0 with 2 N NaOH

PBS

2.74 M NaCl
 54 mM KCl
 30 mM KH₂PO₄
 130 mM Na₂HPO₄ in ddH₂O
 Adjust to pH 7.5 with HCl

Eidesstattliche Versicherung

Venkata Surya Narayana Murthy, Darisipudi

Name, Vorname

Ich erkläre hiermit an Eides statt,

dass ich die vorliegende Dissertation mit dem Thema

Chemokines and Cysteine Proteases in Diabetic Kidney Disease

selbständig verfasst, mich außer der angegebenen keiner weiteren Hilfsmittel bedient und alle Erkenntnisse, die aus dem Schrifttum ganz oder annähernd übernommen sind, als solche kenntlich gemacht und nach ihrer Herkunft unter Bezeichnung der Fundstelle einzeln nachgewiesen habe.

Ich erkläre des Weiteren, dass die hier vorgelegte Dissertation nicht in gleicher oder in ähnlicher Form bei einer anderen Stelle zur Erlangung eines akademischen Grades eingereicht wurde.

Munich

Ort, Date

Unterschrift Doktorandin/Doktorand

CURRICULUM VITAE

VENKATA SURYA NARAYANA MURTHY DARISIPUDI

Research fellow

AG Prof. Hans-Joachim Anders

Medical Klinik and Polyklinik IV

Schillerstrasse- 42, 80336 Munich

Work: +49 89 218075856

Mobile: +49 176 35793871

Email: Narayana-Murthy.Darisipudi@med.uni-muenchen.de



Current position (Oct 2009 to April 2013)

Doctoral Research Fellow at Nephologisches Zentrum, Medizinische Klinik und Poliklinik IV, Ludwig-Maximilians University, Munich, Germany

Principal Investigator: Prof. Dr. Hans-Joachim Anders, Munich

Research project: Chemokines and cysteine proteases in diabetic kidney disease

Research experience (Aug 2008 to Jun 2009)

Research Fellow at Department of Biochemistry, All India Institute of Medical Sciences (AIIMS), New Delhi, India

Principal Investigator: Prof. D. N. Rao

Academic profile

2008 Master of Science in Biochemistry (**Gold medalist**) from Sri Venkateswara University, Tirupati, India with an aggregate of 79.63%

2006 Bachelor of Science (Biotechnology, Biochemistry, and Chemistry) from Andhra University, Visakhapatnam, India with an aggregate of 76%

2003 Diploma in Pharmacy and qualified as a Pharmacist from 'Andhra Pradesh Pharmacy Council of India', India

Publications

Allam R, **Darisipudi MN**, Rupanagudi KV, Lichtnekert J, Tschopp J, Anders HJ. Cutting edge: cyclic polypeptide and aminoglycoside antibiotics trigger IL-1 β secretion by activating the NLRP3 inflammasome. *J Immunol.* 2011 Mar 1;186(5):2714-8.

Darisipudi MN, Kulkarni OP, Sayyed SG, Ryu M, Migliorini A, Sagrinati C, Parente E, Vater A, Eulberg D, Klusmann S, Romagnani P, Anders HJ. Dual blockade of the homeostatic chemokine CXCL12 and the proinflammatory chemokine CCL2 has additive protective effects on diabetic kidney disease. *Am J Pathol.* 2011 Jul;179(1):116-24

Lech M^{*}, Weidenbusch M^{*}, Kulkarni OP, Ryu M, **Darisipudi MN**, Susanti HE, Mittrucker HW, Mak TW, Anders HJ. IRF4 deficiency abrogates lupus nephritis despite enhancing systemic cytokine production. *J Am Soc Nephrol.* 2011 Aug;22(8):1443-52.

Lichtnekert J^{*}, Rupanagudi KV^{*}, Kulkarni OP, **Darisipudi MN**, Allam R, Anders HJ. Activated protein C attenuates systemic lupus erythematosus and lupus nephritis in MRL-Fas(lpr) mice. *J Immunol.* 2011 Sep 15;187(6):3413-21

Darisipudi MN, Allam R, Rupanagudi KV, Anders HJ. Polyene macrolide antifungal drugs trigger interleukin-1 β secretion by activating the NLRP3 inflammasome. *PLoS One.* 2011;6(5):e19588

Allam R^{*1}, Scherbaum Ch^{*1}, **Darisipudi MN^{*1}**, Mulay SR, Hägele H, Lichtnekert J, Hagemann JH, Rupanagudi KV, Ryu M, Hohenstein B, Hugo C, Uhl B, Reichel ChA, Krombach F, Monestier M, Moreth K, Schaefer L, Liapis H, Anders HJ . Histones release from dying renal cells aggravates acute kidney injury via Toll-like receptor-2 and 4 activation. *J Am Soc Nephrol.* 2012 Aug;23(8):1375-88 (***equal contribution**)

Darisipudi MN^{*}, Thomasova D^{*}, Kulkarni OP, Mulay SR, Brech D, Nossner E, Liapis H, Anders HJ. Tamm-Horsfall protein/uromodulin forms nanoparticles that trigger interleukin-1 β -dependent innate immunity by activating the NLRP3 inflammasome in mononuclear cells. *J Am Soc Nephrol.* 2012 Nov;23(11):1783-9

Mulay SR, Kulkarni OP, Rupanagudi KV, Migliorini A, **Darisipudi MN**, Vilaysane A, Muruve D, Shi Y, Munro F, Liapis H, Anders HJ. Calcium oxalate crystals induce renal inflammation by NLRP3-mediated IL-1 β secretion. *J Clin Invest.* 2013 Jan 2;123(1):236-46

Book chapter

Darisipudi MN, Mulay SR, Anders HJ. L'inflammasome NLRP3: un nouvel element de signalisation du danger qui favorise l'inflammation renale. In Actualites Nephrologiques Jean Hamburger. *Medicine Sciences Publications*. Paris 2013

Oral presentations

“Dual blockade of the homeostatic chemokine CXCL12 and the proinflammatory chemokine CCL2 has additive protective effects on diabetic kidney disease” at Kongress für Nephrologie, Berlin, Germany (Sept 2011)

Poster presentations

Accepted as “Dual blockade of the homeostatic chemokine CXCL12 and the proinflammatory chemokine CCL2 has additive protective effects on diabetic kidney disease” for “Kongress der Deutschen Gesellschaft für Innere Medizin e.V. (DGIM)” at Wiesbaden, Germany (April 2011)

Accepted as “Polyene macrolide antifungal drugs trigger interleukin-1 β secretion by activating the NLRP3 inflammasome” for “The IL-1 Family of cytokines conference” at Clear water beach, Florida (May 2011)

Academic achievements

- 1 Received "**Dasaradha Ramayya Gold medal award**" from Sri Venkataswara University, Tirupati, India
2. **Momento “Rajeev Pratibha Puraskar Award”** from National Students Union of India (NSUI) for academic excellence in Masters' at Sri Venkateswara University, Tirupati.
- 3 Secured 2nd Rank and qualified in National level entrance test for Masters' program in Biochemistry at Sri Venkateswara University, Tirupati, India
4. Secured 10th Rank and qualified in National level entrance test for Masters' program in Biochemistry at Andhra University, Visakhapatnam, India

Personal profile

Name : Venkata Surya Narayana Murthy.Darisipudi
Marital Status : Single
Nationality : Indian
Current Address : Hermann-Lingg- Straße 18,
3rd stock, App 311
80336, Munchen

References

Prof. Dr. Hans-Joachim Anders

Nephrologisches Zentrum der LMU
Medizinische Klinik und Poliklinik IV
Ziemsenstr. 1
80336 Munich, Germany
Tel: +49 89-51603583
Email: hjanders@med.uni-muenchen.de

Prof. D. N. Rao

Department of Biochemistry
All India Institute of Medical Sciences (AIIMS)
Ansari nagar
110029 New Delhi, India
Tel: +91 11 6593545
Email: dnrao311@rediffmail.com

Declaration

I hereby declare that the above-mentioned particulars are true to the best of my knowledge and belief.

(Venkata Surya Narayana Murthy Darisipudi)